Identifying Configurations of Plus-energy Curtain Walls for the perimeter zone using the Analysis of Variance (ANOVA) approach

Angel LAM Tze Chun

A Thesis
in
The Department
of
Building. Civil and Environmental Engineering

Presented in Partial Fulfillment of the Requirements
For the Degree of
Master of Applied Science (Building Engineering) at
Concordia University
Montreal, Quebec, Canada

August 2015

CONCORDIA UNIVERSITY

School of Graduate Studies

This is to certify that the thesis prepared by

By: Tze Chun Angel Lam

Entitled: Identifying Configurations of Plus-energy Curtain Walls for the Perimeter Zone Using the Analysis of Variance (ANOVA) Approach

and submitted in partial fulfillment of the requirements for the degree of

Master of Applied Science (Building Engineering)

complies with the regulations of the University and meets the accepted standards with respect to originality and quality.

Signed by the final examining committee:

_____ Chair
Dr. B. Lee

_____ Supervisor
Dr. H. Ge

_____ Examiner
Dr. Y. Zeng

_____ Extemal (to program) Examiner
Dr. A. Athienitis

_____ Examiner
Dr. B. Lee

Approved by _____
Dr. F. Haghighat, GPD
Department of Building, Civil and Environmental Engineering

_____
Dr. Amir Asif, Dean
Faculty of Engineering and Computer Science

Date: _____

Abstract

Identifying Configurations of Plus-energy Curtain Walls for the perimeter zone using the Analysis of Variance (ANOVA) approach

Angel LAM Tze Chun

Curtain walls are believed to be "energy sinks" because of their low thermal performance, however, the integration of energy generating technologies such as photovoltaic (PV) panels may enable converting curtain walls to "plus-energy" curtain walls. The "plus-energy" curtain wall is defined as the energy generated by the curtain wall façade exceeds the energy consumption of a perimeter zone office. To design plus-energy curtain walls, design parameters of curtain walls are prioritized by sensitivity analysis and the most critical design parameters corresponding to specific energy efficient measures that bring major energy benefits with minor modifications are identified.

An office unit with five adiabatic faces and one exterior façade completed with curtain walls is developed as the energy model in EnergyPlus. The indoor environmental parameters are set based on ASHRAE energy standard.

In this study, global sensitivity analysis is conducted to prioritize the energy impact of ten design parameters, U-value of glazing, solar heat gain coefficient of glazing, visible transmittance of glazing, U-value of spandrel panel, U-value of frame, window wall ratio, infiltration, depth of overhang, inclination of overhang, and effective efficiency of photovoltaic panels. The three most significant design parameters are identified for four orientations. Plus-energy curtain wall configurations at different window-to-wall ratio (WWR) and orientations are identified according to the total sensitivity indices. The significance of this study is to provide design recommendations of plus-energy curtain wall configurations under different WWRs and orientations, which are not covered in the current design guidelines.

Acknowledgement

It has been a long journey for me ten thousand kilometres away all starting from an email with Dr. Paul Fazio. He gave me the courage to cross the ocean and the confidence to take on one of his projects on “plus-energy curtain walls”. It has been my privilege to work with a great scholar such as Dr. Fazio. His passion towards research, his patience towards his students, his perseverance in his argument, all make him a unique scholar whom I admire greatly. I can still remember that he returned to research meeting immediately after long journey from the IBPC Japan conference. In his last few days, Dr. Fazio still returned to school and cared about his research and students; all this persistent attitude leave me no room in making any excuse in life not to do or not to achieve anything.

My work will never be completed without the persistent effort and vigilant supervision of Dr. Hua Ge. She is meticulous and yet caring. She attends to needs and characteristics of each of her students. She mentors me when I am confused, gives me support when I feel alone, encourages me when I feel weak and she offers me a home away from home. I learned from her the patience to every detailed problems, not to avoid from difficulties. There were so many happenings in the past three years, and Dr. Ge guided me through each of them. I should say thank you for her tolerance towards my stubbornness. I am grateful for her patience to answer all my questions and her tolerance towards my mistakes. She is a great research supervisor.

Dr. Andreas Athienitis is the theme leader of this SNEBRN (Smart Net-zero Energy Buildings strategic Research Network) project. Through the network, he exposes us to numerous research and network opportunities. I am glad to be part of the SNEBRN family.

It has been my pleasure to work at Concordia, where I am surrounding with great people, whom I would like to mention in the order of our encounter. I must thank Dr. Jiwu Rao for his assistance and constructive discussion throughout these years. I treasure the time Dimitri and I started the new office from scratch at the beginning of my study. The office will be dull without Colin, he makes every day cheerful, I appreciate all his offers, all his sharing throughout these years. Ramy always offers ready help and is full of wits. Vincent brings us so much fun and energy with his lively spirit. Asok is full of wisdom towards life, I can still remember many of our conversation. I appreciate very much the many constructive inputs for my research from Costa. Sam, thanks for

sharing your vision and passion with me, they are inspiring. I wish Shaghayegh and Mohammed good luck in their new venture. Ali is the best companion in travelling, I shall remember all the laughter and support when I was in difficult moment. Sarah is the best listener. Lin and I have very lively discussion on sensitivity analysis. I appreciate all his kind offers that ease my life. Clement, my personal French teacher, accompanied me for the many ups and downs. The year Xiangwei spent here makes our office like home, I wish you and Li all the success in Shanghai. Special thanks goes to Dr. Jian Li Hao for her moral support. Even though it has been just a few months, Kim, I miss sharing with you. Dr. Bruno Lee's advices on simulation and optimization were very valuable. There are so many encounters in the last three years, Daniel, German, Edvinas, Malak, Jennifer, Stephanie, Stijn, and many others. I appreciate all your help and encouragement.

Indeed, so many things happened in the last year. I wish my mother could be with me now to share my joy in finalizing the thesis. My mother not only brought me to the world, fed me with sweat and tears, but also empowered me with freedom and trust that allow me to explore the world on my own. She cheered on my achievement and yet tolerated many of my short comings. I will remember all the overnights she accompanied me. She had faith in all my decisions and allowed me to learn from my own failure. This thesis witnesses the last moment of her and the most difficult time for me. With the birth of my baby boy, Sage, on Aug 3rd, 2015, I am also crossing the finish line of my thesis. I know it is under the blessing of my mother. I would like to delicate this thesis to my mother, to whom has set up a role model for me to follow as being a great mother.

Table of contents

List of figures

List of tables

Chapter 1 Introduction

1.1 Background

The Net Zero Energy Building (NZEB) is a complex concept lacking commonly agreed NZEB definition (Marszal et al., 2011; Torcellini et al., 2006) or consistently confirmed type of energy balance. The most favoured definition is the balance between the energy demand or consumption and the renewable energy generation (Noguchi et al., 2008; Torcellini et al., 2006; Gilijamse, 1995; Rosta et al., 2008). The greatest challenge of NZEB is to strive to fulfil the energy balance of a building equipped with on-site renewable energy generation systems. To design NZEB is not an easy task at the design stage during which the building information is still being devised, such as building forms, building envelope design, orientation, and geometry, mechanical and electrical systems. These are important parameters in ascertaining building energy performance, which are most crucial attributes to achieve the NZEB goals.

Building envelope, including fenestration, opaque elements and shadings, has strong impact on heating, cooling and electric lighting energy demands as well as on daylight. Building envelope design is a key factor in enhancing the energy efficiency in the perimeter zone of buildings because building envelopes play an important role in regulating the indoor conditions of perimeter zone by filtering the unwanted heat and retaining useful heat. Typically, the interior zone of buildings is subjected to the high cooling demand due to the internal gains such as artificial lighting, occupancy and electrical appliances while the perimeter zone of buildings is subjected to both cooling and heating demand due to the variation of climatic conditions (Gutherz & Schiler, 1991). Therefore high performance building envelope deign is an essential step in reducing the energy consumption in the perimeter zone of buildings.

Building envelopes, which can greatly reduce the energy consumption, integrated with energy generation, such as Building Integrated Photovoltaic Panels (BIPV), provide means to achieve NZEB goals. There is abundant research on the optimal tilt for fixed photovoltaic technologies. (Duffie & Beckman, 1994; Gopinathan, 1991; Gunerhan & Hepbasli, 2007; Lewis, 1987; Lorenzo, 2011; Prasad & Snow, 2014; Roberts & Guariento, 2009). Without optimized building envelope and BIPV design, the energy demand of perimeter zone of buildings is typically higher than the

energy yield from the BIPV despite the advances in photovoltaic technologies. It implies that thorough careful building envelope and BIPV design with optimized performance is significant for the NZEB design.

Curtain wall is one of the commonly used building envelopes in office buildings. An important element of curtain walls is the glazing portion. The aesthetic effect offered by a high portion of glazing in curtain walls is popular for most of office building design. While the glazing units provide the same functions as the rest of the curtain walls such as insulation, glazing units also allow daylight and solar heat gains to pass through, which can help offset lighting and heating energy demand of the perimeter zone. Despite the aesthetic and the energy benefits, glazing units are typically the worst insulation compared to the spandrel part of the curtain walls and are subjected to high unwanted solar heat gain during warm periods and high heat loss during cold periods. Therefore glazing units have a significant impact on the heating, cooling, and lighting energy demand of the perimeter zone. Given the typical large glazing area in curtain walls and the relatively low thermal performance of metal and glass, the energy consumption of buildings with curtain walls, especially the perimeter zone, is more sensitive to the climatic conditions and the variation of façade design (Poirazis et al., 2008) and less sensitive to the occupancy usage (Hoes et al., 2009) compared to buildings with opaque insulated façade. To reduce the energy consumption of office buildings, it is necessary to have careful design of the curtain wall configurations.

The advancement of technologies in the thermal and optic properties of glazing can help improve the overall performance of curtain walls. Many high performance curtain walls can be achieved by integrating advanced glazing units, better insulated mullion and applying shading and daylighting control strategies (Jelle et al., 2012; Dussault et al., 2012; Ge, 2002; West, 2001; Kim & Kim, 2010; Lee & Tavil, 2007; Geoffrey et al., 2007; Tzempelikos & Athienitis, 2007; Nielsen et al., 2011; Shen & Tzempelikos, 2012; Silva et al., 2012). The significance of different energy saving measures for curtain walls is altered by the interaction among the parameters which affect the building performance. Carmody et al., (2004) compared the annual energy consumption of a perimeter office space and a school classroom located in Chicago with six different window systems. Due to a higher internal heat gain generated by computers in the office space in comparison to the school classroom, a lower SHGC (0.27 v.s.0.34) resulted in slightly greater

energy savings in the office space. The results indicated that to reduce the energy consumption of perimeter zones through effective curtain walls design, the design process should be able to take into account both the individual impact and the combined impact of variables, such as façade design parameters, climatic conditions and the building operation parameters.

With the high solar potential in cold climate zone and the advancements in curtain wall component to enhance the thermal properties, curtain walls integrated with photovoltaic modules are highly possible to become "plus-energy" curtain walls for NZEB. The "plus-energy" curtain wall is defined as a curtain wall with energy generation on the façade exceeds energy consumption of the perimeter zone of buildings enclosed by the façade. The key is to minimize energy consumption and maximize energy generation by proper façade design.

1.2 Motivation

Most of building design solutions can be identified by optimization process. The state of the art of simulation-based building performance optimization has been summarized in the study (Attia et al., 2013). Although optimization is capable of figuring out a proper "plus-energy" curtain walls design, it still remains a research subject and has yet to evolve into common industry practice due to the lack of expertise in properly carrying out optimization process (Roy et al., 2008). Simulation-based building performance optimization tools can identify the optimal parameter values for the best performance under the studied conditions, but optimal parameter values do not hold true when the studied conditions change. Repeated analyses of the simulation under new studied conditions are necessary to seek new sets of optimal parameters values. An optimum solution is a point in the search-space that satisfies an optimality condition. The design variables determine the search-space. Design variables can be quantitative such as temperature or U-values and qualitative such as aesthetics. In the optimization process, the quantitative design variables are given a minimum and maximum value, are called the bounds of the variable. Therefore the effectiveness in searching the optimal solutions is controlled by the bounds of the variables. However, the results from simulation-optimization tools cannot provide the insights of how much the performance deteriorate or improve due to the alterations of design parameters. Furthermore, the quantification of specific improvement or deterioration due to alterations of design values is not consistent, specific improvement appeared to be significant under prescribed conditions may not appear to be

significant under other conditions. To quantify the efficacy of specific improvement, it is necessary to investigate the impact of specific improvement within the bounds of the variables.

To study the individual impact of curtain wall design parameters on the building energy performance, parametric analysis of different fenestration configurations can be employed (CIBSE, 2004; Hausladen, 2008). The impact of design parameters is studied by generating many potential design alternatives and comparing their impact on the building energy performance. The process can be a valuable tool to assess the performance of different curtain wall configurations at early stages, however, the exploration of the design space cannot be complete, that is, not all the potential design alternatives can be extracted and therefore, it is impossible to determine the optimum solution. With the increasing number and complexity of design options, evaluating the impact of individual building parameters on building energy performance becomes more arduous by solely parametric analysis. The process becomes time-consuming and requires high computational cost. In addition, parametric study cannot capture the complex interaction among all the design parameters. Hence, to effectively apprehend the impact of parameters, a different approach should be sought.

Proper “plus-energy” curtain wall design at the early design stage is critical to achieve NZEB. Curtain wall design parameters, such as window wall ratio (WWR), types of glazing units, types of spandrel panels, types of mullions, configurations of PV modules, are involved in the design process, while other building parameters, such as building form, orientations, mechanical and electrical systems and occupancy usage pattern are not yet confirmed at the early design stage. Currently there is no systematic methodology for performing the analysis to quantify the impact of curtain wall designs on the energy consumption of the perimeter zone, or to quantify the influence of specific curtain wall design parameters on the building energy performance. A general integrated methodology that could provide curtain wall designers with a process and guidelines for selection of curtain walls properties without case by case evaluation is necessary.

1.3 Objectives and scope

The objective of this study are:

- To develop a methodology to quantify the impact of curtain wall's design variations on the energy performance of the perimeter zone of curtain wall buildings;
- To quantify the impact of particular façade design parameters on the energy performance of the perimeter zone of curtain wall buildings;
- To develop a methodology to identify curtain wall configurations that can achieve energy balance in the perimeter zone of buildings in cold climates;
- To develop general design recommendation on the "plus-energy" curtain walls that can be used at the conceptual design stage.

The developed design methodology to identify plus-energy curtain wall configurations was applied in highly energy efficient office buildings in the cold climate. Although some of the criteria used for selecting design options can be similar to the other types of commercial buildings with curtain wall façades such as hotels and institutions, the developed methodology was not intended to those commercial buildings which have different mechanical and electrical systems, occupant pattern and indoor condition requirements. There may exist variations in the resultant configurations of "plus-energy" curtain walls when the developed methodology is employed in other types of commercial buildings.

The generic energy model used in this study is a 4m (Length) x 4m (Width) x 3.6m (Depth) typical office unit in perimeter zone. It is modeled in the whole building performance simulation tool, EnergyPlus (DOE, 2013a; DOE, 2013b). This generic energy model, known as "Perimeter Zone Optimization Method" (ASHRAE, 2011a) is simulated in a series of permutations on different "Plus-energy "curtain walls configurations. This method provides consistent results between early design stage and the whole-building energy modeling at later construction stage.

Finally, this study is not intended to produce a database of office building energy consumption. The generated results of energy consumption are not intended for the comparison of energy performance of perimeter office spaces. Instead, this work aims to provide a methodology for evaluating the impact of varying curtain wall configurations, assessing the influence of individual

curtain wall design parameters, and developing the recommendations on selecting the configurations of "plus-energy" curtain walls at the early design stage.

1.4 Outline of the thesis

Chapter 2 presents a review of related literature. The state of the art curtain wall components and photovoltaic technologies are presented. Methods for identifying configurations of "plus-energy" curtain walls are discussed. Methods for quantifying the impact of varying configurations and the influence of individual curtain wall design parameters are discussed. The need for investigating the impact is justified and limitations of using existing tools are analyzed, followed by the identification of research needs.

Chapter 3 presents the developed methodology. The workflow of performing iterative simulation for design is discussed and theoretical basis for the methodology is presented. The detailed description of sampling procedure is provided. By investigating the combined impact of design parameters, a means for selecting specific design solutions is provided. The configurations of "plus-energy" curtain walls is identified.

The uncertainty and sensitivity results of the proposed methodology for perimeter zone of office buildings in Montreal are presented in Chapter 4. Different design solutions for the "plus-energy" curtain walls are given. Finally, recommendation of designing "plus-energy" curtain walls is presented.

Chapter 5 demonstrates a new design tool which is developed from the database of the simulation results.

Chapter 6 provides a conclusion of the study, presents its limitation on applications, and identifies the future research opportunities.

Chapter 2 Literature review

While curtain walls have the advantages of providing occupants with better visual connection between indoor space and outdoor environment, they often introduce greater heat loss and cold draft compared to well-insulated opaque envelopes (Ge, 2002). The large area of glazing and the metal mullion bear much of the blame. However, from the energy point of view, the large portion of glazing area could become beneficial by introducing solar heat gain and daylight indoors. A high performance curtain wall system is expected to harvest passive and active solar energy and to lower artificial lighting demand. Over recent decades, a lot research effort was made to improve the performance of curtain walls in terms of thermal, optical and energy aspects. The "plus-energy" curtain wall is defined as the energy generated by the curtain wall façade exceeds the energy consumption of a perimeter zone office enclosed by this curtain wall façade. Building Integrated Photovoltaic Panels (BIPV), provides means of harvesting active solar energy to facilitate the "plus-energy" curtain wall design.

Section 2.1 provides a market review of the state of the art curtain walls and photovoltaic technologies and their contribution to improving building energy performance is summarized. Efficacy of energy saving measures are discussed. A summary of optimized design of façades for different design objectives is also presented. The first section explains the importance of quantifying the impact of curtain walls design and also the impact of individual parameters.

Section 2.2 reviews different design support tools that are commonly used. Simulations programs and statistical tools are presented. This section highlights the needs of formulating a systematic workflow for designing façades.

2.1 Design aspects

2.1.1 Advancements in curtain walls

Glazing is one of the most important components of curtain walls. Improvement in thermal and optics properties of glazing can significantly improve the energy performance of curtain walls.

Multilayer glazing is the most popular commercially available glazing because of its low U-value (0.49 - 0.64 W/m^2K) (Jelle et al., 2012). Basically a gas, either argon or krypton is filled in a multilayer glazing. The multilayer glazing filled with krypton has lower U-values and krypton filled glazing enables compact gas cavity. The compact gas filling cavity reduces the overall weight of the window because thinner frames can be employed due to the reduced cavity thickness.

A similar product to multilayer glazing is suspended coated film glazing. The suspended films can be installed in between the outer and inner panes. These films are often regarded as a third or fourth glass pane in glazing units. The idea of using films instead of adopting glass panes not only reduces the overall weight of the window but also allows a larger gas cavity thickness in the same volume of window cavity as ordinary multilayer glazing because the films are normally thinner than glass panes. The U-values can range from 0.28 – 0.62 W/m^2K (Jelle et al., 2012).

Vacuum glazing units also offer thinner overall thickness of glazing unit. Basically vacuum glazing units consists of double panes with a narrow vacuum space. An array of support pillars in the vacuum space is used to separate the two panes and keep the two panes evenly apart. Low-e coated glass panes can be adopted in the vacuum glazing unit to produce glazing units with very low U-values ($0.7W/m^2K$). However, compared to low-e triple glazing units, the thickness of vacuum glazing units can be almost half of that of low-e triple glazing units.

The previous research shows that the trend of improvement in glazing units is mainly to reduce the U-value because highly glazed curtain walls are commonly used. In cold climate zone, glazing units with high solar heat gain coefficient are also popular since such glazing units can provide the energy benefit in heating energy consumption in perimeter zone of buildings in winter. However, glazing units with low U-values always come along with low solar heat gain coefficient (Manz & Menti, 2012). Figure 2.1 shows the U-values and solar heat gain coefficients of different glazing units. The single glazing units have relatively high U-values and high solar heat gain coefficients while the triple glazing units have relatively low U-values and low solar heat gain coefficients. The graph indicates that glazing units with higher U-values have higher solar heat gain coefficients or glazing units with lower U-values have lower solar heat gain coefficients. Glazing units with low U-values and high solar heat gain are rarely available in the current market. At first glance, installing glazing units with high solar heat gain is an obvious choice in heating dominated areas.

However, with the high cooling energy consumption and high peak cooling loads during hot summer afternoons in buildings, glazing units with lower solar heat gain coefficients also provide the benefits in reducing cooling energy consumptions. It is always challenging to choose glazing units with higher solar heat gain coefficients to reduce heating energy consumption in winter or glazing units with lower solar heat gain coefficient to benefits from the cooling energy reduction in summer. This will be discussed in section 2.1.3.

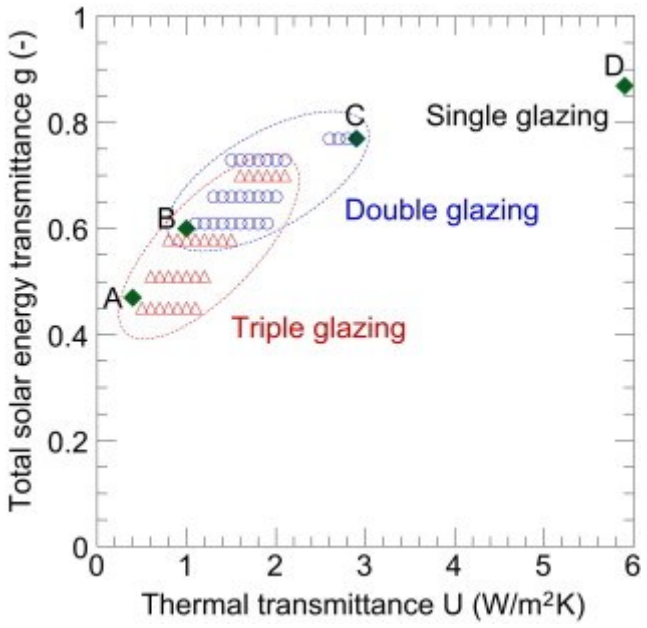

Figure 2.1. The U-value and the solar heat gain coefficient of different glazing units (Manz & Menti, 2012).

2.1.2 Advancement in solar photovoltaic technologies

Photovoltaic systems and some other renewable energy systems are excellent choices to achieve the net-zero energy building design. The major attraction of the photovoltaic systems is that the process of producing electric power brings relatively less damage to the environment, by directly converting a free source of energy, from the solar energy into electricity without any heat engine to interfere. Photovoltaic systems require relatively less maintenance. The output of photovoltaic systems can range from microwatts to megawatts. Van der Zwaan, (2003) presented current photovoltaic cell production cost ranges including the single crystalline silicon, multi-crystalline silicon, amorphous silicon and other thin film technologies according to the learning-curve

methodology. The decreasing cost of photovoltaic panels and increasing efficiency in the photovoltaic technologies imply a promising role for renewable energy systems in the building sector in the near future. Compared to the grid-tied photovoltaic systems, the price of an energy unit generated from a grid-tied photovoltaic system is much higher than that from off-grid photovoltaic system (Singh, 2013).

The basis of the photovoltaic effect is to convert lighting energy into electricity in solar cells. The light absorbing materials in all solar cells absorb photons and generate free electrons via the photovoltaic effect. The sunlight striking on the photovoltaic cells imparts the energy to some negatively charged electrons to raise their energy level and thus the electrons become mobile. Voltage is created by a built-in-potential barrier in the cell, and the voltage is used to drive a current through a circuit.

Silicon is the dominant material for the supply of power modules into photovoltaic applications. The proportion of silicon in multi-crystalline silicon and monocrystalline silicon is currently increasing to produce high-efficiency solar cells.

Amorphous (uncrystallized) silicon is one of the most popular materials in thin-film technology. Amorphous silicon can produce the cell efficiencies of 5-7% and the double and triple junction designs of amorphous silicon cell can have cell efficiencies up to 8-10%. However, the amorphous silicon cell are prone to degradation. The varieties of amorphous silicon are amorphous silicon carbide, amorphous silicon germanium, microcrystalline silicon, and amorphous silicon-nitride (a-SiN).

Yang et al., (2003) summarized the development and the advantages of amorphous-silicon photovoltaic technology. The essence of the roll-to-roll manufacturing process and the advantages of solar panels on flexible substrates are discussed. The cell efficiency can be achieved to 13%. Tawada & Yamagishi, (2001) developed a series of production technologies for stable 8% efficiency direct-super-straight-type modules along with large area monolithic amorphous-silicon pin single-junction cell on glass substrate. The modules are proved by the detailed designing, actual installation and the performance evaluation to be suitable for roofing purpose. Figure 2.2 shows the photovoltaic cell made from amorphous (uncrystallized) silicon.

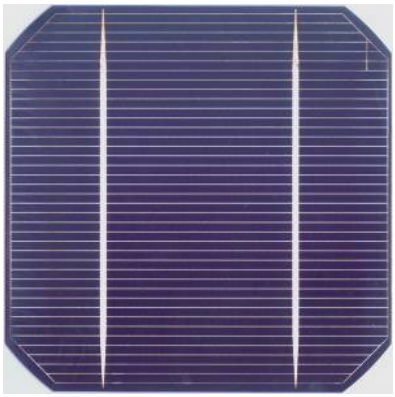

Figure 2.2. A photovoltaic cell made from amorphous (uncrystallized) silicon. Source: www.pveducation.org

Polycrystalline silicon photovoltaic cell are produced from cast square ingots which is made from being cooled and solidified large blocks of molten silicon. Compared to single crystal silicon cells, polycrystalline silicon photovoltaic cells are normally less expensive to produce than, but are usually less efficient. They often come on larger frames than the monocrystalline. Crystalline silicon provides higher cell efficiency when compared to amorphous silicon cell, however, only a small amount of material is used. The commercially available polycrystalline silicon solar cells can achieve an efficiency around 14-19% (Parida et al., 2011). Polycrystalline silicon thin film solar cells are cost-effective among the solar cell production technologies and they retain the advantages of thin film technology and crystalline silicon. Figure 2.3 shows the photovoltaic cell made from amorphous (polycrystalline) silicon.

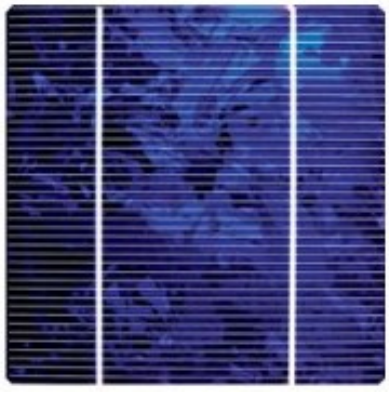

Figure 2.3. The photovoltaic cell made from amorphous (polycrystalline) silicon. Source: http://www.solarpanelbuyersguide.co.uk

Thin-film solar cells are basically thin layers of semiconductor materials applied to a solid backing material. Thin films solar cells play an important role in photovoltaic market because the thin films technology can reduce the amount of semiconductor material required for each cell when compared to silicon wafers and hence lowers the cost of production of solar cells. Gallium arsenide, copper, cadmium telluride indium di-selenide and titanium dioxide are those materials that have been mostly used for thin film photovoltaic cells. However, a primarily unavoidable drawback of a thin-film solar cell is its poor optical absorption, which is caused by the thinner active layer and limits the power conversion efficiency of this type of solar cells. Temperature affects the performance of thin-film solar cells through two possible approaches: one is affecting the optical and electrical parameters of semiconductor material and the other is altering the geometric parameters of the structures. To increase the optical absorption, different light trapping technologies have been extensively used to enhance the light absorption. Barnett et al., (2001) investigated that solar cells utilizing thin-film polycrystalline silicon can achieve photovoltaic power conversion efficiencies greater than 19% as a result of light trapping and back surface passivation with optimum silicon thickness.

Figure 2.4. The photovoltaic cell made from thin-film. Source: http://topdiysolarpanels.com

The previous research shows that the trend of improvement in solar photovoltaic technology is mainly changing the types of materials composited the cell in order to increase the cell efficiency. Since the energy yield from the photovoltaic array depends on not only the cell efficiency of the photovoltaic panels, but also the wiring of the cells, the array pattern, the inclination of the arrays and the outdoor conditions. The evaluation of potential yield from the photovoltaic panels in this study is based on the effective efficiency of the whole array. This is discussed in the chapter 3.

2.1.3 Efficacy of energy saving measures

A lot of research has been carried out on the energy performance of fenestration (Manz & Menti, 2012; Chaiyapinunt et al., 2005; T. R. Nielsen et al., 2000; Chow et al., 2010). Manz & Menti, (2012) compared the energy flow of four types of glazing, four façade orientations in eight case study locations in Europe namely Bucharest, London, Madrid, Moscow, Rome, Stockholm, Warsaw and Zurich. The result showed that modern triple glazings perform the best and enable net energy gains at south façades in December even in Moscow and Stockholm.

Chaiyapinunt et al.,(2005) studied different types of windows with clear glass, tinted glass, reflective glass, double pane glass, and low-e glass in the aspect of heat flow. The analysis indicated that the values of heat gain due to solar radiation effect were larger than the values of heat gain due to conduction effect for all glass windows and glass windows with films. Adhered film to the glass windows resulted in lowering the heat gain due to solar radiation in the amount corresponding to the film properties. However, the film shows little effect on the relative heat gain due to conduction. The heat gain values were varied linearly with the total transmittances of the glass windows with and without films. The relative heat gain values were also varied inversely with the absorptance of glass windows with and without with films linearly.

Nielsen et al., (2000) simplified the comparison of the energy performance of different glazing because it is difficult to select the glazings or windows in terms of energy performance in a particular case without detailed evaluation. A number of diagrams were produced to provide the net energy gain with respect to the orientation, the tilt, the U-value and the solar heat gain factor of the glazing or windows. A single diagram showing the net energy gain in a one-family house was produced according to the orientation of the windows in the building. By using the diagrams the best glazings can be chosen in particular case.

Chow et al., (2010) introduced the concept of water-flow window and their potential areas of application were discussed. Their research showed that this new design was able to support hot water supply system, reduced air-conditioning load and enhanced thermal and visual comfort.

Lee, (2010) compared the trade-off in different façades design options by examining the impact of typical and high performance windows on the energy performance of perimeter offices in a high-

rise commercial building located in Southern Ontario. His results showed that window properties had insignificant impact on the building energy performance of the perimeter zone with high internal heat gain. Windows with low U-values and high solar heat gain coefficient (SHGC) were preferred over the windows with similar U-values but low SHGC. Low U-values contributed to a significant energy saving in commercial buildings with mid to low internal heat gain in all window wall ratio. Static and dynamic shading had very little effect on energy performance of mid to low internal heat gain offices.

Previous research focused on comparing the energy performance of different fenestration technologies, however, the impact of the geometrical and thermophysical characteristics of fenestration on the energy demand of buildings under different conditions has neither been thoroughly analyzed, nor quantified. Without a quantification scheme, it is always difficult for the façade designers to choose a fenestration product among the wide variety of technologies.

2.1.4 Optimized design of façades

In the study by Thalfeldt et al., (2013), the design parameters of curtain walls influencing the energy performance of a building, such as window type, wall insulation, window wall ratio and shading devices were optimized in the case of a generic office floor model for the lowest life cycle cost and alternatively for the best achievable energy performance. The results show that the window sizes resulting in the best energy performance for double and triple glazing were 22 and 24% respectively as small as daylight requirements allowed. For quadruple and hypothetical quintuple glazing, the optimal window-to-wall ratios were larger, about 40% and 60% respectively, because of daylight utilization and better solar factor naturally provided by multi panes. The cost optimal façade solution was highly transparent triple low emissivity glazing with window-to-wall ratios of about 25% and external wall insulation thickness of 200 mm (U = 0.16W/m^{2}K).

Kasinalis et al., (2014) presents a method for quantifying the impact of seasonal façade adaptation on building performance, based on coupled building energy and daylight simulations, which were conducted under multi-objective optimization scenarios with genetic algorithms with respect to the building energy performance and the indoor environmental quality. Window wall ratio as well

as thermophysical and optical material properties were determined by optimization. The results showed that a south facing office zone with a monthly adaptive façade in the Dutch climate can have up to 15% energy savings and largely improve thermal comfort requirements in comparison with the best performing non-adaptive façade.

Previous research shows the challenges of the optimization, which requires high computational time for the façade designers to undergo iterative optimization process before obtaining the direction of the design trend. The optimization approach requires comprehensive knowledge of what needs to be optimized and what algorithm needs to be adopted. Another issue is that the resulting optimized design solutions only work for the defined design objectives. If a design objective is changed or more additional objectives are the subject of interest, then another vigorous optimization process has to be performed.

2.1.5 Summary

Based on the previous research, curtain walls theoretically have high potential to act as a positive energy source for buildings when they are integrated with photovoltaic technology. In reality, the selection of design options that strikes the balance between energy harvesting and energy conservation increases the complexity in decision making among a wide variety of design options. Therefore, it is necessary to seek the design trend without undergoing the repeated case-by case simulation or iterative optimization process.

2.2 Design support tools

2.2.1 Curtain wall performance simulations

With the large portion of glazing in curtain walls, the selection of assessment method of glazing performance becomes critical. The pre-evaluation of glazing unit designs with the help of simulation programs can facilitate identifying more energy efficient options.

Most of the building energy performance simulation programs, such as EnergyPlus, ESP-r and TRNSYS, provide different approaches to model glazing portion in fenestration. Those approaches allow different ways to specify the glazing properties and present different restrictions on certain

configurations of glazing units. All approaches differ in terms of level of detail and applicability. Detailed models require a considerable amount of detailed information as the input parameters. Increasing the level of detail increases the difficulty in performing the simulations. Decreasing the level of details degrades the model fidelity, which may lead to greater uncertainty in the modelling results.

An appropriate modelling approach should be able to reproduce predictions which fit with the experimental data regardless of unforeseen errors and uncertainties (Van Buren et al., 2014); however, the norm tends to steer the approach selection towards the detailed approach which fits better with the experimental data. The approach selection strategy loses ground when the experimental data is not available at the early design phase.

One previous study by Peter et al., (2010) compared the discrepancies in the predicted energy consumption by using different glazing modeling approaches. They concluded that the energy consumption predicted using the Simple Window Model, in which simplified window performance indices including U-value of glazing (U_{gl}), solar heat gain coefficient (SHGC), and the optional input, visible transmittance (Tv), are used to specify the glazing properties, agreed well with the results from the Full Spectral Method, which is the only recommended model in EnergyPlus (DOE, 2013b; DOE, 2013a). Due to lack of literature support, users typically choose the glazing modeling approach based on subjective judgement or the availability of input parameters.

One study by Lam et al., (2013) discussed the advantages and limitations of each glazing modelling approach and suggested selecting an appropriate approach based on three criteria: computational cost, ability to reproduce consistent results and uncertainty. The paper concluded that the Average Spectral Method, in which the transmittance and reflectance of glazing are weighted over the spectrum, can produce consistent results as the Full Spectral Method. In this study, Simple Window Model is found to have higher variation in predicting the cooling and the total energy consumptions.

It is clear that there is no specific glazing modeling approach that is absolutely superior to others. All methods have their own requirements in terms of the level of expertise manipulating those programs, the key assumptions and the limitations.

2.2.2 Building performance simulation

The building energy performance simulation tools do not take into account all the complex interactions of energy transfer such as thermal bridge within a building system, however, by comparing the performance indices that the user specified, the designers can still make decision based on the performance.

Computer simulations are also able to provide inexpensive and quick results that allow designers and researchers to easily make changes to the building design and compare the relative differences in performance, making them suitable tools for design and research. While full field tests or experiments may provide better results, they are often very expensive and time intensive. Many of these building simulation programs are developed with validation from laboratory measurements. With the advancement of computer technology and further understanding of energy transfer in buildings, building simulation programs continue to evolve and improve with greater accuracy, making them ideal for such applications. In the past, designers and researchers have used computer programs such as EnergyPlus, ESP-r, and TRNSYS. Crawley et al., 2008 provide a comprehensive comparison of the features and capabilities of twenty major building energy simulation programs.

EnergyPlus is an energy analysis and thermal load simulation program. Based on a user's description of a building from the perspective of the building construction, associated mechanical systems, etc., EnergyPlus developed from two programs BLAST (Building Loads Analysis and System Thermodynamics) and DOE-2 programs in 1996 by Department of Energy (DOE) from the United States of America (USA). There is no user interface in EnergyPlus. It is a simulation engine in which the inputs and outputs are in simple ASCII text format. EnergyPlus allows external GUI (graphical user interface) such as Sketchup, AutoCAD for building geometry and Simergy for HVAC mechanical systems.

ESP-r is another building performance simulation. ESP-r uses a finite volume conservation approach in which all problems with inputs (specified in terms of geometry, construction,

operation, leakage distribution, etc.) are converted into a set of conservation equations (for energy, mass, momentum, etc.), which are then integrated at successive time-steps in response to climate, occupant and control system influences. ESP-r comprises a central Project Manager and the support databases, a simulator, various performance assessment tools and a variety of third party applications for CAD, visualisation and report generation.

TRNSYS is made up of two parts. The first is an engine (called the kernel) that reads and processes the input file, iteratively solves the system, determines the convergence, and plots system variables. The kernel provides the functions that determine thermophysical properties of building materials, invert matrices, perform linear regressions, and interpolate external data files. The second part of TRNSYS is an extensive library of components for building systems performances. The standard library includes approximately 150 models such as building system components, wind turbines, weather data, basic HVAC equipment, some cutting edge emerging technologies and also some multizone building examples. Users can modify existing components or create their own, or extend the capabilities of the simulated scenarios.

In fact, building simulation models can accurately quantify building energy loads, but are not amenable to the early design stages when architects need an assessment tool that can provide rapid feedback by altering the design parameters.

2.2.3 Application of cloud simulation

OpenStudio is a free, open source Software Development Kit (SDK) and application suite to conduct building energy modeling and analysis. The OpenStudio Parametric Analysis Tool (PAT) was extended to allow cloud-based simulation for iterative parametric study. Multiple building parameters can be varied over multiple iterations to model simulation results, as calculated and visualized in the GUI. Simulations are performed in parallel using the Amazon Elastic Compute Cloud service. OpenStudio highlights model measures used for parametric study and design optimizations.

The cloud supplements the manual process with more automated, optimization-based processes that are used with data visualization to help modelers have fast comparison of results whose impacts on the model are visualised in GUI.

2.2.4 Application of parametric study

The influence of particular parameters and their interacting effects among them is not easily determined unless full design space exploration is investigated. The number of design options is enlarged by vast number of design parameters. Identifying the design alternatives can be achieved by parametric study or comparing the outcomes. Typically, parametric study is performed by one-at-a-time method, it can never cover the entre design parameter range. Any design options identified by the parametric study can be only valid for the investigated range of parameters. The process involves high computational cost. Especially, evaluating all design options with large number of design parameters is not a viable approach.

2.2.5 Application of optimization

Façade design is quite a complicated task with the design team trying to counterbalance various antagonistic parameters, which in turn are subject to various constraints and design objectives. Simulation-optimization tool is an efficient way to seek the design options with global minima or maxima with the help of appropriate optimal algorithm subject to a number of constraints. Design options are sought by the building performance simulation programs integrated with optimization methods which act as a decision aid. Summary of building design optimization methods is conducted to explain the selection of optimization algorithms (Machairas et al., 2014).

Most of the building design problems face the difficulties in decision making, which are in fact multi-objective optimization problems, characterized by the existence of multiple and competing objectives. The methods for solving multi-objective optimization problems are (1) enumerative algorithms, (2) deterministic algorithms, and (3) stochastic algorithms. Limitations of different algorithms are discussed (Attia et al., 2013). Since the building simulations can sometimes be time-consuming, abundant research are focusing on investigation of boosting rapid optimal solutions. The best optimal design options are not always guaranteed to be found by any one of these algorithms. The optimal solutions obtained from the optimization methods are often showed in the decision space, which consists of a set of feasible solutions that are not predefined but are implicitly defined by a set of parameters and constraints that should be taken into account, however, the interdependent relationship among the parameters are not explicitly indicated. Due

to the lack of information of interdependent relationship, it is difficult to compare the near-optimal design options.

Simulation-optimization tools identify the optimal parameter values for best performance under the prescribed conditions, but optimal parameter values do not hold true when the prescribed conditions changes. Repeated analyses of the simulation with new prescribed conditions are necessary for seeking new sets of optimal parameters values. The results from simulation-optimization tools cannot provide the insight of how much the performance deterioration or improvement due to the ad hoc changes to the design parameters. Furthermore, the performance of specific improvement or deterioration due to the ad hoc changes to design values does not keep consistent, specific improvement appeared to be significant under prescribed conditions may not appear to be significant under other conditions. To quantify the efficacy of specific improvements, it is necessary to ensure the complete design space exploration such that the impact of specific improvements are investigated.

2.2.6 Application of sensitivity analysis

Sensitivity analysis has long been used to derive diagnostic insights from building performance models by identifying the key input factors controlling building performance (Tian, 2013). It helps to identify the influence of input parameters in relation to the outputs. It can also be used as a tool to understand the behavior of the model and can then facilitate its development. Their applications include the following (Saltelli et al., 2008; Spitz et al., 2012).

Implication of model quality - Sensitivity analysis indicates the appropriate setting of the base model. For example, dramatic discrepancy may occur in output variables when one influential input is kept at fixed values in the model and the influential input is changed to another value. Such information is important when the computational cost is high.

Factor fixing - A fixed value can be assigned to the insensitive inputs for simplifying the optimization problems.

Factor mapping- The regions of the whole input space where a particular input is most sensitive are identified.

Factor prioritization - The input parameters are ranked according to their importance.

Increase the robustness of the model - The output uncertainty is minimized when the uncertainty of the influential parameters are reduced.

Investigation of interaction between parameters - Influential parameters can be attested as important in local sensitivity analyse but it may appear to be non-influential when their effect are cancelled by the effect of other parameters. The cancellation occurs when the influence of parameters is not superimpose together.

The methods for sensitivity analyses can be classified into screening methods, local and global methods.

Screening methods is OAT approach (one parameter at each time) in which each design parameters is evaluated individually. The standard values of the design parameters are used as control. Two extreme values on both sides of standard values of the individual design parameters are chosen such that the different results from the control and the two extreme values are compared. The larger the range of difference, the more sensitive.

The local method, OAT approach, also evaluates the variability of the model output by one changing parameter and keeping the other parameters fixed at a nominal value. Local methods provide the sensitivity indices of parameters relative to a single point (or base case) in the multivariate space of a model. The interaction effect between the design parameters is isolated. Therefore local sensitivity analysis does not quantify the influence of individual parameters under the changing impact by other parameters. Local sensitivity analysis cannot measure the interaction among the parameters.

Global methods can evaluate the importance of a parameter throughout the entire multivariate space of a model. The global method is regarded as a more superior method. There are many techniques in global methods, include sampling-based methods such as Partial Correlation Coefficients (PCC), Standardized Regression Coefficient (SRC), Reliability algorithms such as First-Order Reliability Method (FORM) and Second-Order Reliability Method (SORM), and variance-based methods.

The variance-based methods are the analysis of variance, known as ANOVA (Archer et al., 1997), such as Sobol', First Amplitude Sensitivity Test (FAST) (Saltelli et al., 2000) and later extended-FAST. The ANOVA is to portion the variance of an output over the different input variables. Two attractions of ANOVA are to provide quantitative insight of (1) the contributions of design parameters to the variation of building energy performance (2) the interacting effects among the design parameters on the variation of output. Therefore the sensitivity of individual design parameters can be prioritized.

Parameters are concluded to be significant according to its ability to contribute large variation in outputs. Parameters are altering the variation in outputs by two ways. (1) large possible range in which the input parameter is propagated throughout all the model evaluations; (2) output results are highly correlated to the parameters so slightly alternating the input values result in major variation in the output values. There is difference between "importance" and "sensitivity", important parameters are always sensitive so that important parameters can produce large variations in outputs. Sensitive parameters are defined as parameters that can produce significant variation in outputs for small alternations in inputs (Hamby, 1994), but sensitive parameters are not always important. In the case of sensitive parameters with small possible range throughout all model evaluations may not easily detected in the output variation. Therefore the range and distribution pattern affect the sensitivity results and they are defined with great care in order to ensure the reliability of the resulted sensitivity index.

The first step of conducting global sensitivity analysis is sampling. There are various sampling procedures that are commonly used. They are (i) random sampling, (ii) stratified sampling and (iii) quasi-random sampling. The selection of the sampling procedures is subjected to the types of global sensitivity analysis to be implemented, nature of parameters, computational cost and accuracy. Table 2.1 shows the comparison of these three methods.

In random sampling, random numbers are generated. In stratified sampling, the sample space of input parameters is partitioned into N disjoint strata. One particular stratified sampling method, Latin hypercube sampling, is widely used in the global sensitivity analysis. Various types of quasi-random samplings were reviewed by (Bratley & Fox, 1988). The superiority of quasi-random

samplings is due to its enhanced rate of convergence. Table 2.1 lists the advantages and disadvantages of three sampling methods.

Table 2.1. Comparison of three sampling methods.

	Advantages	**Disadvantages**
Random sampling	• produce unbiased mean and variance • suitable for large sample size • easy to implement	• clumps of samples in certain regions • poor representation for small samples • not suitable for model with high computational cost
Stratified sampling	• better coverage of sample space • produce unbiased means and distribution function for LHS • suitable for situations that large samples are not computational feasible	• convergent rate of $1/\sqrt{N}$
Quasi-random sampling	• suitable for large samples are not computational feasible • Sobol' sequence are suitable for monotonic relationship • fewer simulations are needed	

2.2.7 Application of uncertainty analysis

As discussed in the previous section, the sensitivity analysis can quantify the contribution of individual parameters to the variation of the models, in other words, the sensitivity analysis quantify the impact of individual parameters on the studied systems.

Uncertainty analysis can quantify the variation of outputs due to the variation of input parameter set, in other words, the uncertainty analysis quantify the impact of whole set of input parameters on the models. The larger the variation, the more significant the whole set of input parameters.

The application of uncertainty analysis in this study is different from the common application in engineering systems. In general application, the term "uncertainty "defined as the lack of perfect information concerning the phenomena, process, or the resulted data.

Uncertainty can be broadly divided into two groups, epistemic uncertainty and aleatory uncertainty.

The word aleatory derives from the Latin alea, which means the rolling of dice. Thus, an aleatory uncertainty is one that is presumed to be the intrinsic randomness of a phenomenon. Interestingly, the word is also used in the context of music, film and other arts, where a randomness or improvisation in the performance is implied.

The word epistemic derives from the Greek επιστημη (episteme), which means knowledge. Thus, an epistemic uncertainty is one that is presumed as being caused by lack of knowledge (or data). The reason that it is convenient to have this distinction within an engineering analysis model is that the lack-of-knowledge-part of the uncertainty can be represented in the model by introducing auxiliary non-physical variables. These variables capture information obtained through the gathering of more data or use of more advanced scientific principles. An uttermost important point is that these auxiliary variables define statistical dependencies (correlations) in a clear and transparent way (Kiureghian & Ditlevsen, 2009).

Epistemic uncertainty refers to lack of knowledge about phenomena and usually translates into uncertainty about the parameters of a model used to describe random variation. Whereas epistemic uncertainty can be reduced, aleatory uncertainty cannot be reduced and for this reason it is sometimes called irreducible uncertainty (Helton & Burmaster, 1996). Table 2.3 summarizes two types of uncertainty, epistemic uncertainty and aleatory uncertainty (Apostolakis, 1990; Hanna, 1993).

Table 2.2. Summary of two types of uncertainty, epistemic uncertainty and aleatory uncertainty.

Epistemic	Aleatory
• Subjective probability function • Knowledge-related • Reducible • Lack of knowledge about the phenomenon • Lack of data	• Limiting relative frequency probability • Stochastic • Irreducible • Variation of population

Uncertainty exists when knowledge about specific factors, parameters (inputs), or models are incomplete. Models have two fundamental types of uncertainty:

Model framework uncertainty, results from the underlying assumptions and simplifications. Those assumptions and simplifications originate from mitigating the lack-of-knowledge for the complicated phenomenon interaction and reducing the computational cost. Since model formulation varies over a wide spectrum, ranging from simple empirical equation to sophisticated partial differential equations with computer simulations. A model is only an abstract of reality, which generally involves certain degrees of simplifications and idealizations. Therefore model uncertainty reflects the inability of the model to represent the system's true physical behavior.

Two types of uncertainty are associated with the model framework uncertainty. The first type results from the use of an inadequate model with correct parameter values. The second type results from the use of a perfect model with parameters subject to uncertainty.

Parameters uncertainty results from the inability to accurately quantify model inputs and parameters. All models involve physical or empirical parameters that cannot be quantified accurately. In building problems, parameters uncertainty could be caused by changes in the operation conditions of buildings in building design problems, the inherent variability of building materials properties in time and spatial domain and a lack of sufficient data.

Data uncertainty includes the measurement errors, analytical imprecision, inconsistency and non-homogeneity of data, and limited sample size during collection and treatment of the data used to characterize the model parameters.

Operational uncertainty includes those associated with the construction, manufacture, procedure, deterioration, maintenance and workmanship.

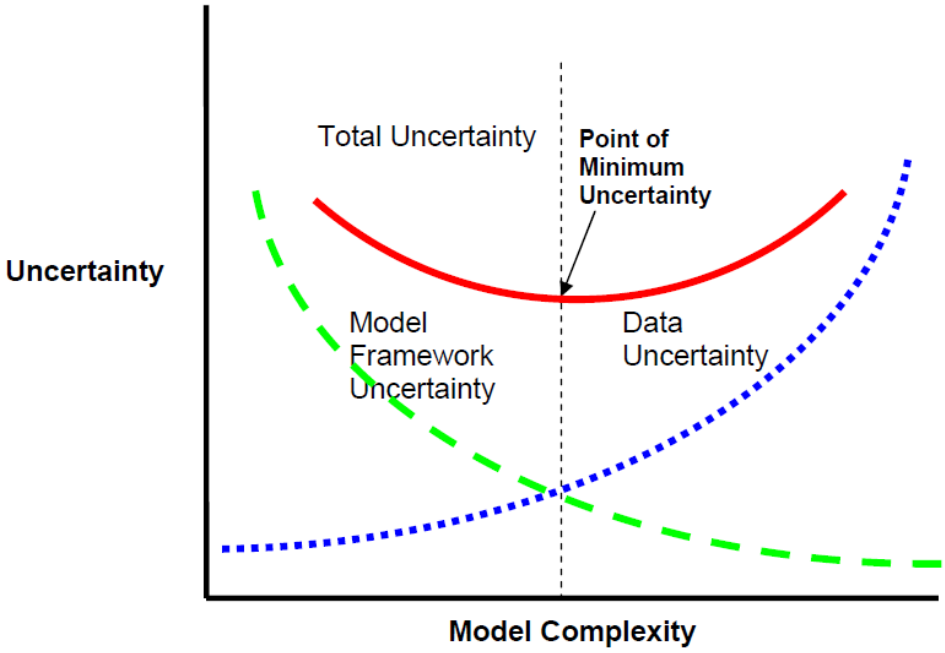

Figure 2.5. The relationship between the Data (Parameters) uncertainty and Model Uncertainty (Hanna, 1993).

These two types of uncertainty have a reciprocal relationship, with one increasing as the other decreases. Thus, as illustrated in Figure 2.5, an optimal level of complexity (the "point of minimum uncertainty") exists for every model.

All simulation programs are subjected to model uncertainty and parameter uncertainty (Macdonald, 2002). Model uncertainty is the assumption and parameter uncertainty can be physical uncertainty due to the irregularity and workmanship of building materials, can be scenario uncertainty due to variation of outdoor climate or indoor occupancy, and can be design uncertainty due to alternations in planning phases (Hopfe & Hensen, 2011).

2.2.8 Summary

In most building design problems, it is almost impossible for the designers to make decision based on a single simulation result. In some cases, iterative simulation process are involved. Early design decisions may not require a detailed simulation program to deal with mass data. It is necessary to adopt a suite of tools integrate with the simulation programs, which would support the decision making process.

2.3 Conclusion

Based on the previous research, curtain walls theoretically have high potential to act as a positive energy source for buildings when they are integrated with photovoltaic. In reality, the selection of design option that strikes the balance between energy harvesting and energy conservation increases the complexity in decision making among a wide variety of design options.

There is no single design support tool that is clearly superior to all others. Each design support tool has its own key assumptions and limitations, its own demands regarding the time and effort to apply the method and interpret the results and has strengths and limitations regarding the type of insight that it can provide.

Due to the lack of systematic approach for seeking rapid design solutions by changing design parameters, it is necessary to develop an assessment methodology to identify the configurations of "plus-energy" curtain walls.

In order to derive the design alternatives of "plus-energy" curtain walls, it is essential to investigate the impact of varying curtain walls configurations on the building energy performance in perimeter zone, the impact of individual design parameters and also the interdependency relationship among the design parameters.

Since the uncertainty analysis provides the insight of the impact of variations in inputs on the variations in outputs, it is used to investigate the impact of curtain walls configurations on the building energy performance in perimeter zone. Global sensitivity analysis assists to quantify the impact of particular inputs on the variations in outputs. It is employed to quantify the impact of

individual design parameters on energy performance. Appropriate global sensitivity analysis methods can illustrate the interdependency relationship among the design parameters.

Chapter 3 Methodology

The energy performance of the perimeter space of buildings is heavily dependent on façade configurations including the fenestration. In this chapter, the influence of curtain wall configurations and the impact of individual parameters on the energy performance of perimeter spaces of office buildings is examined. This discussion is divided into five sections: 1) work flow of the analysis; 2) input parameters and their range selected; 3) description of the generic energy model created in EnergyPlus and modeling approach; 4) sampling procedure; and 5) procedure for sensitivity analysis.

3.1. Overview of the workflow

Figure 3.1 and Figure 3.2 show the flow chart of the analysis.

1. Simlab 2.2 (Simulation Laboratory for Uncertainty and Sensitivity Analysis) (Bieda, 2010) is used to generate samples. Simlab is a software designed for Monte Carlo analysis that is based on performing multiple model evaluations with selected model inputs.
2. A generic energy model is built in EnergyPlus. The sample files are stored as text files that are input to the base model in EnergyPlus.
3. The outputs from EnergyPlus in terms of annual heating, cooling, lighting, total energy consumption and energy generation for four orientations are consolidated using Excel.
4. The dispersion of end-use energy consumption, annual heating, cooling, lighting, total energy consumption and the energy balance for four orientations indicate the impact of curtain walls configurations on the end-use energy consumption and the energy balance. The dispersions of end-use energy consumption are quantified by the coefficient of variation (i.e. the ratio of the standard deviation to the mean) using excel.
5. An open-source statistical computing program R with a customized code is used to calculate the first-order and total sensitivity index of individual design parameters (Pace, 2012). The first order sensitivity indices quantify the impact of each individual input on the variation of outputs. The total sensitivity indices quantify the total contributions of each individual input on the output variances, which include both first order and higher-order effects due to the interaction among inputs. In this study, total sensitivity indices are used to quantify the impact of parameters by taking into account of the interacting effect of design parameters.

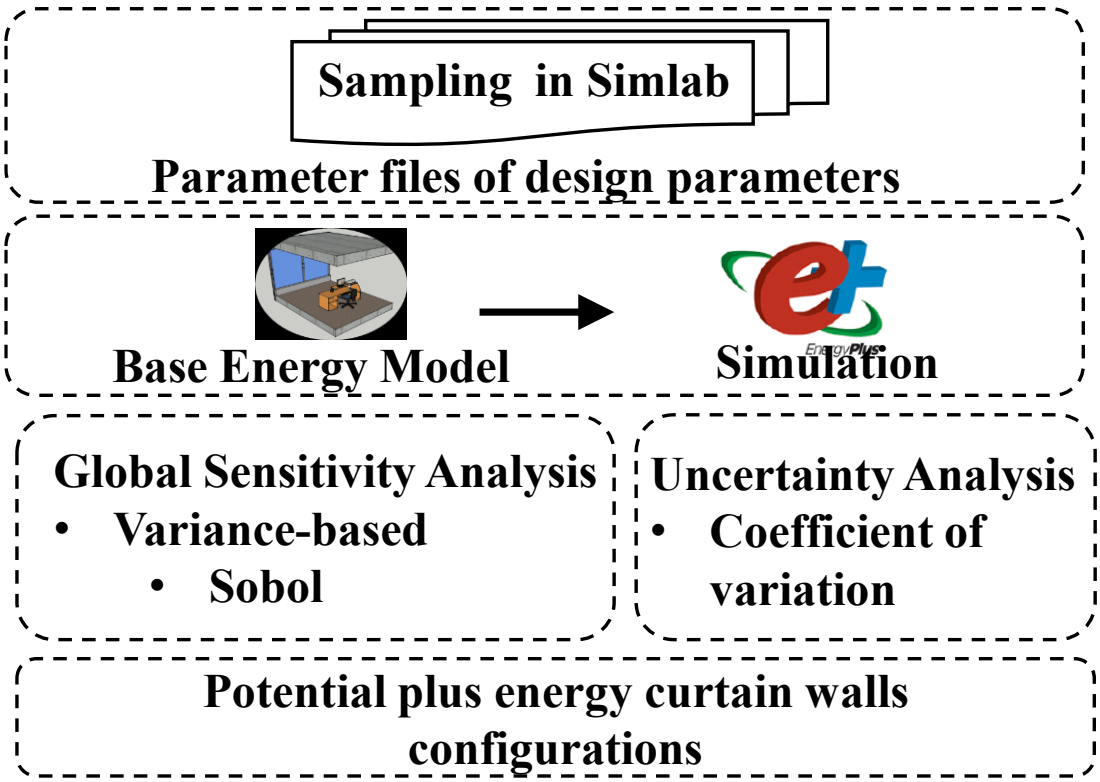

Figure 3.1. Flow chart of the analysis.

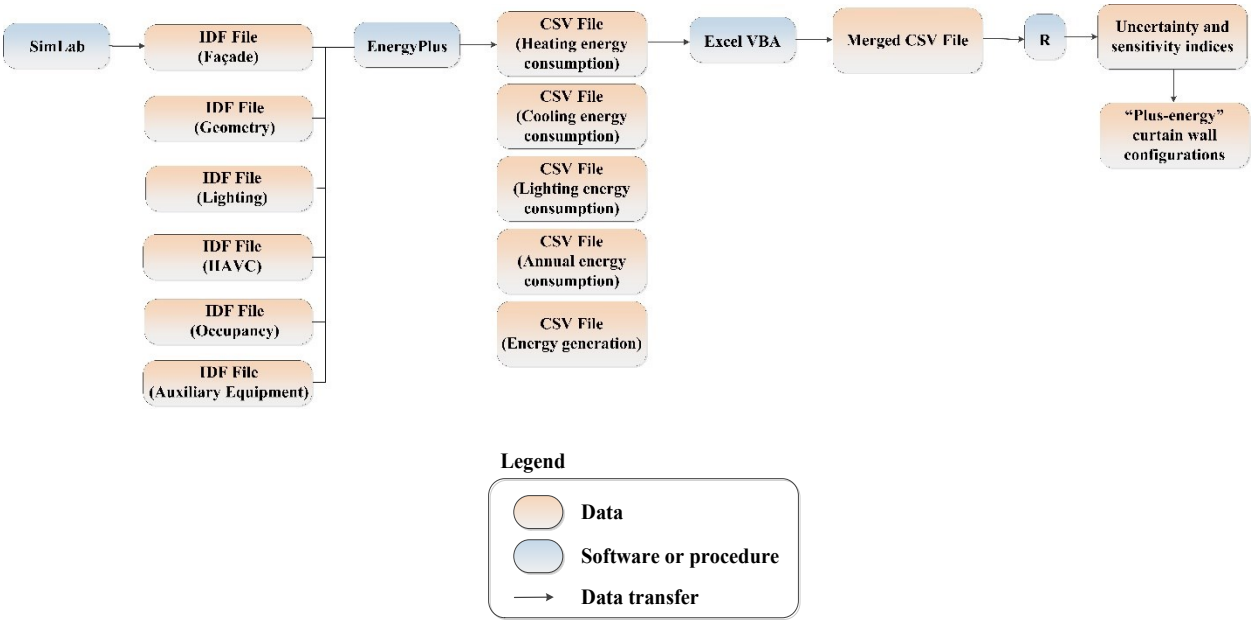

Figure 3.2. The flow chart of the analysis.

3.2. Parameters affecting the building energy performance

The evaluation of the impact of curtain wall configurations on building energy performance cannot be directly indicated by energy consumption since curtain walls are not energy consumers, however, the energy transfer processes take places through the curtain walls in buildings. As a result, the configurations of "Plus-energy" curtain walls can only be identified by comparing the building energy performance due to the variation of curtain wall configurations. The building energy performance is influenced by the factors in Table 3.1.

The selection of design parameters to be varied in the energy models is based on the subject of interests. For example, the building design problems are related to enhancing the COP of HVAC system, the user may need to select the types of systems, and the types of refrigerants as design parameters which are to be varied in order to investigate the impact of those parameters on the performance indices. In this study, the subject to be investigated is the façade curtain wall.

To run the generic energy simulation model, an extensive set of inputs such as building geometry, internal loads, outdoor environment, equipment, and occupancy schedules are required to define. For façade design, only a small subset of inputs related to the performance of façades are varied. The remaining inputs can be fixed at default values. The choice of input subsets and the associated ranges of their values determine the design space to be explored and they are summarized as in Table 3.2.

The design parameters include window wall ratio, U-value of glazing, solar heat gain coefficient, visible transmittance, U-value of spandrel panel, U-value of mullion, infiltration rate, types of shadings and PV Modules efficiency. It is obvious that façade orientation has great impact on building performance (Nielsen et al., 2011; Shen & Tzempelikos, 2012). However, the orientation is not a factor that can be fully controlled. So the analysis is performed for each main orientation in this study.

Table 3.1. The parameters affecting the building energy performance.

	Parameters
Exterior environmental parameters	• Solar radiation • Ambient temperatures • Wind direction and speed • Air humidity • Geographical locations
Building information parameters	• Orientation • Building shape • Building type
Curtain walls design parameters	• Window wall ratio • U-value of glazing • Solar heat gain coefficient • Visible transmittance • U-value of spandrel panel • U-value of mullion • Air tightness • Type of shading • PV Modules efficiency
Indoor environmental parameters	• Occupancy schedule • Occupancy consumption

3.2.1 Range and justification of design parameters

The range and distribution of the ten design parameters studied are listed in Table 3.2.

Table 3.2. The range and distribution of ten design parameters.

Design Variable	**Symbol**	**Unit**	**Distribution**	**Range**
Types of glazing		-		
i. U-value of glazing	Ugl	$W/m^2 \cdot K$	PDF	1.10 to 2.50
ii. Solar heat gain coefficient	SHGC	-	PDF	0.33 to 0.70
iii. Visible transmittance	Tv	-	PDF	0.16 to 0.79
U-Value of frame	Ufr	$W/m^2 \cdot K$	Uniform	0.80 to 8.80
U-Value of spandrel	Usp	$W/m^2 \cdot K$	Uniform	0.15 to 0.28
Window wall ratio	WWR	-	Uniform	0.10 to 0.90
Infiltration	Infil	$L/m^2 \cdot s$	Uniform	0.01 to 0.22
Depth of overhang	D_h	-	Uniform	0.10 to 1.00
Inclination of overhang	Da	degree	Uniform	0.00 to 90.0
Efficiency of modules	PV	-	Uniform	0.09 to 0.19

The three primary thermal and optic properties of glazing, U-value of glazing, solar heat gain coefficient and visible transmittance are often correlated. For example, glazing with a high solar heat gain coefficient might also have a high U-value (Figure 2.1.) Such properties are not completely independent and they cannot be combined together randomly. Given the fact that these three properties are interrelated, to assign a realistic distribution for their ranges, curtain wall products that are available in the commercial market are investigated.

In the website of National Fenestration Rating Council (NFRC), there is a certified products directory. The properties of the certified curtain walls products can be found in this directory. A database is formed based on 40 manufactures and 2858 certified curtain walls. The ranges of U-value of glazing, solar heat gain coefficient (SHGC) and visible transmittance (T_v) are set according to the distribution of these certified curtain walls.

Figure 3.3 shows the scattered plot of solar heat gain coefficient against U-value of glazing. The graph shows that the solar heat gain coefficient ranges from 0.1 to 0.5 when the U-value of glazing is under 2 W/m^2·K, while the solar heat gain coefficient has a larger range (0.1-0.7) when the U-value of glazing is over 2 W/m^2·K. Figure 3.4 shows the scattered plot of visible transmittance against U-value of glazing. The graph shows that the visible transmittance ranges from 0.1 to 0.7 when the U-value of glazing ranges from 1 to 3.5 W/m^2·K. Figure 3.5 shows the scattered plot of visible transmittance against solar heat gain coefficient. The graph shows that in general the visible transmittance increases with the increasing solar heat gain coefficient.

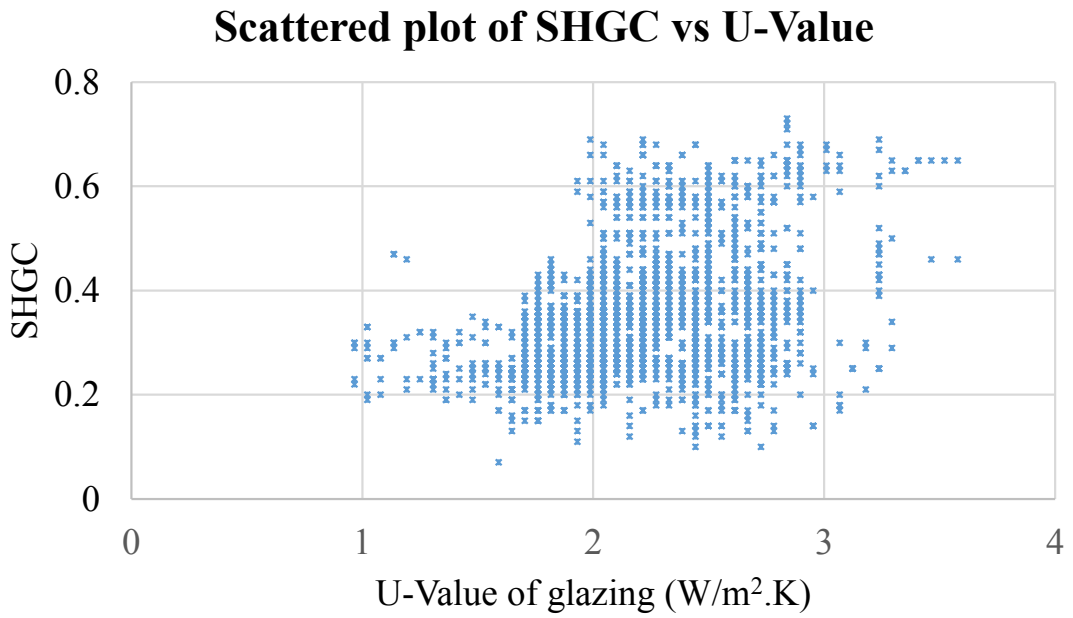

Figure 3.3. The scattered plot of solar heat gain coefficient against U-value of glazing.

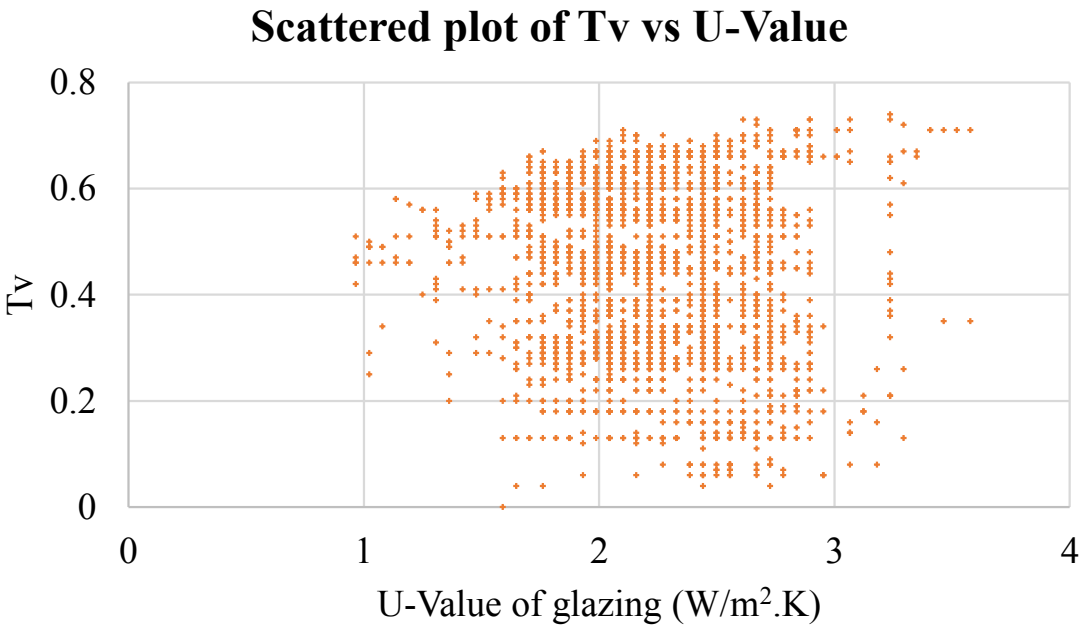

Figure 3.4. The scattered plot of visible transmittance against U-value of glazing.

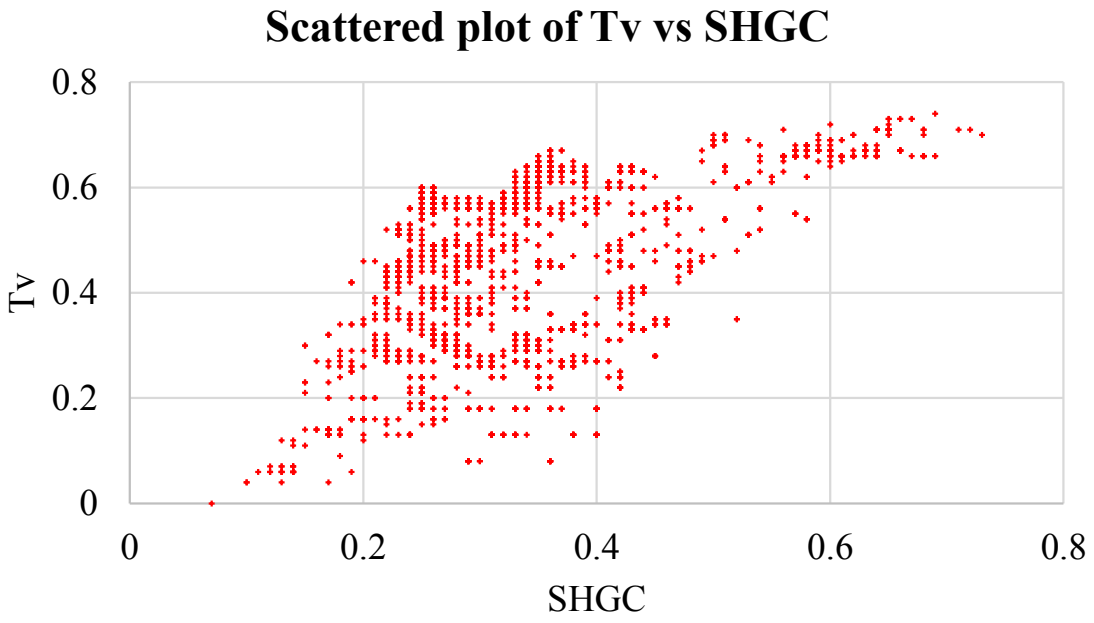

Figure 3.5. The scattered plot of visible transmittance against solar heat gain coefficient.

The probability distribution functions of U-value, solar heat gain coefficient and visible transmittance should be sought to better reflect their distribution.

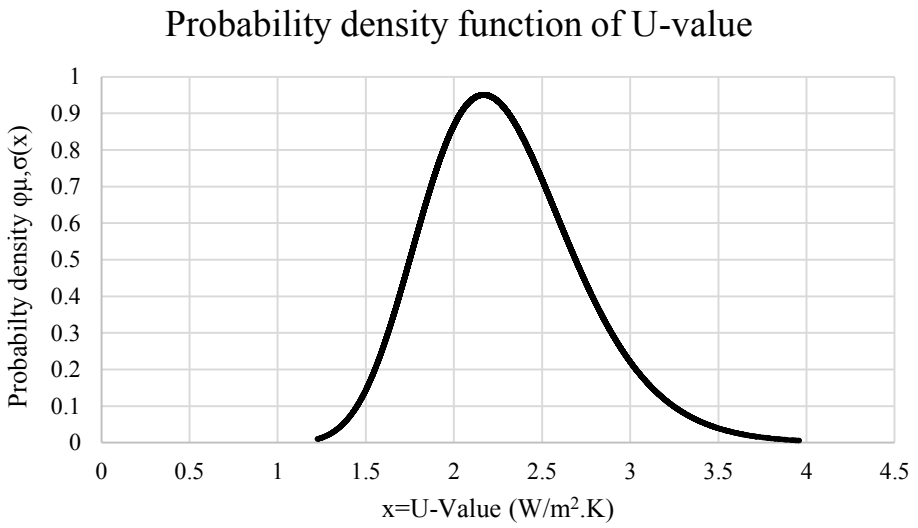

Figure 3.6. The probability density function of U-value of glazing of certified products in NFRC.

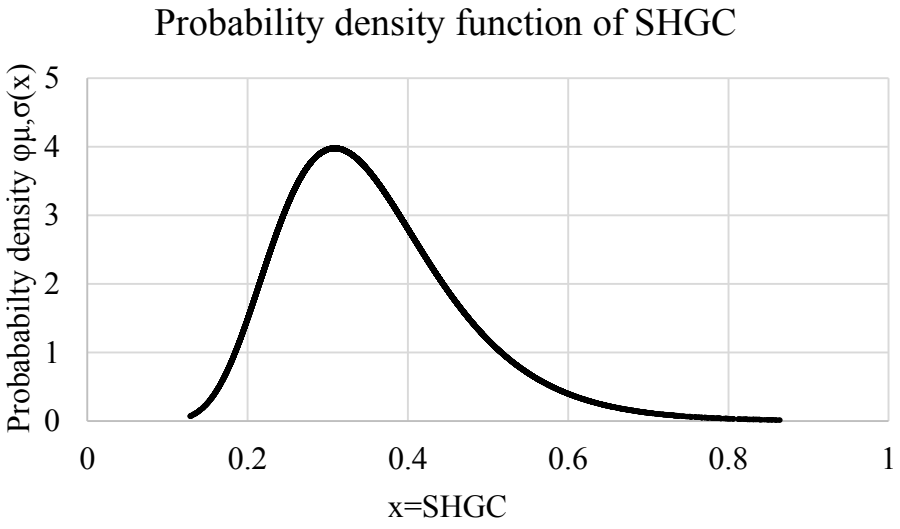

Figure 3.7. The probability density function of solar heat gain coefficient of certified products in NFRC.

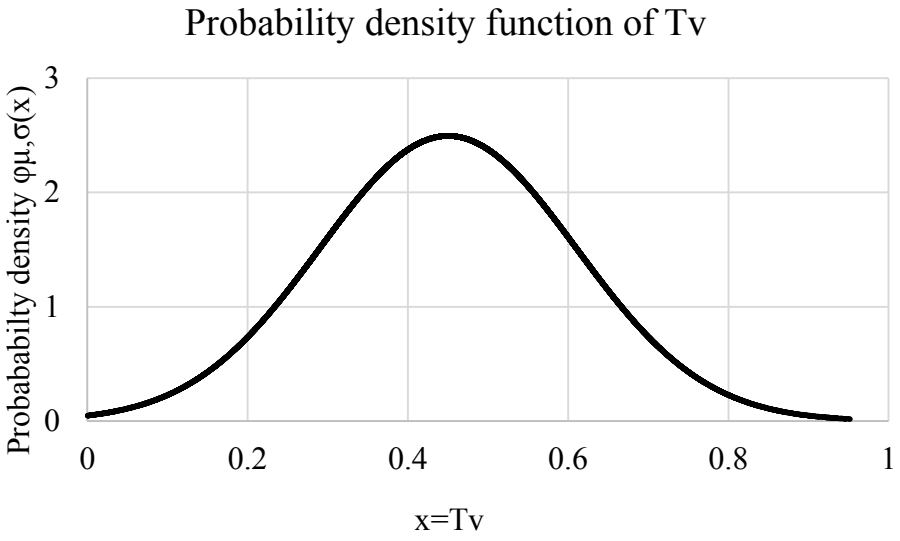

Figure 3.8. The probability density function of visible transmittance of certified products in NFRC.

Figure 3.6 – 3.8 show the probability density functions of U-value, solar heat gain coefficient and visible transmittance. Both U-value and solar heat gain coefficient follow a lognormal distribution (Equation 3.1). The distribution of visible transmittance follows a normal distribution (Equation 3.2).

Lognormal distribution

$$f(x) = \frac{1}{x\sigma \cdot \sqrt{2\pi}} \exp\left\{\frac{-1}{2}\left[\frac{\ln x - \mu}{\sigma}\right]^2\right\}$$ ---------- Equation 3.1

where $\mu = 0.79$ and $\sigma = 0.19$, x=value of parameter for glazing U-value

where $\mu = -1.10$ and $\sigma = 0.32$, , x=value of parameter for glazing SHGC

Normal distribution

$$f(x) = \frac{1}{\sigma \cdot \sqrt{2\pi}} \exp\left\{\frac{-1}{2}\left[\frac{x-\mu}{\sigma}\right]^2\right\}$$ ---------- Equation 3.2

Where μ = 0.45 and σ = 0.17, x=value of parameter

The other seven parameters are assumed with a uniform distribution as follows:

Uniform Distribution (rectangular distribution) is

$$f(x) = \frac{1}{n}$$ ---------- Equation 3.3

Where n is the sample size

The uniform distribution or rectangular distribution is a family of symmetric probability distributions such that for each member of the family, all intervals of the same length on the distribution's support are equally probable.

The range of U-value for curtain wall mullion is determined as 0.8 W/m^2·K for a framing configuration made of wood (Jelle et al., 2012) and 8.8 W/m^2·K for a standard aluminum mullion with thermal break (Ge, 2002). The range for U-spandrel panel is determined as 0.15 W/m^2·K for vacuum insulation panels as insulation (Alam et al., 2011) and 0.28 W/m^2·K for mineral wool as insulation (Ge, 2002). The efficiency of commercially available multi-crystalline silicon solar cells is around 14–19% (Parida et al., 2011). The range of photovoltaic modules effective efficiency is set from 9% to represent amorphous (uncrystallized) silicon cells to 19% representing crystalline silicon cells (Parida et al., 2011).

Retaining solar heat in heating season can be achieved by measures such as low U-value of glazing, U-value of spandrel panel and the mullion and high SHGC. Filtering unwanted solar heat gain in cooling seasons can be achieved by internal shading or exterior overhang. The operation of internal shading is stochastic in nature and it is not the focus in this paper. The width and the inclination of overhang are two controlling factors that affect the performance of overhang for cooling energy

reduction, so these two parameters are included in the analysis. An overhang above the vision panel of the curtain wall is added as a fixed shading device. The range of depth is set as 0.1-1.0 m to represent a practical depth and the range of inclination is set between 0^0 (horizontal) to 90^0 (vertical).

In order to convert a known leakage rate at a fixed building pressure to a corresponding input for the Energy Plus wind-driven infiltration model, it is necessary to figure out the baseline infiltration rate range.

The actual wind-driven infiltration rates at different floors of the building calculated by EnergyPlus should sum to equal that calculated using a surface average pressure coefficient and the building roof height. For infiltration models, where the infiltration rate varies linearly with the wind speed, it is possible to apply an adjustment factor to the wind-driven infiltration component in EnergyPlus equal to the ratio of the wind speed (U_H) at building roof height to the average wind speed impinging on the building face (U_{avg}). The latter can be found by integrating the wind profile with respect to height (up to the building roof height) and then dividing by the building roof height.

The base wind profile used by EnergyPlus is of a power law form

$$U_H = U_{met}\left(\frac{\delta_{met}}{H_{met}}\right)^{\alpha_{met}}\left(\frac{H_{building}}{\delta_{building}}\right)^{\alpha_{building}}$$ ---------- Equation 3.4

$U_{met} = 4.9 ms^{-1}$ (Climate, 2015)

4.9 m/s anemometer wind speed for a height H_{met} of 10 m at a nearby airport, so the wind speed U_H at roof level H = 36 m for a 10-floor building located in a large city centers

$\delta_{met} = 270m$, $\delta_{building} = 370m$

$H_{met} = 10m$, $H_{building} = 36m$

$\alpha_{met} = 0.14$, $\alpha_{building} = 0.22$

$$U_H = 4.9\left(\frac{270}{10}\right)^{0.14}\left(\frac{36}{370}\right)^{0.22} = 4.655 ms^{-1}$$

To get the average wind speed, integrate the equation (Equation 3.5) and divide the height of building

$$\frac{U_{avg}}{U_{met}} = \frac{1}{H_{building}}\frac{1}{\left(\alpha_{building}+1\right)}\left(H_{building}\right)^{\alpha_{building}+1}\left(\frac{\delta_{met}}{H_{met}}\right)^{\alpha_{met}}\left(\frac{1}{\delta_{building}}\right)^{\alpha_{building}} \text{ ---------- Equation 3.5}$$

While EnergyPlus calculates the wind speed at the centroid of each exterior surface, use of the average wind speed across the building height top to bottom is a simplifying assumption.

$$\frac{U_{avg}}{U_H} = \frac{1}{\left(\alpha_{building}+1\right)} \text{ ---------- Equation 3.6}$$

U_H is greater than the average wind speed impinging on the surface. The infiltration rate referenced to the wind speed at roof height is multiplied by the $\left(\alpha_{building}+1\right)$ for use

$$I_{design} = \left(\alpha_{building}+1\right)\cdot I_{@75Pa}\left(\frac{0.5C_s\rho U_H{}^2}{75}\right)^n \text{ ---------- Equation 3.7}$$

Where $U_H = 4.655 ms^{-1}$

$\rho = 1.18 kgm^{-3}$

$C_s = 0.1617$

$n = 0.65$

$\alpha_{building} = 0.22$

$I_{@75Pa} = 0.1 L/m^2 \cdot s$

$$I_{design} = (1+0.22)\times 0.1\times 10^3 \left(\frac{0.5\times 0.1617\times 1.18\times 4.655^2}{75} \right)^n = 0.011819 L/m^2 \cdot s$$

All building height-related impacts on wind speed and subsequent wind-driven infiltration in the building are handled within EnergyPlus simulation software based on the linear wind velocity coefficient.

Therefore the range of infiltration is set from 0.01L/m^2·s (75Pa) to 0.22 L/m^2·s (300Pa) due to curtain walls being normally tested under 300Pa for high rise buildings (Ge, 2002).

3.3. Modeling objectives and modelling approach

3.3.1 Modeling objectives

In order to fully assess the impact of curtain walls configurations on energy consumption in highly energy efficient building, building simulation models were developed and their results were analyzed.

The objective of the building simulations is to quantify and understand the influence of curtain wall design parameters on building energy performance, such as annual heating, cooling, and artificial lighting consumption. The impact of these different curtain wall design parameters was evaluated for the four cardinal orientations.

The results of these simulations should provide reference to designers for creating an energy-efficient building enclosure for the office buildings in heating dominated region such as Montreal. These results are only used for quantifying the influence of varying curtain walls configurations and the influence of individual curtain wall design parameters, since the actual energy consumption will greatly depend on the mechanical and electrical systems in the building along with the different occupancy schedules and set-points.

3.3.2 Generic energy model description

A hypothetical office unit in Figure 3.9 represents a typical office space in the perimeter zone of a multi-storey office building in Montreal is set in EnergyPlus as a case study. Figure 3.10 shows

the layout of an office unit on a typical floor. The hypothetical office unit is 4m deep, 4m wide and 3.6 m high (floor to ceiling).

One exterior façade is completed with the curtain walls with various configurations. The other three walls are regarded as internal walls. The adjacent spaces are all conditioned to the same temperature, therefore, the adiabatic boundary conditions are assumed at the three internal walls, floor and ceiling to ensure there is no heat exchange across these partitions. Gypsum board, acoustic tile and carpeted concrete are assigned as the interior finishing of internal walls, ceiling and floor, respectively. Realistic thermal, solar and optic properties are assigned for these surfacing materials so that radiative and convective heat transfer among surfaces and between the surface and indoor air can be taken into account properly. This set-up of the building model facilitates the comparison of potential energy saving due to different curtain wall system configurations.

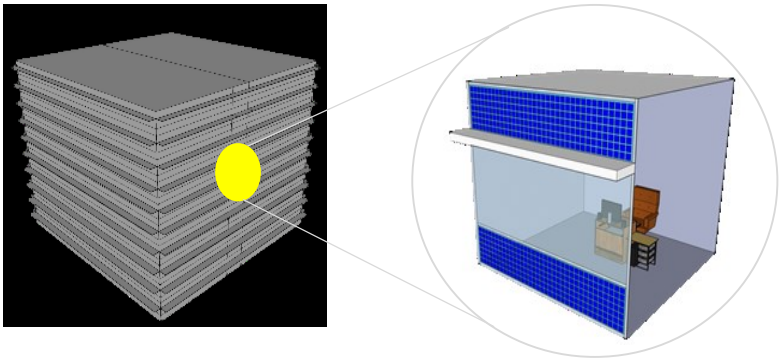

Figure 3.9. The office unit in a typical multi-storey office building.

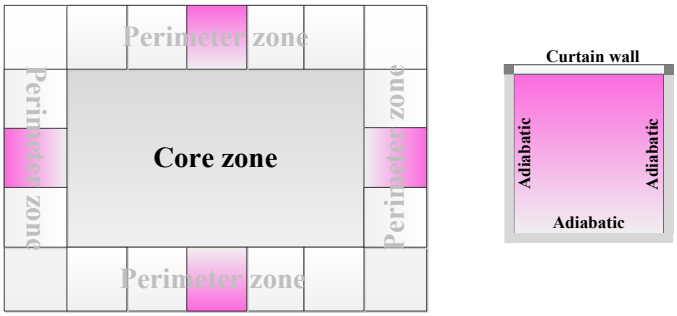

Figure 3.10. The layout of office unit in one of intermediate-level floors.

The façade is constructed by curtain wall with the building integrated photovoltaic conversion system (photovoltaic panel with crystalline silicon solar cells) mounted on the spandrel panels for the energy generating, as shown in Figure 3.10 and Figure 3.11. The curtain walls are popular in the office buildings but curtain walls integrated with photovoltaic panels on spandrel panels are still not common façades. An overhang is installed above the vision panel as the shading device.

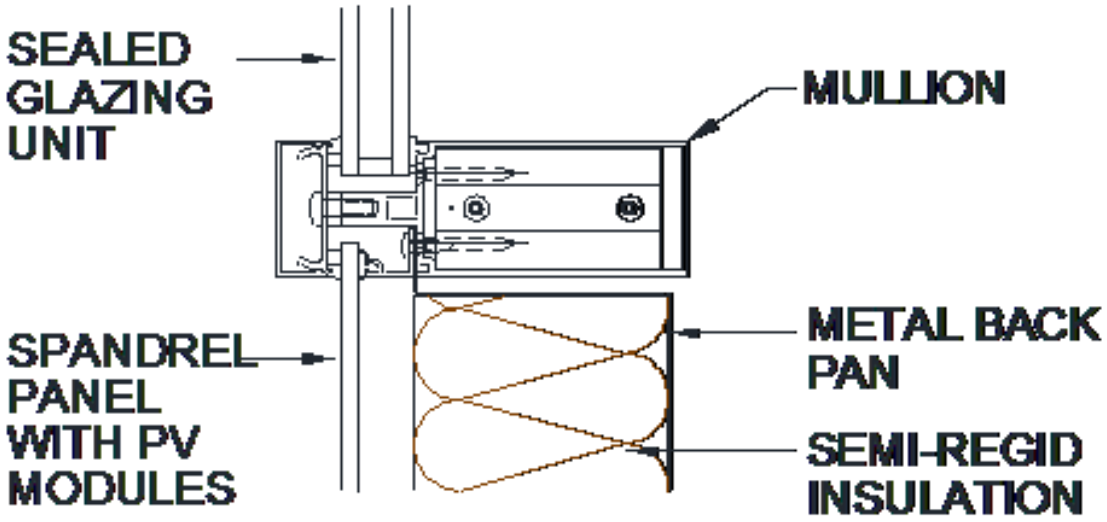

Figure 3.11. The configuration of curtain wall integrated with photovoltaic panels.

The hypothetical office unit is constructed for a single occupant according to common building practices for commercial offices (ASHRAE, 2010). The internal loads in the office room is assumed as highly energy efficient design usage which consists of the heat generated by the occupant (90 W), one desktop computer (54W) and monitor (24 W) (ASHRAE, 2011a). The occupancy schedule is listed in Table 3.3. The plug load consumption schedule is listed in Table 3.4.

Table 3.3. The office occupancy schedule.

	Start (hour)	End (hour)	Number of occupants	Internal heat gains from the occupant [W]
Weekdays	0	8	0	0
	8	18	1	90
	18	24	0	0
Saturdays	0	10	0	0
	10	16	1	90
	16	24	0	0
Sunday	0	8	0	0
	8	18	0	0
	18	24	0	0
Holidays	0	8	0	0
	8	18	0	0
	18	24	0	0

Table 3.4. The plug load consumption schedule.

	Start (hour)	End (hour)	Diversity factor	Plug load consumption [W]
Weekdays	0	8	0.4	0
	8	18	0.9	70
	18	24	0.5	0
Saturdays	0	10	0.4	0
	10	16	0.5	39
	16	24	0.3	0
Sunday	0	8	0.2	0
	8	18	0.2	0
	18	24	0.2	0
Holidays	0	8	0.2	0
	8	18	0.2	0
	18	24	0.2	0

The artificial lighting is provided by four 32W T8 fluorescent tubes with a total load of 120W and a lighting power density (LPD) of 7.5 W/m^2 (ASHRAE, 2011a). All of the lighting is set to operate on the lighting schedule as Table 3.5.

Table 3.5. The lighting schedule.

	Start (hour)	**End (hour)**	**Diversity factor**	**Lighting consumption [W]**
Weekdays	0	8	0.05	6
	8	18	0.90	108
	18	24	0.50	60
Saturdays	0	10	0.05	6
	10	16	0.50	60
	16	24	0.30	36
Sunday	0	8	0.05	6
	8	18	0.20	24
	18	24	0.05	6
Holidays	0	8	0.05	6
	8	18	0.20	24
	18	24	0.05	6

The occupancy, plug load and lighting load schedule represent an internal heat gain level that is comparable to common offices with normal occupant pattern. Offices with higher internal heat gain levels are typically older offices that uses less energy efficient equipment and lighting systems, or high-density offices which up to four occupants would occupy the same space in the office considered. In both cases the energy consumption intensity is higher. As technology improves, the energy consumption intensity is expected to decrease with more efficient office equipment and lighting, which gears to lower internal heat gains.

Daylighting controls are also incorporated into the model. The continuous dimming of the auxiliary lighting is assumed to maintain an illuminance level of 500 lux at the centre of the room at a work plane height of 0.8 m (2.5 ft).

Discomfort glare is also controlled with interior drapes, which are deployed once a glare index rating of 22 is reached in the model. The glare index is calculated from the centre of the room, at a 90^{o} angle from the window, facing the glazed façade.

Since the annual heating and cooling energy consumption are used as performance indicator for the analysis, a simplified packaged heat pump is specified to provide heating and cooling for this office unit. The COP for heating is set at 2.75 and the COP for heating is set at 3, to keep the air temperature between its heating and cooling set points.

The thermostat settings are 20ºC for heating and 25ºC for cooling during working hours of 08:00 to 18:00, with a night setback temperature of 13ºC in the winter and 30ºC in the summer (ASHRAE, 2011b). The heating and cooling set points schedule are listed in Table 3.6.

Table 3.6. The Design values of building information.

Building information	Design value (SI units)
Dimension of office unit	4m, 4m and 3.6m (D x W x H)
Heat gain from occupant	Single 90W
Plug load	One desktop computer and monitor (78 W)
Lighting power density	7.5W/m^2
Dimming control setpoint	500 lux setpoint by sensor located at room centre
HVAC Type	Package type Heat pump Heating COP=2.75 Cooling COP=3
Operating hours	08:00-18:00 (weeksdays) 09:00-13:00 (weekends)
HVAC setpoints	Heating 20ºC (set back temperature 13ºC) Cooling 25ºC (set-back temperature 30ºC)
Spandrel panel	Photovoltavaic panels with insulation and backpan

The building is located in Montreal, and weather data of the same location from WYEC2 is used, as created by WATSUN Simulation Laboratory, which contains hourly weather observations representing an artificial one-year period specifically designed for building energy calculations. Montreal is chosen as a typical cold climate zone with temperatures ranging from approximately -25°C to +35°C. Table 3.6 shows the summary of the details of building and systems setting in the base case model.

Exterior shading is designed to control the unwanted solar heat from the glazing. Two types of exterior shading are included in the energy model, including static external fixed overhang and dynamic interior shading. Static shading took the form of overhangs. The projecting depth and the inclination of the overhang is assigned as variables. The transparent portion composes two glazing panes whose width of the glazing is 1.95m, total 3.9m.

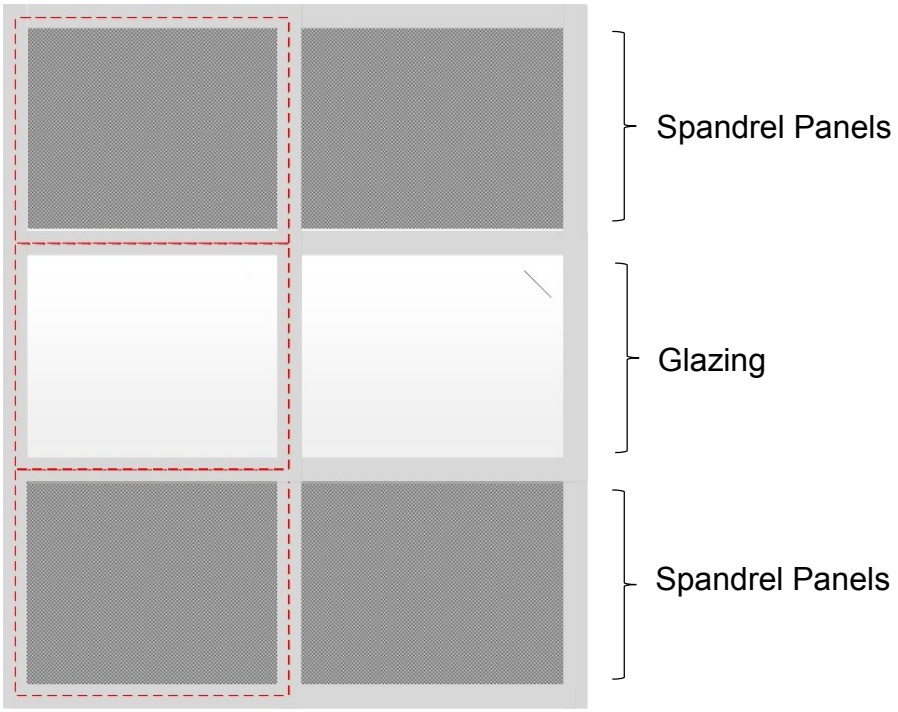

Figure 3.12. The plan view of the curtain wall section.

Dynamic interior shading is in the form of internal drapes, and has been programmed to block incident solar radiation when deployed once a glare index rating of 22 is reached.

3.3.3 Modeling approach

Modeling approaching for glazing

EnergyPlus provides six approaches to model glazing portion in fenestration, including the Full Spectral Method (FSM), the Aver-age Spectral Method (ASM), the WINDOW 5 Report Method (WRM), the Bi-directional Scattering Distribution Functions Method (BSDF), the Refraction Extinction Method (REM), and the Simple Window Model (SWM) (DOE, 2013a;DOE, 2013b). The six approaches allow different ways to specify the glazing properties but present different restrictions on certain configurations of glazing units. The six approaches differ in terms of level of detail and applicability. Detailed models require a considerable amount of detailed information as the input parameters. Increasing the level of detail increases the difficulty in performing the simulations. Decreasing the level of details degrades the model fidelity, which may lead to greater uncertainty in the modelling results.

The FSM requires the wavelength-by-wavelength spectral data (transmittance, front reflectance, and back reflectance) covering the solar spectrum from about 0.25 to 2.5 microns as inputs. The ASM requires the inputs of transmittance, front and back reflectance of solar spectrum and visible light, infrared transmittance, front and back emissivity and conductivity of each layer of glazing. The WRM includes the U-value, the SHGC, and the calculated values of optical properties such as the transmittance, the absorptance, the front and back reflectance for the glazing unit at different incidence angles. BSDF, which consists of Bi-directional Reflectance Distribution Function or BRDF and Bi-directional Transmittance Distribution Function or BTDF, describes how light coming from a certain direction is transmitted and reflected in different directions. In REM, the index of refraction and extinction coefficient are used to specify glazing properties. In SWM, simplified window performance indices including U-value of glazing (Ugl), solar heat gain coefficient (SHGC), and the optional input, visible transmittance (Tv), are used to specify the glazing properties.

An appropriate modelling approach should be able to reproduce predictions which fit with the experimental data (Van Buren et al., 2014); however, this norm tends to steer the approach

selection towards the detailed approach. The approach selection strategy loses ground when the experimental data is not available in early design phase.

Although an appropriate approach should be selected based on three criteria: computational cost, ability to reproduce consistent results and uncertainty, simple window mode is used in this study because this is the only one modeling approach to vary the U-value, solar heat gain and visible transmittance in order to investigate the impact of these three design parameters on end-use energy consumption. However, the SWM has the largest variation in predicting cooling and the total energy consumption (Lam et al., 2014)

Modeling approaching for spandrel panel

To estimate the overall U-value of the curtain wall, the area and its corresponding U-value for mullion, center-of glass, and edge-of-glass (based on a 65 mm band around the perimeter of each glazing unit as shown in Figure 3.11) are determined. The area-weighted U-value is the overall U-value of the curtain wall assembly.

The change of U-value of spandrel panel is due to the range of insulation products that can be used in the spandrel panels. The U-value of spandrel panel is adjusted by changing the thickness of the insulation instead of changing the type of insulation to simplify the simulation process.

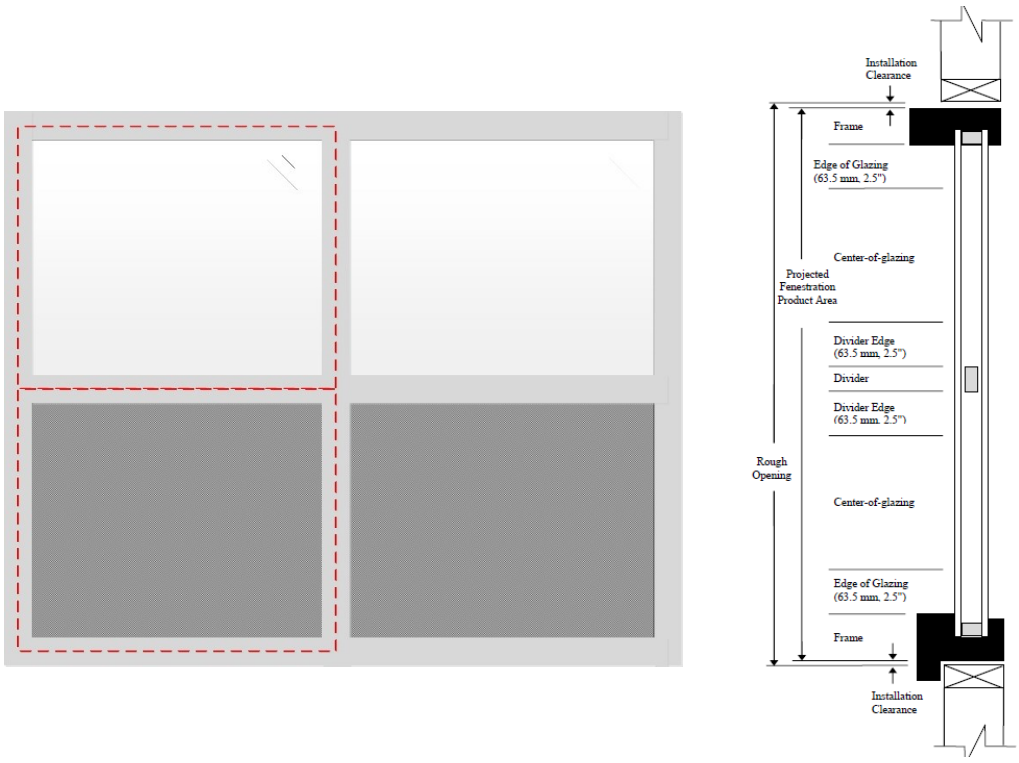

Figure 3.13. (a) The layout of glazing and spandrel panel. (b) The cross section of curtain wall. (c) The glazing panel. (d) The spandrel panel.

Modeling approach for photovoltaic panel

In EnergyPlus, there are three PV performance models to evaluate the generation by the PV arrays, Simple Model, Equivalent One-diode and Sandia models.

The simple model to calculate the electrical power produced by a photovoltaic surface in EnergyPlus is as following (DOE, 2013a; DOE, 2013b).

In the Simple PV performance model, a constant efficiency assumed during whole range of solar irradiation and cell temperature effect is not taken into account. Here the constant efficiency is an effective efficiency.

$$P = A_{surf} \cdot f_{activ} \cdot G_T \cdot \eta_{cell} \cdot \eta_{invert}$$ ---------- Equation 3.8

Where

P Electrical power produced by photovoltaics [W]

A_{surf} Net area of surface [m^2]

f_{activ} Fraction of surface area with active solar cell [-]

G_T Total solar radiation incident on PV array [W/m^2]

η_{cell} Module conversion efficiency [%]

η_{invert} DC to AC conversion efficiency [%]

The equivalent One-Diode model is known as four or five parameters TRNSYS (TRaNsient SYstem Simulation Program, an energy simulation program) model for photovoltaics in which modules are modeled using an equivalent one-diode circuit. The list of parameters in equivalent one-diode model of PV module includes short circuit current, open circuit voltage, voltage at maximum power, current at maximum power, temperature coefficient of short circuit current,

temperature coefficient of open circuit voltage, number of cells in series per module, cell temperature at NOCT (Nominal Operating Cell Temperature) condition, and module area.

Sandia conducts detailed outdoor performance tests on about 500 commercially available modules, and a database of the associated module performance parameters is maintained on the Sandia website. The Sandia model incorporated in EnergyPlus is based on empirical coefficients assembled by Sandia National Laboratory for each specific type and brand of PV modules.

The results of equivalent one-diode and Sandia models in EnergyPlus are validated with experimental data.

To justify the application of simple PV model in this study, an investigation is performed. The same generic energy model and eleven types of photovoltaic (PV) modules on the south façade are simulated in EnergyPlus. Each PV modules are modelled repeatedly for seven WWR ranged from 0.1 to 0.7 with interval 0.1. Table 3.7 lists the eleven PV modules selected. The products chosen are all crystalline modules. It is confirmed to have good agreement between one-diode model and Sandia models when the crystalline modules are the subjects of interest.

The annual energy yield of modules are predicted with three PV performance models and the annual solar radiation received by the modules is predicated in EnergyPlus. The effective efficiency obtained by the Simple PV model is compared to the other two validated PV performance models, the One-diode model and the Sandia model.

The effective efficiency is calculated as follows:

$$\eta_{effective} = \frac{\text{Generation (W/m}^2\text{)}}{\text{Radiation (W/m}^2\text{)}} \quad \text{---------- Equation 3.9}$$

The variation of simple PV model from the accredit approaches (One-diode and Sandia models) is quantified by the Coefficient of Variation of the Root Mean Square Error (CVRMSE) and Normalized Mean Bias Error (NMBE). The required values are dependent of data sampling frequency as listed in Table 3.8.

Table 3.7. Specifications of the eleven PV modules selected.

Photovoltaic panels	Peak efficiency [%]	Area of modules [m^2]	Number of cells in series
Photowatt PW1000	9	0.898	36
AstroPower AP-100	10	0.974	36
Solarex MSX-110	11	1.098	72
AstroPower AP-120	12	0.974	36
AstroPower AP-130	13	1.121	42
BP Solar SX3140	14	1.018	36
BP Solar BP2150S	15	1.260	72
Kyocera Solar KC158G	16	1.277	48
Sharp ND-167U1F	17	1.310	48
Sanyo HIP-HO97	18	1.148	96
BP Solar SX3190	19	1.406	50

ASHRAE Guideline 14 (ASHRAE, 2002) is intended to be a guideline that provides a minimum acceptable level of performance in the measurement of energy and demand savings from energy management projects applied to residential, commercial or industrial buildings. In section 5.3.2.1 requires that the calibration data such as energy consumption of baseline model shall meet the Coefficient of Variation of the Root Mean Square Error (CVRMSE) and Normalized Mean Bias Error (NMBE) requirement.

The Normalized Mean Bias Error (NMBE) is computed from

$$NMBE = \frac{\sum_{i=1}^{n}\left(y_i - \hat{y}_i\right)}{\left(n-p\right)\times \bar{y}} \times 100 \quad \text{---------- Equation 3.10}$$

The Coefficient of Variation of the Root Mean Square Error (CVRMSE) indicates the uncertainty inherent in the model, which is computed from

$$CVRMSE = \frac{1}{\bar{y}}\sqrt{\frac{\sum_{i=1}^{n}\left(y_i - \hat{y}_i\right)}{\left(n-p\right)}} \times 100$$ ---------- Equation 3.11

y_i is the current value

$\hat{y}_i$ is estimated value

$\bar{y}$ is mean value

n is number of observations

p is number of parameters in the regression model

Table 3.8. Required value for baseline model from ASHRAE Guideline 14.

	Hourly
Coefficient of Variation of the Root Mean Square Error	30%
Normalized Mean Bias Error	10%

In Table 3.9, it lists the effective efficiency calculated by three PV models. The results shows that the effective efficiency is consistent in seven WWR.

Since the one-diode model and the Sandia model are the validated PV modelling approach in EnergyPlus, the effective efficiencies obtained by Simple PV models are compared with respect to those obtained by the one-diode model and the Sandia model. Table 3.10 lists the Coefficient of Variation of the Root Mean Square Error (CVRMSE) and Normalized Mean Bias Error (NMBE) of Simple PV model compared to One-diode model. Table 3.11 lists the CVRMSE and

NMBE of Simple PV model compared to Sandia model. The results shows that Simple PV model fulfils the requirements of ASHRAE Guideline 14.

Table 3.9. Comparison of effective efficiency obtained by simple model to one-diode model.

		Calculated effective efficiency [%]		
Photovoltaic panels	**Peak Efficiency [%]**	**Simple PV**	**One diode**	**Sandia**
Photowatt PW1000	9	9.8	9.6	10.0
AstroPower AP-100	10	10.5	10.7	10.3
Solarex MSX-110	11	10.1	10.2	10.1
AstroPower AP-120	12	12.3	11.9	12.7
AstroPower AP-130	13	11.8	11.8	11.8
BP Solar SX3140	14	13.7	13.4	13.7
BP Solar BP2150S	15	11.7	11.3	12.1
Kyocera Solar KC158G	16	12.3	11.8	12.8
Sharp ND-167U1F	17	12.8	12.5	13.0
Sanyo HIP-HO97	18	15.6	15.9	15.3
BP Solar SX3190	19	13.5	13.2	13.7

Table 3.10. Comparison of effective efficiency obtained by simple model to one-diode model.

WWR	**CVRMSE [%]**	**NMBE [%]**
0.1	2.50	-1.41
0.2	2.50	-1.40
0.3	2.49	-1.39
0.4	2.49	-1.39
0.5	2.49	-1.38
0.6	2.48	-1.38
0.7	2.48	-1.37

Table 3.11. Comparison of effective efficiency obtained by simple model to Sandia model.

WWR	CVRMSE [%]	NMBE [%]
0.1	2.50	1.41
0.2	2.50	1.40
0.3	2.49	1.39
0.4	2.49	1.39
0.5	2.49	1.38
0.6	2.48	1.38
0.7	2.48	1.37

3.4. Sampling

3.4.1 Sampling of glazing parameters

As discussed in section 3.2.1, the glazing properties cannot be combined randomly in sampling, it is necessary to investigate the relationship among the U-value of glazing, solar heat gain coefficient and visible transmittance. The relationship is quantified by the correlation coefficient r which is a measure of the strength of the straight-line or linear relationship between two variables. Correlation is a statistical measure that indicates the extent to which two or more variables change together. If the relationship is known to be linear, or the observed pattern between the two variables appears to be linear, then the correlation coefficient provides a reliable measure of the strength of the linear relationship. If the relationship is known to be nonlinear, or the observed pattern appears to be nonlinear, then the correlation coefficient is not useful.

$$r = \frac{\sum_{i=1}^{n}\left(z_{x_i} \times z_{y_i}\right)}{n-1}$$ ---------- Equation 3.12

where n is the sample size;

$$z_{x_i} = \frac{x - \mu_{x_i}}{\sigma_{x_i}}$$ ---------- Equation 3.13

where μ_x is the mean of sample set x;

σ_x is the standard deviation of sample set x

$$z_{y_i} = \frac{x - \mu_{y_i}}{\sigma_{y_i}}$$ ---------- Equation 3.14

where μ_y is the mean of sample y;

σ_y is the standard deviation of sample set y

The correlation coefficient takes on values ranging between +1 and -1. The following points are for interpreting the correlation coefficient.

- r = 0 indicates no linear relationship.
- r = +1 indicates a perfect positive linear relationship: as one variable increases in its values, the other variable also increases in its values via an exact linear rule.
- r = -1 indicates a perfect negative linear relationship: as one variable increases in its values, the other variable decreases in its values via an exact linear rule.
- Values between 0 and 0.3 (0 and -0.3) indicate a weak positive (negative) linear relationship.
- Values between 0.3 and 0.7 (0.3 and -0.7) indicate a moderate positive (negative) linear relationship.
- Values between 0.7 and 1.0 (-0.7 and -1.0) indicate a strong positive (negative) linear relationship via a firm linear rule.

The results in Table 3.12 show that the correlation between U-value and solar heat gain coefficient is moderate positive linear relationship while the correlation between U-value and visible transmittance is no linear relationship.

Table 3.12. The correlation among the U-value of glazing, solar heat gain coefficient and visible transmittance.

Correlation	
U-value and solar heat gain coefficient	0.406
U-value and visible transmittance	-0.015
Solar heat gain coefficient and visible transmittance	0.5486

In Simlab, there are three methods to induce correlations .(i) the dependence-tree/copula method (Meewissen & Cooke, 1994; Morris, 1987), (ii) the Iman and Conover method (Iman, Ronald L., 1982), and (iii) the Stein method (Stein, 1987).

The dependence-tree method is used for modelling the correlation between factors. The Simlab user can specify correlations among input factors that form a tree structure. Whatever correlation values are imposed by the user in this way, it is guaranteed that a joint PDF exists. The joint PDF has minimum information amongst all those joint distributions which satisfy the criteria given by the users.

The Iman-Conover method is used to induce a desired rank correlation on pairs of input factors. Its characteristics are:

- rank correlations can be set independently on marginal distributions,
- the original form of the marginal distributions is preserved,
- may be used with many sample schemes,
- if the correlations imposed are too strong, then the correlation matrix is not positive definite, and a message is displayed.

Stein method is used in this study to sample the glazing properties because it allows the user to generate a correlated Latin Hypercube Sampling (LHS). The users must provide an ASCII file that contains a correlated sample (such as a random sample, or even an empirical sample generated by an experiment). The method generates an LHS sample with the same correlation of the sample provided by the user.

The database of available curtain wall products, which is formed based on 40 manufactures and 2858 certified curtain walls in National Fenestration Rating Council (NFRC), is used to from the ASCII file for the Stein Method. Therefore, the correlated sample among U-value of glazing, solar heat gain coefficient (SHGC) and visible transmittance (Tv) is the same as the database formed by 2858 certain walls in National Fenestration Rating Council (NFRC).

Figure 3.13 and Figure 3.14 show the scattered plots of the sampled solar heat gain coefficient v.s. U-value, and sampled visible transmittance v.s. U-value. The samples generally have a good representation of the manufacturer data. Figure 3.15 to Figure 3.17 show the comparison in distribution function between manufacturers' data and the sampled data, which has generally good agreements.

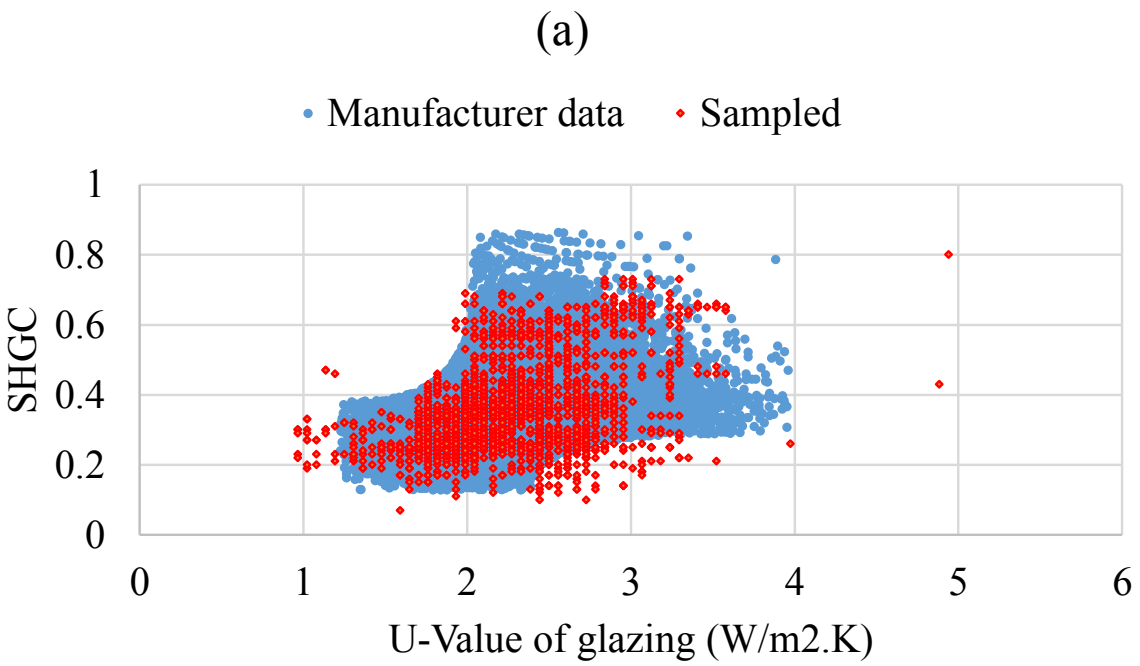

Figure 3.14. The scattered plots of the sampled solar heat gain coefficient vs. U-value.

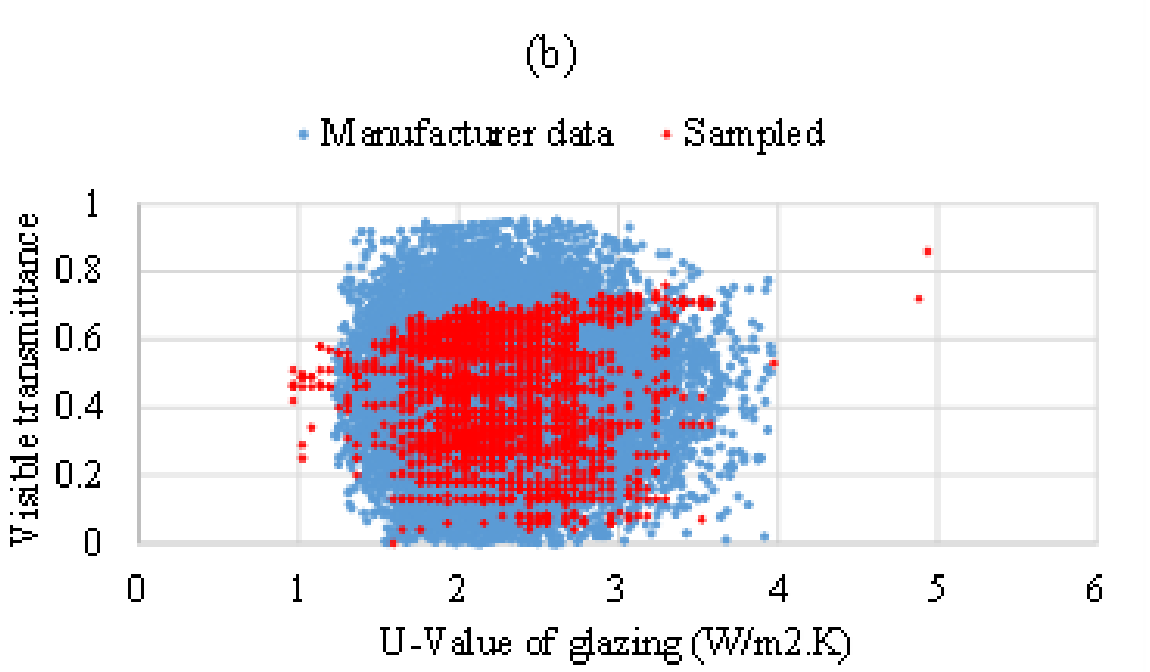

Figure 3.15. The scattered plots of the sampled Tv vs. U-value.

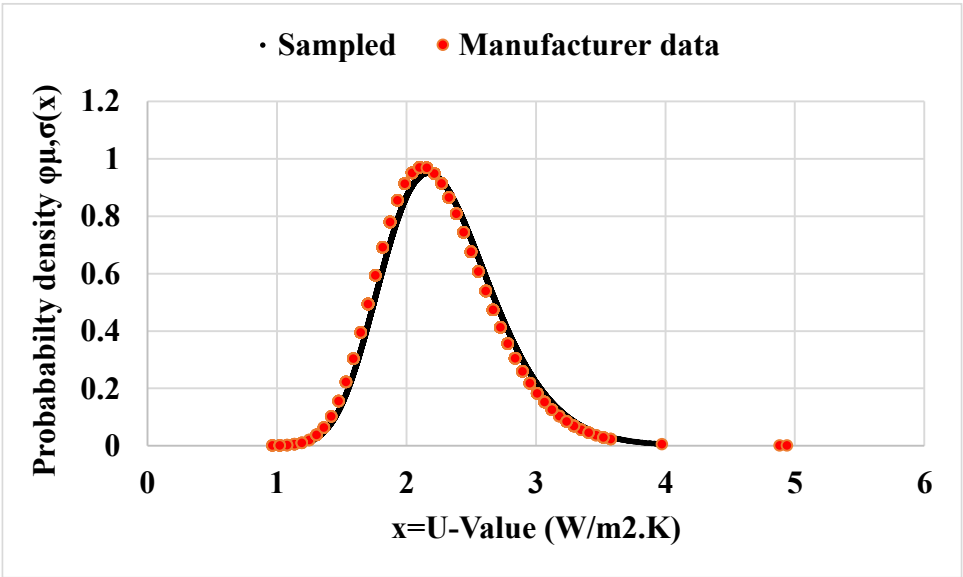

Figure 3.16. Comparison of PDF of glazing U-value between manufacturers' (Lognormal: μ=0.79 and σ=0.19) and sampled data (Lognormal: μ=0.81 and σ=0.19.

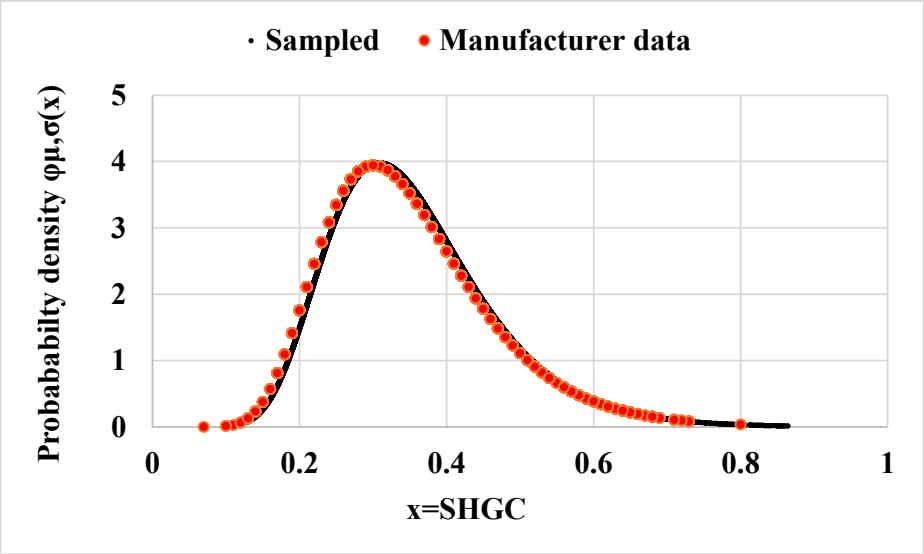

Figure 3.17. Comparison of PDF of SHGC between manufacturers' (Lognormal: μ=-1.10 and σ=0.32) and sampled data (Lognormal: μ=-1.08 and σ=0.31).

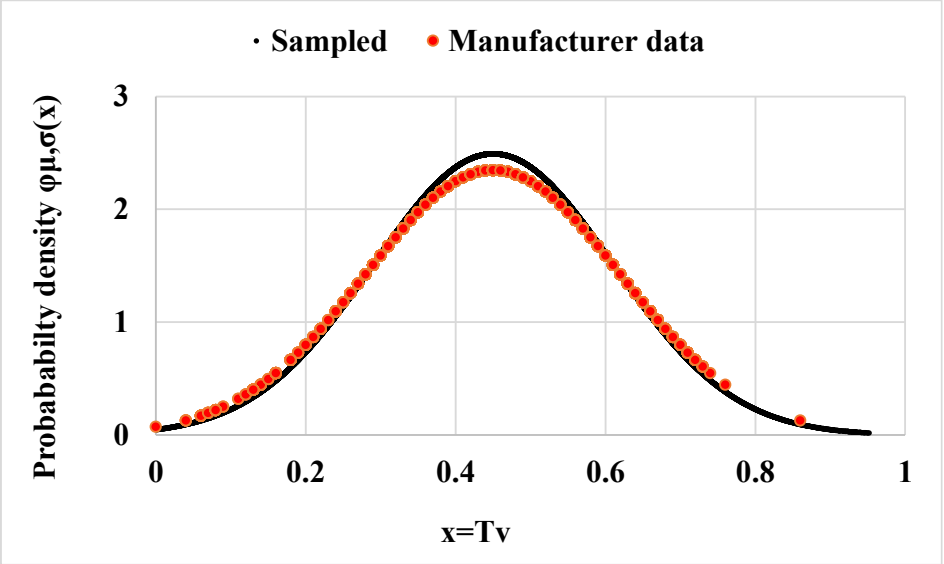

Figure 3.18. Comparison of PDF of Tv between manufacturers' (Normal: μ=0.45 and σ=0.17) and sampled data (Lognormal: μ=0.45 and σ=0.16).

3.4.2 Sampling procedure

In this study, Sobol' is used for the sensitivity analysis and therefore the sampling method of Sobol' sequences, a quasi-random sampling technique, is used.

k column is number of parameter

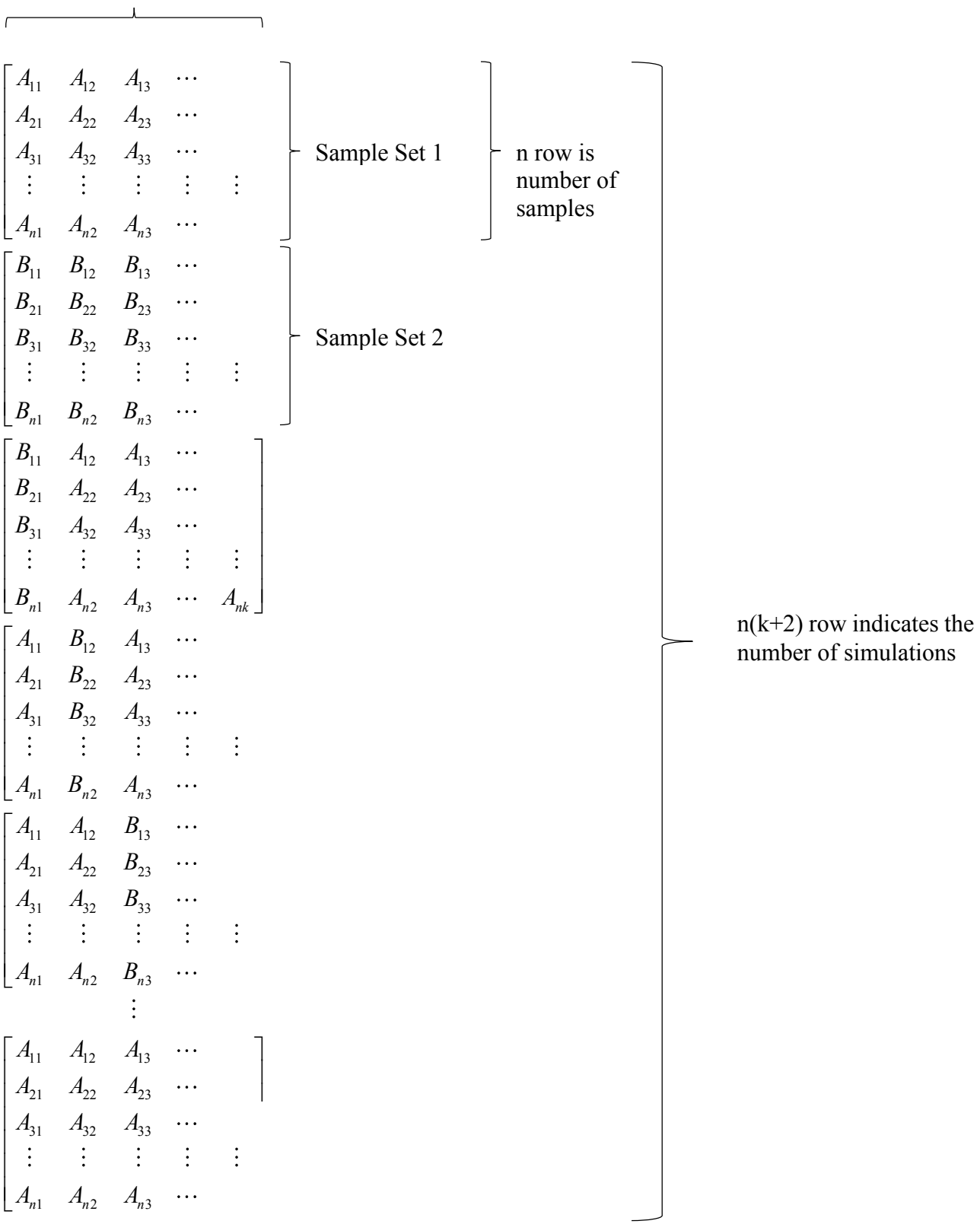

A sequence of sampling is generated by changing one input variable at a time. The new input variables are sampled in a fixed cyclic order.

The output is evaluated after generating each input variables sampling, yielding a sequence of output variables.

3.5. Uncertainty analysis

The purpose of uncertainty analysis is to quantify the variations of end-use energy consumption as a result of the variation in curtain wall design parameters. After the sample has been generated and the corresponding simulations have been carried out, the primary computational portions of the uncertainty analysis component have been completed.

There are two measures commonly used. The first is the results represented by single number (Scalar result) such as coefficient of variation. The second is the results represented by functions such as the probability density function and the cumulative density function. In this study, we adopted the scalar result.

3.5.1 Measure of uncertainty

The uncertainty is quantified by the coefficient of variation (ν), which is the ratio of the standard deviation (σ) to the mean value (μ) given by Equation 3.15 to Equation 3.16. n is the number of data, y_i is the exact data point. The coefficient of variation (ν) in Equation 3.17 indicates the dispersion of the outputs. The smaller the coefficient of variation, the less the deviation of the predicted value from the mean value.

$$\sigma = \sqrt{\frac{1}{n-1}\sum_{i=1}^{n}(y_i - \mu)^2}$$ ---------- Equation 3.15

$$\mu = \frac{1}{n}\sum_{i=1}^{n} y_i$$ ---------- Equation 3.16

$$\upsilon = \frac{\sigma}{\mu}$$ ---------- Equation 3.17

3.6. Sensitivity analysis

3.6.1 Selection of global sensitivity analysis methods

The methodology for sensitivity analysis is the same in different types of application in building energy analysis. The first step is to select the appropriate methods for sensitivity analysis. As in section 2.2.6, there are local and global sensitivity analysis. In this study, global sensitivity analysis is adopted.

The selection of global sensitivity analysis approaches depends on the relationship between output values and the input values (dependency of model), nonlinearity,(non-monotonicity) and offset effect between the input values (non-additivity). The variance-based methods or Analysis of Variance (ANOVA) are strongly favoured in case that non-additivity of model is difficult to decided (A. Saltelli et al., 2000). Both variance-based methods Sobol' and FAST are able to cope with non-linear and non-monotonic models. The capability of ANOVA is evident, however, the computational cost of ANOVA is high. Sobol' method requires totally n(k+2) model evaluations while FAST method requires nk model evaluations where n is the sample size and k is the number of parameters.

The variance-based method is based on the decomposition of the model variance. Variance is a measure of the dispersion of the output. Therefore, variance-based method is to decompose the (dispersion) uncertainty of outputs for the corresponding inputs. In ANOVA, F-test is commonly used to evaluate the significance of the output variations to variations in the inputs, while the Tukey test and Scheffé test are used to evaluate the effect of input value ranges (Frey & Patil, 2002; Montgomery, 2012; Hochberg & Tamhane, 2009). However, the results of the F-test may not be

appropriate for the study which contains correlated inputs (Frey & Patil, 2002). In this study, orientation is a factor which does not have correlated relationship with other parameters, therefore, F-test is used to assess the impact of orientations on the energy consumption. As mentioned in section 3.2.1, the three primary thermal and optic properties of glazing, U-value of glazing, solar heat gain coefficient and visible transmittance are often correlated. Therefore, other ANOVA sensitivity analysis methods such as Sobol' or FAST should be used in order to address the vulnerability of F-test on correlated inputs.

Single-factor F-test can be employed to investigate the effect of the particular factor on the output variable. F-test can also deal with two or more factors for determining the effect of interactions among factors.

In this study, the effect of orientation is quantified by the F-value.

The calculation of F-value is presented from Equation 3.18 – Equation 3.22 (Ott, 2008)

$$\text{F-value}=\frac{\text{mean square between samples}}{\text{mean square within samples}}=\frac{\text{explained variance}}{\text{unexplained variance}} \quad \text{----------Equation 3.18}$$

$$\text{mean square between samples}=\frac{\text{variability between samples}}{\text{degree of freedom between samples}} \quad \text{----------Equation 3.19}$$

Variability between samples = Sum of square between samples (SSB)

$$\text{SSB}=\sum_i n_i\left(\bar{y}_i-\bar{y}\right)^2 \quad \text{---------- Equation 3.20}$$

SSB measures the variability of the sample means $\bar{y}_i$ about the overall mean $\bar{y}$

$$\text{mean square within samples}=\frac{\text{variability within samples}}{\text{degree of freedom within samples}} \quad \text{----------Equation 3.21}$$

Variability within samples = Sum of square within samples (SSW)

$$SSW = \sum_{ij} \left(y_{ij} - \bar{y}_i \right)^2 = \left(n_1 - 1 \right) s_1^{\,2} + \left(n_2 - 1 \right) s_2^{\,2} + \ldots \qquad s_t^{\,2}$$ ----------Equation 3.22

SSW measures variability of an observation y_{ij} about the its sample mean $\bar{y}_i$

The number of degrees of freedom is the number of values in the final calculation of a statistic that are free to vary.

The magnitude of F-value is justified by comparing the F-value to critical values of F-distribution. In hypothesis testing, a critical value is a point on the test distribution that is compared to the test statistic to determine whether to reject the null hypothesis. If the absolute value of the test statistic is greater than the critical value, statistical significance can be declared and the null hypothesis should be rejected. In this study, the null hypothesis is that all group means are equal.

Normally critical values of F-distribution is obtained in tabular form correspond to α (Probability of type I error) and the degree of freedom between groups and the degree of freedom within groups. Types I error is committed if the null hypothesis is rejected when it is true.

The process of deriving the critical values of F-distributions was presented in Didonato & Morris, (1992).

Although Sobol' needs higher computational cost compared to FAST, Sobol' method is used to evaluate the total sensitivity index in this study because sampling based on Sobol' sequences is found to produce the most robust results relative to Latin Hypercube Sample (LHS) when dealing with building simulations (Burhenne, 2011).

Ten parameters are investigated in Sobol'. With sample size of 2048, 24576 model evaluations are needed to evaluate the first order sensitivity index and the total sensitivity index. For four orientations, 98304 model evaluations are needed. For a more accurate model, larger sample size results in high computational cost (Saltelli et al., 2000).

Sobol's is one of the quasi-random sampling methods, which has the advantage of enhanced convergence rate (Bieda, 2010). The Sobol' approach is to decompose the function f(x) into summands of increasing dimensionality (Pace, 2012).

$$f\left(x_1,\ldots \right.$$ … … ---------- Equation 3.23

Where $f_0 = \text{constant}$ and x_i are the design parameter and k is the number of design parameters.

The variance of function f(x_1,……x_k) can be represented as the sum of variances of first order and higher order functions.

The variance of output (D) can then be decomposed as

$$D = \sum_{i=1}^{k} D_i + \sum_{j>i}^{k} D_{ij} + \ldots$$ ---------- Equation 3.24

Where D_i are first order variances, and $D_{123\ldots}$ are higher order variances

The sensitivity index is calculated using Equation 3.25 to Equation 3.27.

The first order sensitivity index

$$S_i = \frac{D_i}{D}$$ ---------- Equation 3.25

The second order sensitivity index

$$S_{ij} = \frac{D_{ij}}{D}$$ ---------- Equation 3.26

The total sensitivity index (TS_i) is defined as the sum of all the sensitivity indices involving the design parameters. We have ten design parameters, the total effect of design parameter 1 on the output variance, denoted by TS_i (1), is determined by

$$TS_i(1) = S_1 + S_{12} + \ldots$$ … … ---------- Equation 3.27

where S_1 is the first-order sensitivity index for design parameter 1. S_{1j} is the second-order sensitivity index for the two design parameters 1 and j($\neq$1), i.e. the interaction between design parameters 1 and j($\neq$1).

When the model is additive, which means that the interacting effect is negligible i.e. the higher order values are negligible, the total sensitivity index is similar to the first-order sensitivity index.

3.6.2 Interpretation of F-values and sensitivity indices

When the F-value is sufficiently large, it means that the explained variance or the mean square between samples is significant (Equation 3.18), it implied that the differences between the group means are significant too. Therefore it can conclude that the single factor contribute significantly to the variation of the output variables. In this study, significant impact of orientation on end-use energy consumption is represented by large F-value. The magnitude of F-value is justified by comparing the F-value to critical values of F-distribution.

The critical value is the number that the F-value must exceed to reject the hypothesis. If the F-value is greater than the critical value at α (Probability of type I error), that implies the results are significant at α % level of significance.

First order sensitivity index represents the individual impact of the uncertainty of the input factor Xi on the output variation. Second order sensitivity index represents the interaction effect due to two parameters in non-additive relationship. Total sensitivity index is the sum of the first order sensitivity index of the factor and the higher sensitivity index involved in the investigated study.

For additive models with no interaction between the factors, first order sensitivity index = total sensitivity index ($S_i=TS_i$) and summation of first order sensitivity indices = 1 ($\sum S_i=1$). The estimation of the pair S_i and TS_i is important to evaluate the difference in the impact of factor X_i alone on output Y and the overall impact of factor X_i through interactions

The first order effects consider the main effects for the output variations due to the corresponding inputs. The total effects account for the total contributions to the output variance due to the corresponding inputs, which include both first order and higher-order effects because of interactions among inputs.

Hence, the difference between the first order and total effects can show the effects of interactions between variables. The first order indices and the total indices are different, indicating factors are involved in significant interactions. If the objective of the research is to fix the factors which are not important in the output results, the total sensitivity effects should be used. In contrast, if the purpose is to prioritize the factors, the first order effects are a better choice (Tian, 2013).

The total effects are much more reliable than the first-order effects in order to investigate the overall effect of each single input on the output (Frey & Patil, 2002). Therefore, total sensitivity indices are used in this study.

The significance of the impact can be classified (Chan et al., 1997, Frey & Patil, 2002).

- very significant $TS_i > 0.8$
- significant $0.5 < TS_i < 0.8$
- insignificant $0.3 < TS_i < 0.5$
- irrelevant $TS_i < 0.3$

Chapter 4 Result

4.1 Uncertainty analysis

Table 4.1 shows the coefficient of variation of end-use energy of the office unit with various curtain wall configurations at four cardinal orientations. The higher value of the coefficient of variation implies greater dispersion of the output data and greater variations of the end-use energy consumption due to random combinations of curtain wall design parameters.

In general, the coefficient of variation is similar for all the four orientations for heating, lighting and total energy consumption, which is about 34-38%, 28%, and 16-20%, respectively. For the cooling energy consumption though, the dispersion is about 55% for the east and west, 65% for the south, and 42% for the north. These results indicate that the variation of curtain wall configurations has generally greater impact on the cooling followed by heating, lighting and total energy consumption. As for cooling, the variation of curtain wall configurations has much less impact on north façade than on the other three orientations while the south façade is the most sensitive to the curtain wall design parameters. The energy generation to energy consumption ratio has the largest coefficient of variation from 61% in the south facing façade to 66% in the west facing façade. Therefore, the variation of curtain wall configurations has more significant impact on the energy balance than on the energy consumption.

Table 4.1. Coefficient of variation (υ) of the end-use energy of the office unit with various curtain wall configurations at four cardinal orientations.

Cardinal Direction	Heating	Cooling	Lighting	Total	Generation to Consumption Ratio
East	0.339	0.550	0.280	0.186	0.645
South	0.378	0.648	0.279	0.165	0.610
West	0.342	0.564	0.283	0.201	0.660
North	0.342	0.421	0.291	0.186	0.640

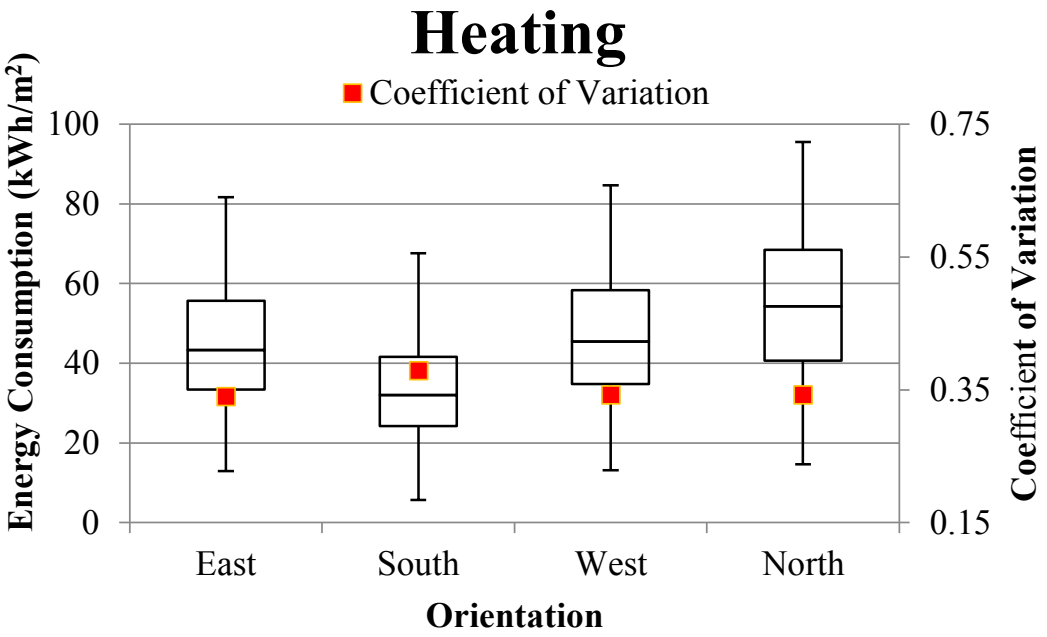

Figure 4.1. The boxplot of heating energy consumption and coefficient of variation in four cardinal orientations.

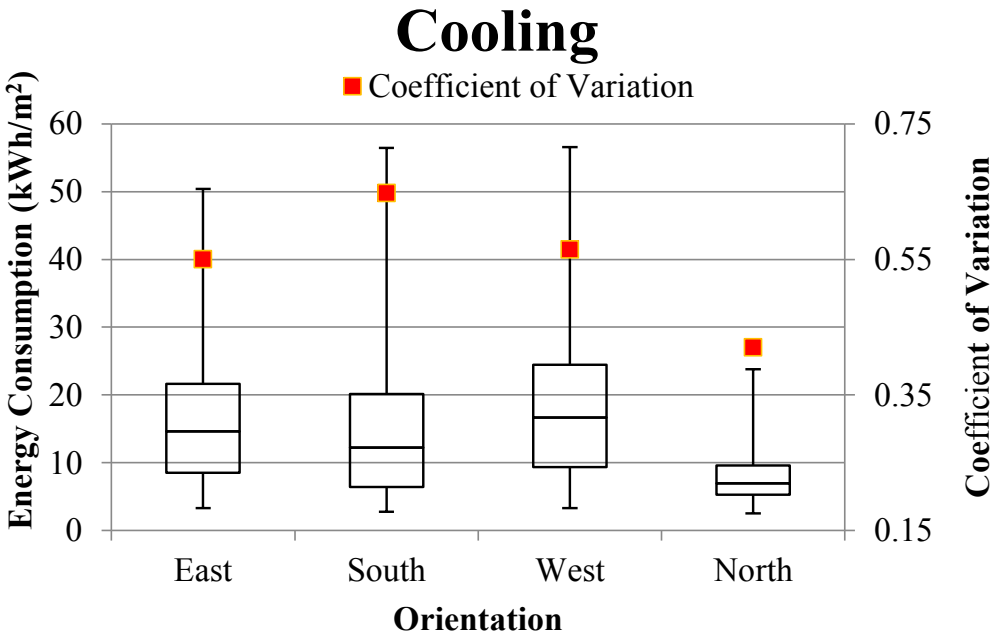

Figure 4.2. The boxplot of cooling energy consumption and coefficient of variation in four cardinal orientations.

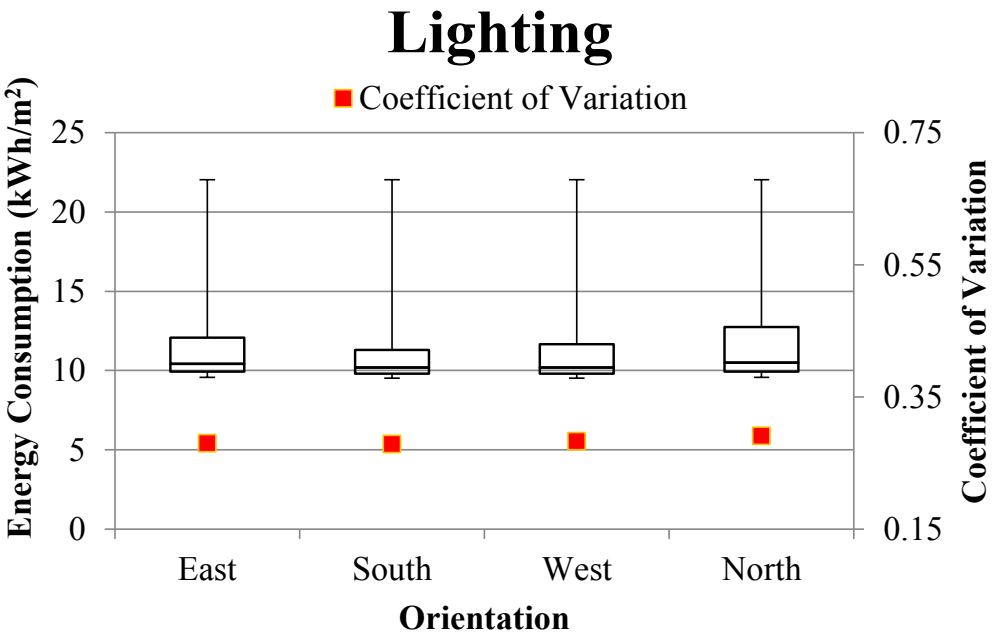

Figure 4.3. The boxplot of lighting energy consumption and coefficient of variation in four cardinal orientations.

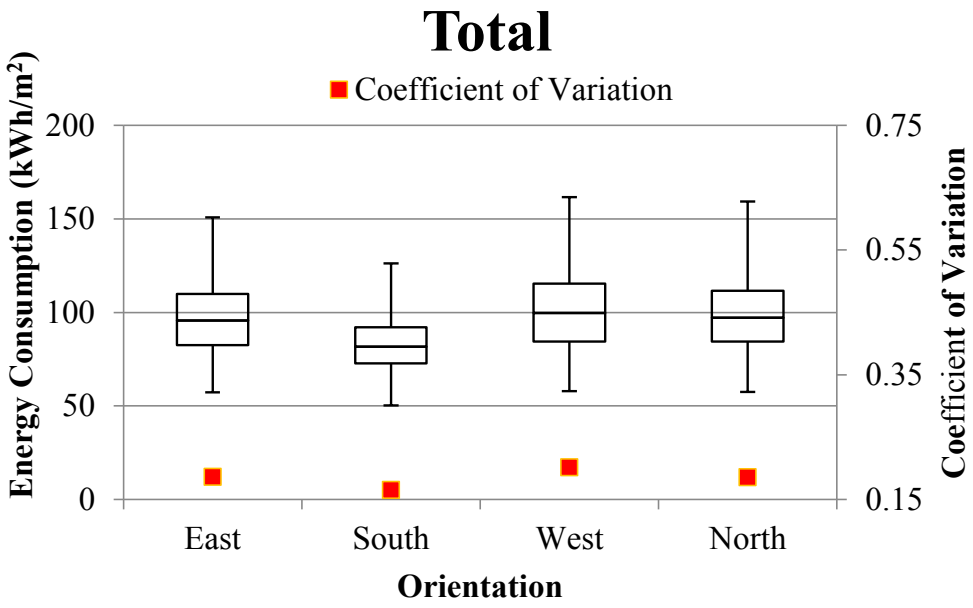

Figure 4.4. The boxplot of lighting energy consumption and coefficient of variation in four cardinal orientations.

Table 4.2. Breakdown of the end-use energy over the total energy consumption for four cardinal orientations.

	East			South			West			North		
	Min	Average	Max	Min	Average	Max	Min	Average	Max	Min	Average	Max
Heating	18%	45%	67%	8%	39%	67%	19%	46%	68%	23%	55%	75%
Cooling	3%	16%	47%	2%	17%	57%	3%	17%	49%	2%	8%	25%
Lighting	7%	13%	33%	7%	14%	33%	6%	12%	33%	6%	13%	33%
Fan power & plug load	17%	25%	40%	19%	29%	45%	16%	25%	40%	15%	24%	40%

Figure 4.1 - 4.4 show the box plot of the heating, cooling, lighting and total energy consumption of this office unit for each cardinal orientation. Table 4.2 shows the breakdown of heating, cooling and lighting energy over the total energy consumption for the four cardinal orientations. On average, heating, cooling and lighting takes 45-55%, 8-17%, 13% of the total energy consumption, respectively.

4.2 Sensitivity analysis

4.2.1 The impact of orientations

As shown in Table 4.3, there is a significant influence of orientations on end-use energy consumption and energy balance. In all end-use energy consumption, F-values are greater than the critical values at 5% significance level with very small p-values which are close to 0. P-value is also called level of significance. It is defined as the probability of obtaining a value of the test statistic that is likely to reject null hypothesis.

The null hypothesis in the case of heating energy consumption is that the average values of heating energy consumptions are the same among four orientations. By the same token, the null hypothesis in case of the rest of the end-use energy consumptions is that the average values of the energy consumptions are the same among four orientations.

Since p-values in heating, cooling, lighting, annual total energy consumption and the energy balance are very small which is smaller than 0.0005, the null hypothesis that the average values of energy consumptions are the same among four orientations can be rejected.

The impact of orientations is quantified by the magnitude of F-values. A large value of F-value represents large variance of end-use energy consumptions among four orientations.

Since the F-values of energy balance is the highest, the variance of energy balance among four orientations is the most significant. It explained the impact of orientation on energy balance is the greatest, followed by heating, total and cooling. The impact of orientation on lighting energy consumption is the least. The results agree with the study by Nasrollahi, (2013).

Table 4.3. F-test results on end-use energy consumption.

	F-values	**Critical values**
Heating energy consumption	($F_{3,98300}$ = 7893 , p < .0005)	1.55
Cooling energy consumption	($F_{3,98300}$ = 6763 , p < .0005)	1.55
Lighting energy consumption	($F_{3,98300}$ = 192 , p < .0005)	1.55
Total energy consumption	($F_{3,98300}$ = 5198 , p < .0005)	1.55
Energy Balance	($F_{3,98300}$ = 8520 , p < .0005)	1.55

4.2.2 The impact of ten parameters

Ranking of the significance of each design parameter is obtained based on their total sensitivity index. As shown in Table 4.4 and Figure 4.5, the window wall ratio (WWR), U-value of glazing and infiltration are the three most significant parameters influencing the annual heating energy consumption in the perimeter zone of the office unit for all the four orientations. The WWR has the most significant impact for all orientations. The total sensitivity index of WWR ranges from 0.63 for the south orientation to 0.8 for the north orientation. The influence of WWR and U-value of glazing is comparable for south orientation while the influence of WWR is twice greater than U-value in the north orientation. The total sensitivity index of U-value of glazing is about 1.7-2 times greater than that of the third most significant parameter, i.e. infiltration. The fourth most significant parameter is SHGC. Other design parameters such as the overhang inclination and depth, U-value of frame and visible transmittance have comparable impact on the annual heating energy consumption for all four orientations. The influence of U-value of spandrel panel is the least for all four orientations.

Table 4.4. Ranking of the nine design parameters for annual heating energy consumption and their corresponding total sensitivity index for the four cardinal orientations.

Rank	East		South		West		North	
1	WWR	0.69	WWR	0.63	WWR	0.71	WWR	0.79
2	Ugl	0.52	Ugl	0.55	Ugl	0.50	Ugl	0.41
3	Infiltration	0.25	Infiltration	0.32	Infiltration	0.23	Infiltration	0.19
4	SHGC	0.19	SHGC	0.29	SHGC	0.18	SHGC	0.14
5	Depth	0.15	Depth	0.26	Depth	0.14	Ufr	0.11
6	Inclination	0.14	Inclination	0.20	Inclination	0.14	Inclination	0.11
7	Ufr	0.14	Ufr	0.19	Ufr	0.13	Depth	0.11
8	Tv	0.14	Tv	0.18	Tv	0.13	Tv	0.11
9	Usp	0.12	Usp	0.16	Usp	0.11	Usp	0.09

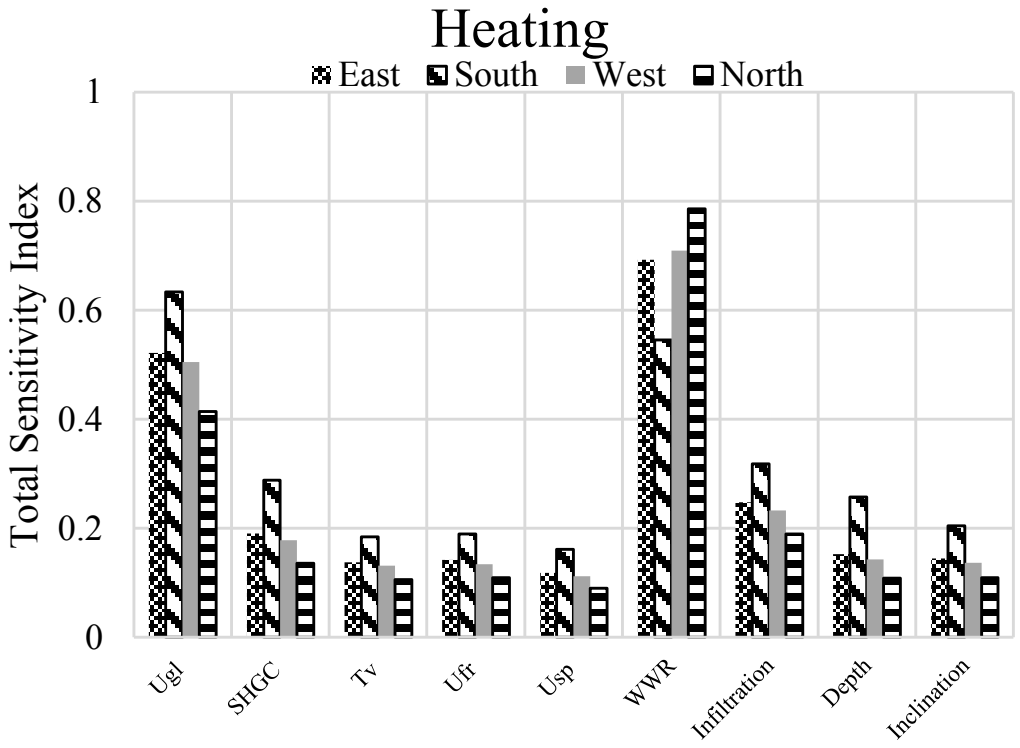

Figure 4.5. Total sensitivity index of the nine design parameters for the annual heating energy consumption.

Table 4.5. Ranking of the nine design parameters for annual cooling energy consumption and their corresponding total sensitivity index for the four cardinal orientations.

Rank	East		South		West		North	
1	WWR	0.75	WWR	0.70	WWR	0.76	WWR	0.60
2	SHGC	0.19	SHGC	0.25	SHGC	0.19	SHGC	0.39
3	Depth	0.06	Depth	0.08	Depth	0.06	Ugl	0.06
4	Ugl	0.03	Ugl	0.04	Ugl	0.02	Depth	0.03
5	Inclination	$7x10^{-3}$	Tv	0.01	Tv	$6x10^{-3}$	Tv	0.02
6	Tv	$4x10^{-3}$	Infiltration	$5x10^{-3}$	Inclination	$6x10^{-3}$	Infiltration	$7x10^{-3}$
7	Infiltration	$2x10^{-3}$	Inclination	$2x10^{-3}$	Infiltration	$1x10^{-3}$	Usp	$7x10^{-3}$
8	Usp	$2x10^{-3}$	Usp	$2x10^{-3}$	Usp	$1x10^{-3}$	Inclination	$6x10^{-3}$
9	Ufr	$2x10^{-4}$	Ufr	$3x10^{-4}$	Ufr	$1x10^{-4}$	Ufr	$2x10^{-3}$

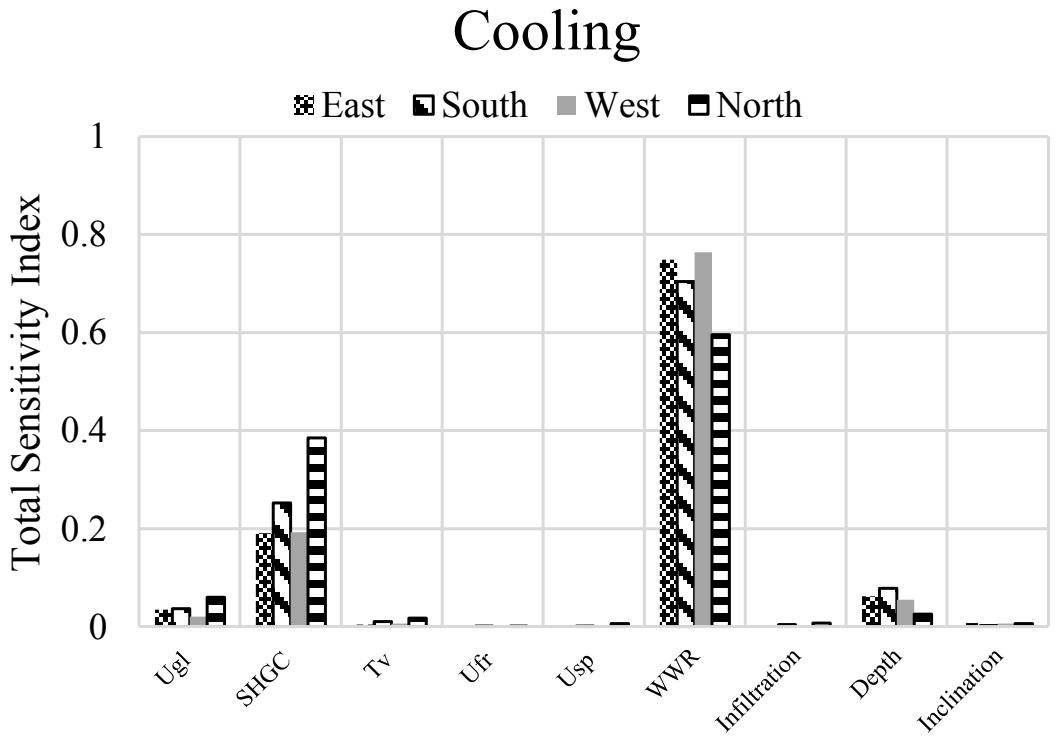

Figure 4.6. Total sensitivity index of the nine design parameters for annual cooling energy consumption.

As shown in Table 4.5 and Figure 4.6, the WWR, SHGC, and the depth of overhang are the three most significant parameters influencing the annual cooling energy consumption in the perimeter zone of the office building. The WWR has the most significant impact with a total sensitivity index of 0.75, which is about 4 times greater than the second most significant parameter, i.e. SHGC on the east and west orientation. For the south façade, the total sensitivity index of WWR is about 0.7, which is 2.8 times greater than SHGC, while on the north façade the total sensitivity index of WWR is 0.6, which is 1.5 times greater than SHGC. The depth of overhang ranks the third for the east, south and the west, however its influence is much smaller (total sensitivity index of about 0.06-0.08) compared to WWR and SHGC. For the north façade, U-value of glazing ranks the 3rd with a total sensitivity index of 0.06. The influence of U-value of frame, infiltration, U-value of spandrel panel, and visible transmittance are negligible on the cooling energy consumption for all the four orientations.

As shown in Table 4.6 and Figure 4.7, the WWR, depth of overhang (Depth) and inclination of overhang (Inclination) are the three most significant parameters influencing the annual lighting energy consumption in the perimeter zone of the office unit for east, south and west orientation. The WWR has the most significant impact with a total sensitivity index of about 0.88, which is about 4-5 times greater than the second most significant parameter, i.e. depth of overhang. The second most significant parameter, i.e. overhang depth, has a total sensitivity index of 0.16 to 0.23, which is about twice greater than the overhang inclination. The visible transmittance ranks the 4th and has similar total sensitivity indices as the overhang inclination. Other design parameters such as SHGC, U-value of glazing, U-value of frame, U-value of spandrel, and infiltration has little influence on the lighting energy consumption.

Table 4.6. Ranking of the nine design parameters for annual lighting energy consumption and their corresponding total sensitivity index for the four cardinal orientations.

Rank	East		South		West		North	
1	WWR	0.88	WWR	0.90	WWR	0.89	WWR	0.86
2	Depth	0.19	Depth	0.23	Depth	0.20	Depth	0.16
3	Inclination	0.09	Inclination	0.11	Inclination	0.10	Tv	0.10
4	Tv	0.08	Tv	0.06	Tv	0.07	Inclination	0.08
5	Ugl	$2x10^{-3}$	SHGC	$6x10^{-4}$	Ugl	$1x10^{-4}$	SHGC	$9x10^{-4}$
6	SHGC	$1x10^{-4}$	Ugl	$7x10^{-5}$	SHGC	$6x10^{-6}$	Ugl	$4x10^{-4}$

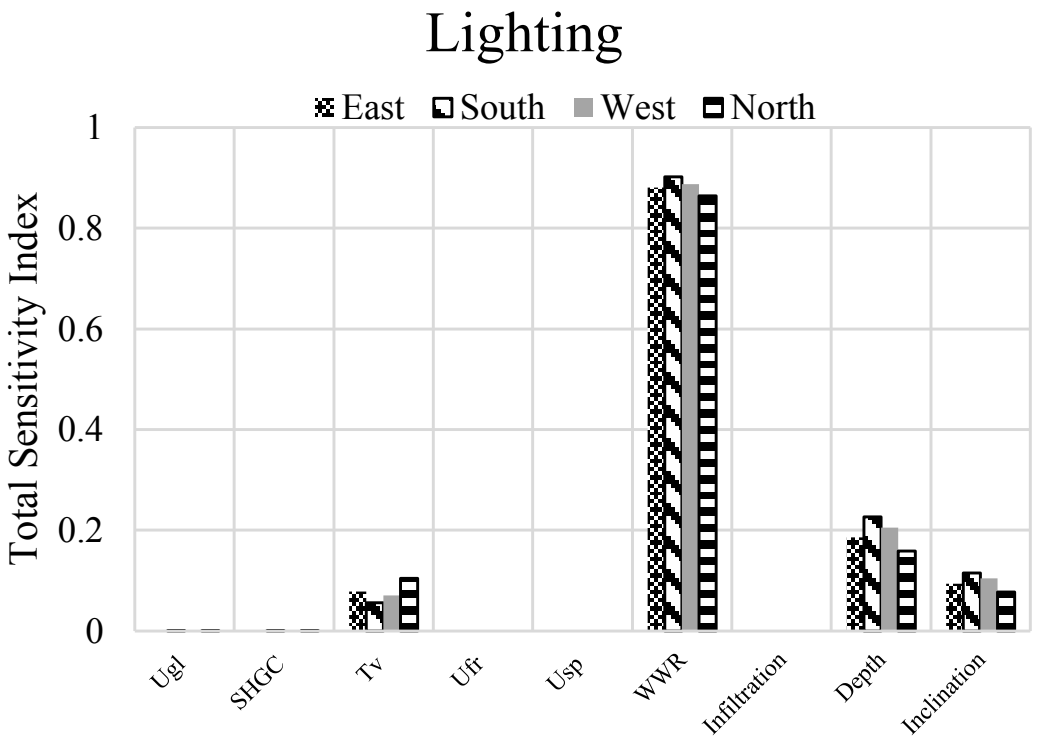

Figure 4.7. Total sensitivity index of the nine design parameters for annual lighting energy consumption.

Table 4.7. Ranking of the nine design parameters for annual energy consumption including heating, cooling and lighting and their corresponding total sensitivity index for the four cardinal orientations.

Rank	East		South		West		North	
1	WWR	0.96	WWR	0.93	WWR	0.95	WWR	0.90
2	Ugl	0.31	Ugl	0.43	Ugl	0.28	Ugl	0.40
3	Infiltration	0.17	Infiltration	0.25	Infiltration	0.15	Infiltration	0.20
4	Inclination	0.11	Depth	0.22	Inclination	0.09	SHGC	0.12
5	Depth	0.11	Inclination	0.19	Depth	0.09	Inclination	0.12
6	Ufr	0.10	SHGC	0.18	SHGC	0.09	Depth	0.12
7	Tv	0.10	Ufr	0.16	Ufr	0.09	Ufr	0.12
8	SHGC	0.10	Tv	0.16	Tv	0.09	Tv	0.11
9	Usp	0.08	Usp	0.13	Usp	0.07	Usp	0.09

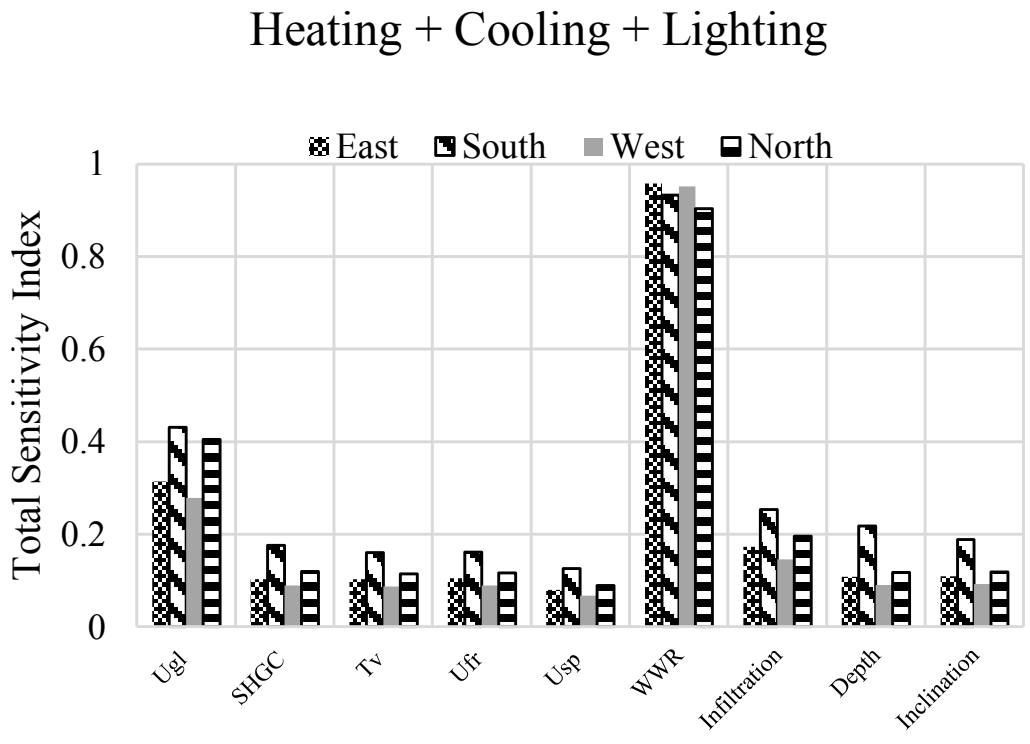

Figure 4.8. Total sensitivity index of the nine design parameters for annual lenergy consumption including heating, cooling and lighting.

As for the annual energy consumption for space conditioning and lighting in Table 4.7 and Figure 4.8, similar to the annual heating energy consumption, the WWR, U-value of glazing, and infiltration are the three most significant parameters. The total sensitivity index of WWR is 0.90 to 0.96, which is about 2-3 times greater than the second most significant parameter. Design parameters such as SHGC, the overhang inclination and depth, U-value of frame and visible transmittance have comparable impact on the annual energy for space conditioning and lighting in all four orientations. The influence of U-value of spandrel panel is the least. It seems that all the design parameters have slightly greater influence on the annual total energy consumption for south façade than on other orientations. Due to the lower solar radiation received, the influence of U-value of glazing and infiltration on north façade is greater than that on the east and west façade.

The difference between annual energy generation and annual energy consumption is the energy balance. As shown in Table 4.8 and Figure 4.9, WWR, PV efficiency, and glazing U-value are the three most significant parameters influencing the energy balance in the perimeter zone. Again, the influence of WWR is the most significant with a total sensitivity index of about 0.90 to 0.96, which is about 4 to 11 times greater than the PV efficiency, the second most significant parameter. As shown in Figure 4.9, the WWR has the most significant influence on the annual energy consumption for space conditioning and lighting, in the meantime, the WWR directly determines the spandrel area available for PV integration since in this paper PV modules are assumed to be integrated within the spandrel panel. The influence of PV efficiency is about 1.8 times greater for the east and west façade, about 2.2 times greater for the south façade than the U-value of glazing and about the same as the U-value of glazing for the north façade. Other design parameters are not significant.

Table 4.8. Ranking of the ten design parameters for energy balance and their corresponding total sensitivity index for the four cardinal orientations.

Rank	East		South		West		North	
1	WWR	0.87	WWR	0.82	WWR	0.88	WWR	0.89
2	PV	0.09	PV	0.09	PV	0.08	PV	0.18
3	Ugl	0.05	Ugl	0.04	Ugl	0.05	Ugl	0.16
4	Infiltration	0.03	Depth	0.03	Infiltration	0.03	Infiltration	0.08
5	Depth	0.02	Infiltration	0.02	Depth	0.02	Depth	0.05
6	Inclination	0.02	Inclination	0.02	Inclination	0.02	Inclination	0.05
7	Ufr	0.02	SHGC	0.01	SHGC	0.02	SHGC	0.05
8	SHGC	0.02	Usp	0.01	Ufr	0.02	Ufr	0.05
9	Tv	0.02	Ufr	0.01	Tv	0.02	Tv	0.05
10	Usp	0.02	Tv	0.01	Usp	0.01	Usp	0.04

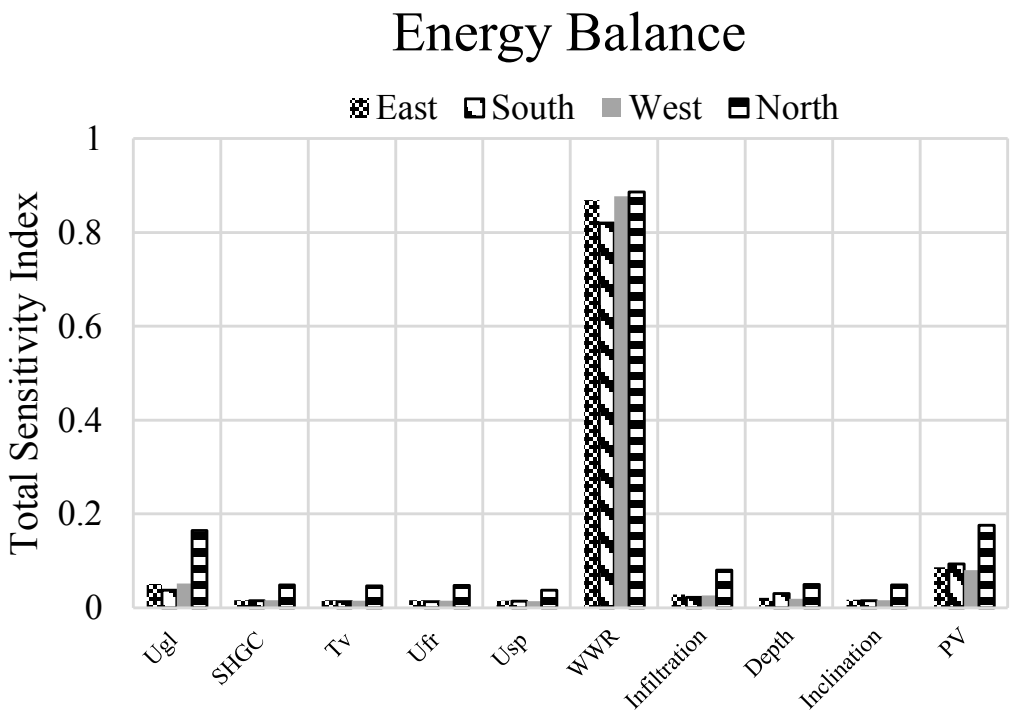

Figure 4.9. Total sensitivity index of the ten design parameters for the energy balance.

4.3 Plus-energy curtain wall configurations

As discussed in section 4.2, WWR, PV efficiency and U-value of glazing are the three most significant parameters influencing the energy balance of the perimeter zone of the office building located in Montreal. The influence of the fourth parameter is comparable to the third design parameter. The influence of other design parameters is not significant.

Among the 98,304 simulations, there are 4250 cases (17%) for the east façade, 9613 cases (39%) for the south façade, 4111 cases (17%) for the west façade, and zero case for the north façade that have achieved the annual energy balance. Table 4.9 shows the range of each of the ten design parameters for all plus-energy curtain wall configurations. Except for WWR, the range of the other nine parameters in plus-energy curtain wall configurations is the same as the original range of parameters propagated throughout all simulations for the east, south and west orientations. There are no configurations that can achieve energy balance for the north façade (Figure 4.10). This implies that WWR is the dominant factor that distinguishes plus-energy configurations and non plus-energy configurations. As shown in Figure 4.11, when the WWR is greater than 50%, no curtain wall configurations sampled can achieve the energy balance for the east façade. At a WWR of 60% for the south façade (Figure 4.12) and 50% for the west façade (Figure 4.13), respectively, no curtain wall configurations sampled can achieve the energy balance. Therefore it is necessary to investigate the range of other nine parameters in each bin of WWR.

Table 4.9. Range of the ten parameters of plus-energy curtain wall configurations.

	East	South	West	North
Total no. of sampled cases	24576	24576	24576	24576
No. of plus energy configuration	4250	9613	4111	0
Percentage of plus-energy configuration	17%	39%	17%	0
Range of WWR	0.10-0.47	0.10-0.61	10-47%	n/a
Range of PV	0.09-0.19	0.09-0.19	0.09-0.19	n/a
Range of U_{gl}	1.10-2.40	1.10-2.40	1.10-2.40	n/a
Range of SHGC	0.33-0.70	0.33-0.70	0.33-0.70	n/a
Range of T_v	0.16-0.79	0.16-0.79	0.16-0.79	n/a
Range of U_{fr}	0.80-8.80	0.80-8.80	0.80-8.80	n/a
Range of U_{sp}	0.15-0.28	0.15-0.28	0.15-0.28	n/a
Range of Infiltration	0.01-0.22	0.01-0.22	0.01-0.22	n/a
Range of Overhang Depth	0.10-1.00	0.10-1.00	0.10-1.00	n/a
Range of Overhang Inclination	0-90	0-90	0-90	n/a

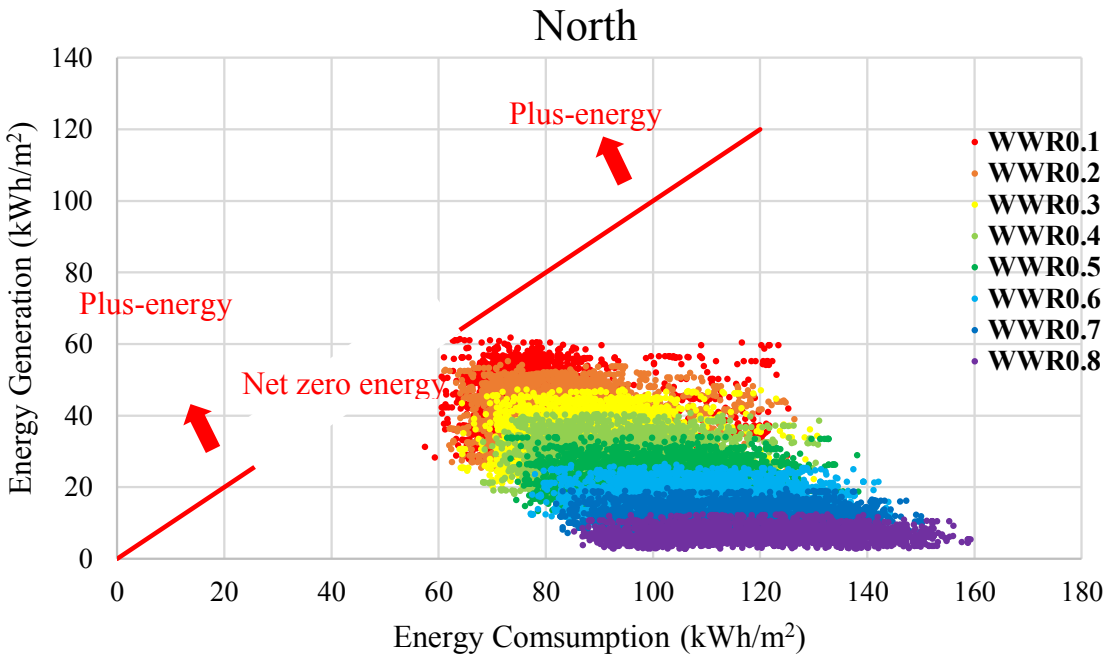

Figure 4.10. Energy generation against energy consumption in north façade with various WWR.

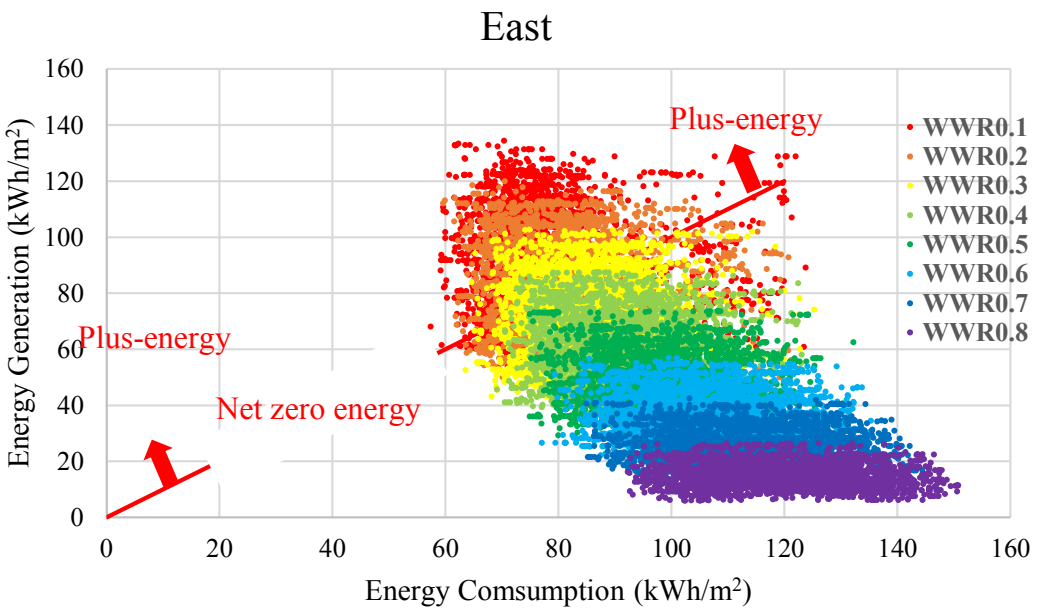

Figure 4.11. Energy generation against energy consumption of east façade with various WWR.

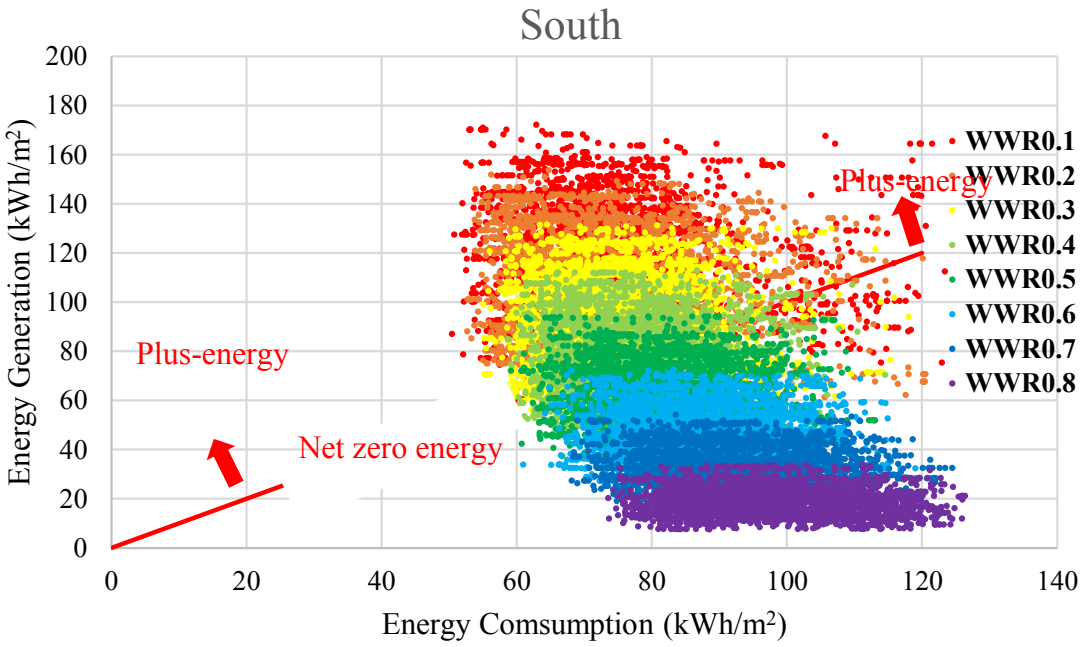

Figure 4.12. Energy generation against energy consumption in south façade with various WWR.

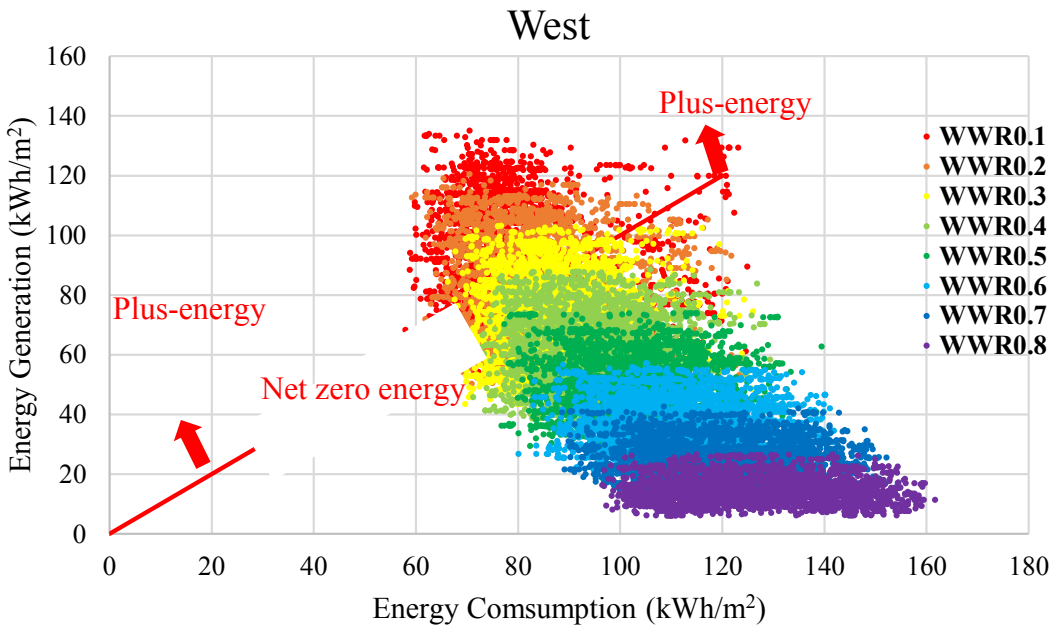

Figure 4.13. . Energy generation against energy consumption in west façade with various WWR.

Table 4.10 shows the breakdown of the range of parameters for each bin of WWR. When WWR is smaller than 40%, the range of design parameters in the plus-energy configurations is similar to the original range for the east, south, and west façades, which implies that with the proper combination these façades can achieve the energy balance using products available. When the WWR increases, the configurations that can achieve energy balance decreases.

To generalize the conclusions, the three most significant parameters, WWR, U-value of glazing and PV efficiency are further analyzed by setting these parameters at intervals with all the other parameters set at the mean values of their range. In total, 1000 configurations for each of the three orientations that have achieved energy balance are assembled and re-simulated. The results are presented in Figure 4.14 to Figure 4.17. The color bars shown in these figures are the differences between the energy generation and the total annual energy consumption. Positive value means that the energy generation is greater than the total annual energy consumption, i.e. plus energy.

Table 4.10. Breakdown of the range of design parameters for each bin of WWR of plus-energy configurations.

East						
WWR	0.1-0.2	0.2-0.3	0.3-0.4	0.4-0.47		
Range of PV	0.09-0.19	0.10-0.19	0.13-0.19	0.17-0.19		
Range of U_{gl}	1.10-2.40	1.10-2.40	1.10-2.40	1.10-1.79		
Range of SHGC	0.33-0.70	0.33-0.70	0.33-0.70	0.33-0.70		
Range of T_v	0.16-0.79	0.16-0.79	0.16-0.79	0.21-0.79		
Range of U_{fr}	0.80-8.80	0.80-8.80	0.80-8.78	1.11-7.71		
Range of U_{sp}	0.15-0.28	0.15-0.28	0.15-0.28	0.16-0.28		
Range of Infiltration	0.01-0.22	0.01-0.22	0.01-0.22	0.01-0.16		
Range of Overhang Depth	0.10-1.00	0.10-1.00	0.10-1.00	0.17-0.84		
Range of Overhang Inclination	0-90	0-90	0-90	5-88		
South						
WWR	0.1-0.2	0.2-0.3	0.3-0.4	0.4-0.5	0.5-0.6	0.6
Range of PV	0.09-0.19	0.09-0.19	0.09-0.19	0.11-0.19	0.14-0.19	0.18-0.19
Range of U_{gl}	1.10-2.40	1.10-2.40	1.10-2.40	1.10-2.40	1.10-2.40	1.23-1.33
Range of SHGC	0.33-0.70	0.33-0.70	0.33-0.70	0.33-0.70	0.33-0.70	0.39-0.42
Range of T_v	0.16-0.79	0.16-0.79	0.16-0.79	0.16-0.79	0.17-0.79	0.47-0.68
Range of U_{fr}	0.82-8.80	0.80-8.80	0.80-8.80	0.80-8.80	0.84-8.78	4.18-6.46
Range of U_{sp}	0.15-0.28	0.15-0.28	0.15-0.28	0.15-0.28	0.15-0.28	0.20-0.24
Range of Infiltration	0.01-0.22	0.01-0.22	0.01-0.22	0.01-0.22	0.01-0.22	0.02-0.07
Range of Overhang Depth	0.10-1.00	0.10-1.00	0.10-1.00	0.10-1.00	0.11-1.00	0.33-0.61
Range of Overhang Inclination	0-90	0-90	0-90	0-90	0-86	33-35
West						
WWR	0.1-0.2	0.2-0.3	0.3-0.4	0.4-0.47		
Range of PV	0.09-0.19	0.11-0.19	0.13-0.19	0.17-0.19		
Range of U_{gl}	1.10-2.40	1.10-2.40	1.10-2.40	1.11-1.79		
Range of SHGC	0.33-0.70	0.33-0.70	0.33-0.70	0.34-0.67		
Range of T_v	0.16-0.79	0.16-0.79	0.16-0.79	0.21-0.78		
Range of U_{fr}	0.80-8.80	0.80-8.80	0.80-8.80	1.20-7.71		
Range of U_{sp}	0.15-0.28	0.15-0.28	0.15-0.28	0.16-0.27		
Range of Infiltration	0.01-0.22	0.01-0.22	0.01-0.22	0.01-0.14		
Range of Overhang Depth	0.10-1.00	0.10-1.00	0.10-1.00	0.17-0.82		
Range of Overhang Inclination	0-90	0-90	0-90	5-88		

Figure 4.14 (a) shows the energy balance of all curtain wall configurations while Figure 4.14(b) shows plus-energy curtain wall configurations with respect to the three most significant parameters for the east façade. With the increase of WWR, to achieve the energy balance curtain wall design with lower glazing U-value and higher PV efficiency is required. At a WWR of 40%, if the PV efficiency is at the maximum of 19%, the glazing U-value can be any value within its range. Similarly as shown in Figure 4.15 for the west façade, when the WWR is higher than 40%, no configurations sampled can achieve the energy balance. For south façade (Figure 4.16), there are more configurations that can achieve the energy balance and the WWR can be generally increased up to 60%. At a WWR of 50%, if the PV efficiency is higher than 17%, the glazing U-value can be any value within its range.

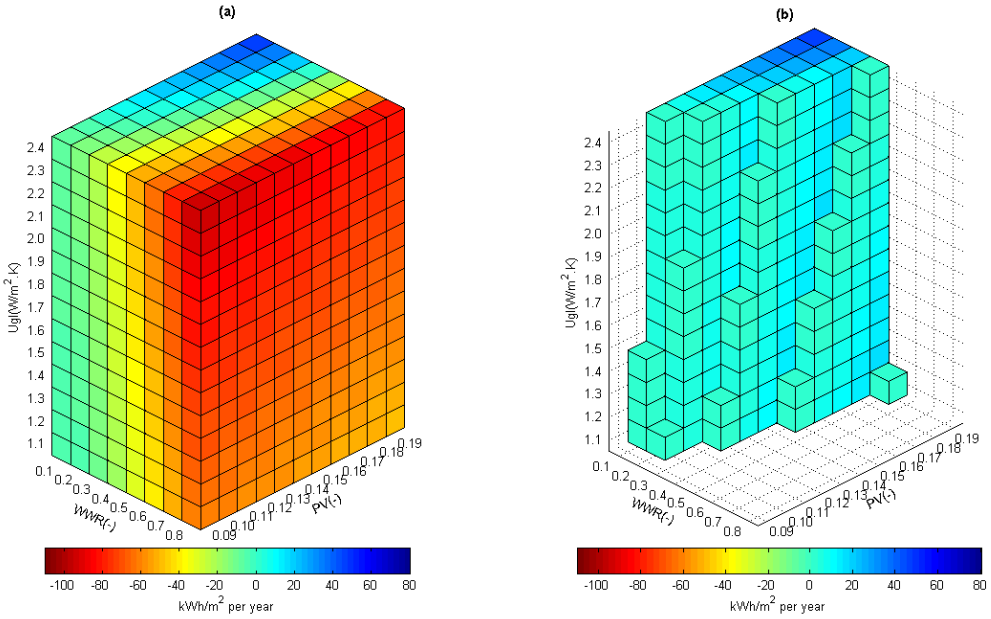

Figure 4.14. Voxel plot of energy performance with respect to the three most significant design parameters in the east façade (a) all curtain wall configurations (b) plus-energy curtain walls configurations. Color bars show the difference between energy generation and energy consumption in kWh/m^2 per year. Positive means “plus energy”.

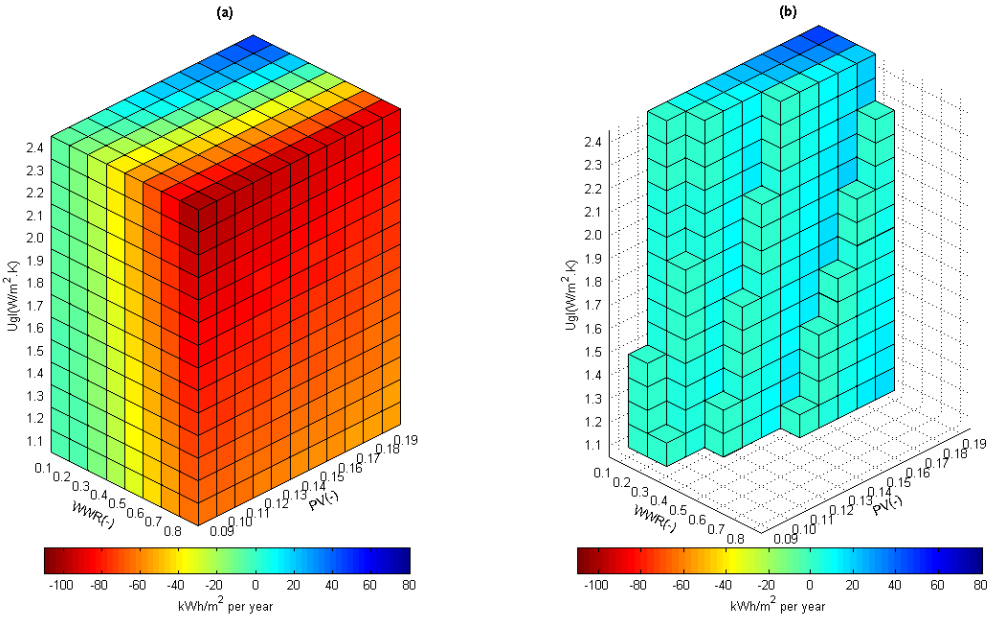

Figure 4.15. Voxel plot of energy performance with respect to the three most significant design parameters in the west façade (a) all curtain wall configurations (b) plus-energy curtain walls configurations.

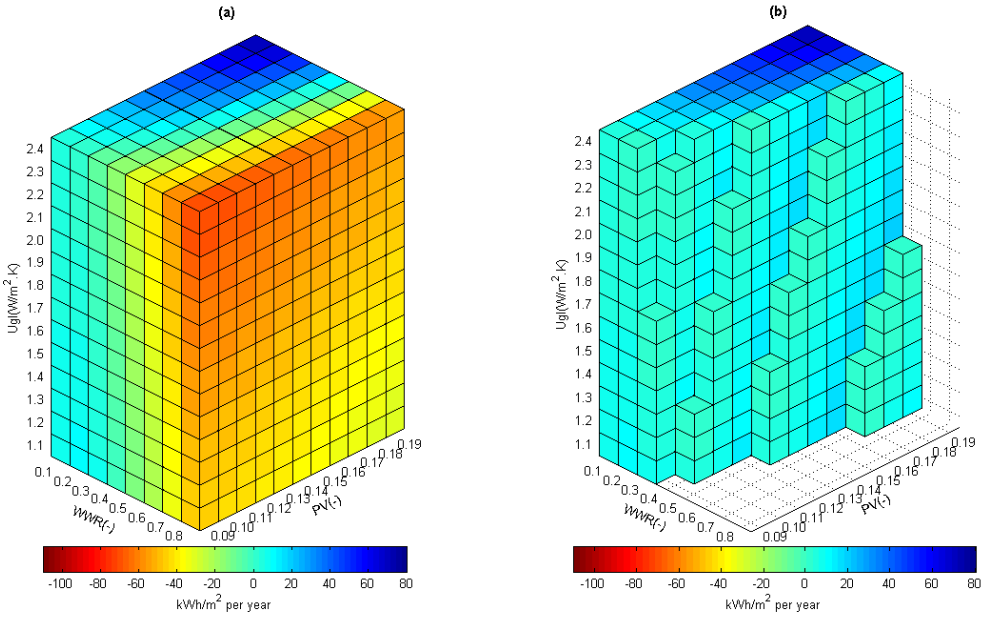

Figure 4.16. Voxel plot of energy performance with respect to the three most significant design parameters in the south façade (a) all curtain wall configurations (b) plus-energy curtain walls configurations.

Chapter 5 Plus-energy curtain wall configurations design tools

5.1 Introduction

Designing the plus-energy curtain wall is not an easy task because curtain walls are not energy consumers and therefore, there is no energy accounting at the curtain wall level. Designing plus-energy curtain walls needs to take into account the interdependency relationship among the design parameters of curtain walls, the outdoor conditions and also the indoor conditions. The current building performance simulations tools can only provide the numerical values of building performance when a particular curtain wall configuration is specified; that is, these tools are ***evaluation tools*** based on user inputs, there is a one-to-one relationship between inputs and results. Solely using building simulations programs cannot easily assess the impact of decisions on building energy performance. During the early design stages, comparing design alternatives is more important than evaluating absolute values of building performance. Most existing building performance simulations tools are only post-design evaluation (Attia et al., 2012). It is difficult to reach the optimum plus-energy curtain walls configurations by going through repeated simulations processes, which can range from an ad-hoc parametric study with no guarantee of optimal solutions. On the other hand, there are ***solution-finding tools***, such as optimization, that result in solutions based on user desired set of performance criteria. The solutions are optimal only with respect to the setting at the time of performing the optimization and therefore are highly constrained.

The result of these processes is a set of solutions, which the designers can either accept or reject, but not interactively involve in the process and make their own choices. This chapter proposes a design tool to generate the desired plus-energy curtain wall configurations and presents the results of the development of such tool. The main objective is to enhance and facilitate the design processes for plus-energy curtain walls. The results demonstrate that the design tool is useful for curtain wall designers. The proposed design tool is currently a developing framework which needs more simulated results in different scenarios and climates zones before being adopted as commercial application.

5.2 Design tool overview

This design tool is based on Microsoft Excel visual basic programming platform. It is meant to facilitate the design process of plus-energy curtain walls, and thus, the tool should offer a user-friendly interface with reduced number of inputs such that the designers could take full control of the design process.

5.3 Design tool workflow

A database is formed based on the previous simulation results. Base on the sensitivity analysis results, the configurations of plus-energy curtain walls are determined by the most three sensitive parameters, the WWR, the efficiency of photovoltaic panels and the u-value of glazing. The impact of the forth and the later sensitivity parameters is little such that the values of them does not affect the performance of plus-energy curtain walls. The barrier to integrate building performance simulation programs during early design phases is too many user inputs in the programs. In such case, the design tool is developed to address this challenge by reducing input parameters. The design tool requires the user to input the values of three parameters only, the database will filter out the configurations from the database which are not belonging to the specified values of the three parameters. The design tool then generates the configurations of plus-energy curtain walls and also their associated energy performance. Figure 5.1 shows the workflow of the design tool.

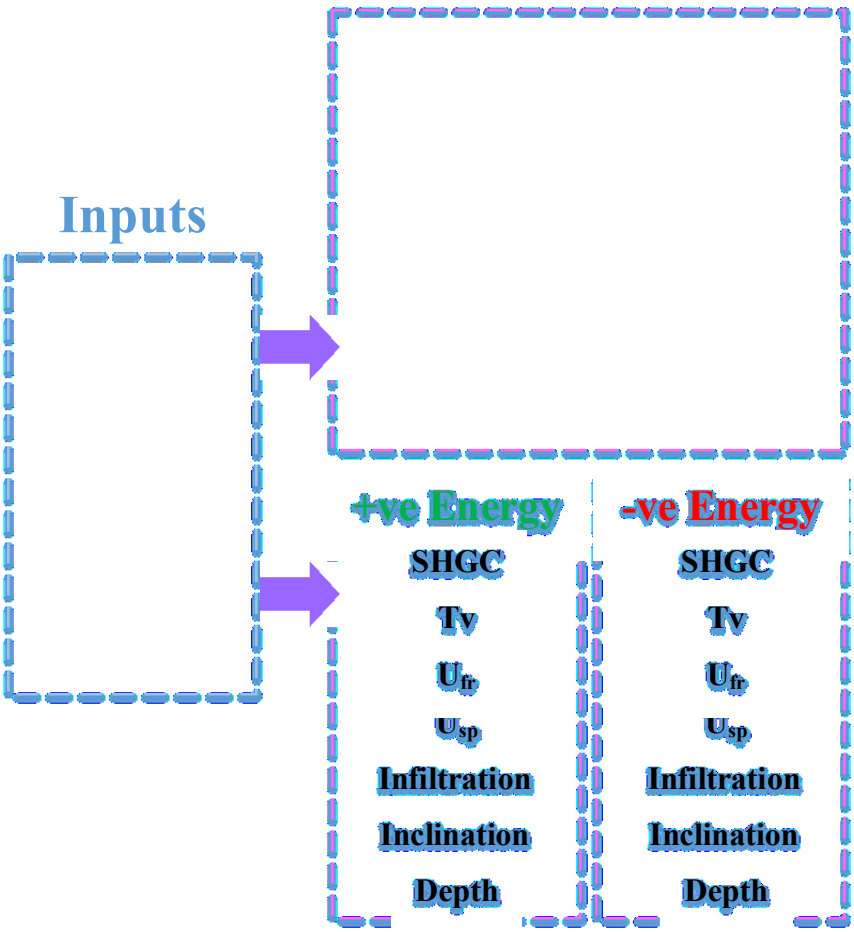

Figure 5.1. The Workflow of the design tool.

5.4 Design tool interface

As suggested, the design tool should offer a user-friendly interface to facilitate the design process. The objective in providing such interface is to allow the designers to explore the design options freely without being constrained by the tool. By contrast, current tools only offer definitive solutions that preclude designers from exploring design alternatives that might offer similar energy performance level with drastically different designs. Figure 5.2 presents the graphical user interface of the proposed design tool.

Figure 5.2. The graphical user interface of the proposed design tool.

As explained in previous section, WWR, the efficiency of photovoltaic panels and the U-value of glazing are found to be the most sensitive input parameters out of the ten parameters that have been investigated, which imply the alteration of any one of these three inputs will have a huge impact to the energy performance of the design. For this reason, it will be of interest to the designers to explore how these input parameters affect the energy performance individually (by changing one input parameter at a time) or collectively (by changing all three inputs at the same time over a range of values for each input).

The primary steps are:

1. Defining the values of Window Wall Ratio (WWR), Effective efficiency of Photovoltaic Panels (PV), and Glazing U-values (U_{gl}),
2. Filtering the configurations. This is done by clicking the icon (Filter Data). All the curtain walls configurations including “plus-energy” and non- “plus-energy” are listed out.
3. Comparing configurations of interest. The user can compare selected configurations side-by-side by scrolling the scroll bar.

Figure 5.3 highlights the interface that allows users to input the values to WWR, the effective efficiency of photovoltaic panels and the u-value of glazing individually. Table 5.1 list the range and the interval of the three parameters.

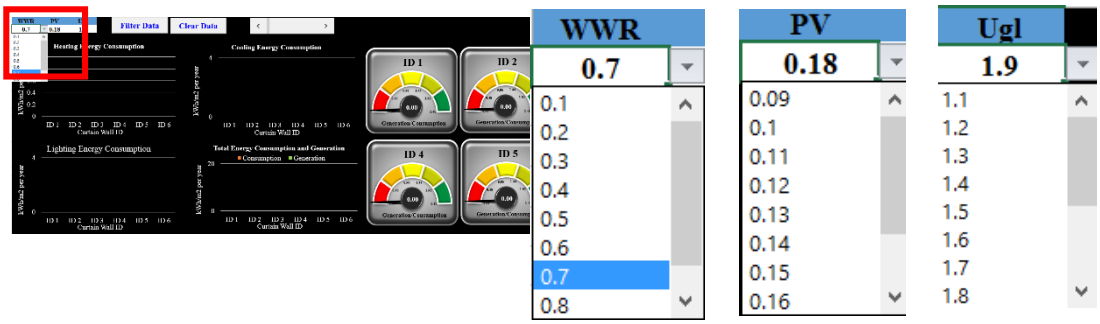

Figure 5.3. The Interface to input values for the three most sensitive parameters.

Table 5.1. The range and the interval of the three parameters.

	Description	Range	Interval
WWR	Window Wall Ratio	0.1-0.9	0.1
PV	Effective efficiency of photovoltaic panels	0.09-0.18	0.01
U_{gl}	Glazing U-value	1.1-2.4	0.01

WWR is allowed to be inputted over a range from 0.1 to 0.9, whereas efficiency of photovoltaic panels and the u-value of glazing can vary from 0.09 to 0.18 and 1.1 to 2.4 respectively. Users can define these values as wish and explore the impact on the fly.

Figure 5.4 highlights the “Filter Data” button which extracts the configurations from the database that correspond to the set of input values.

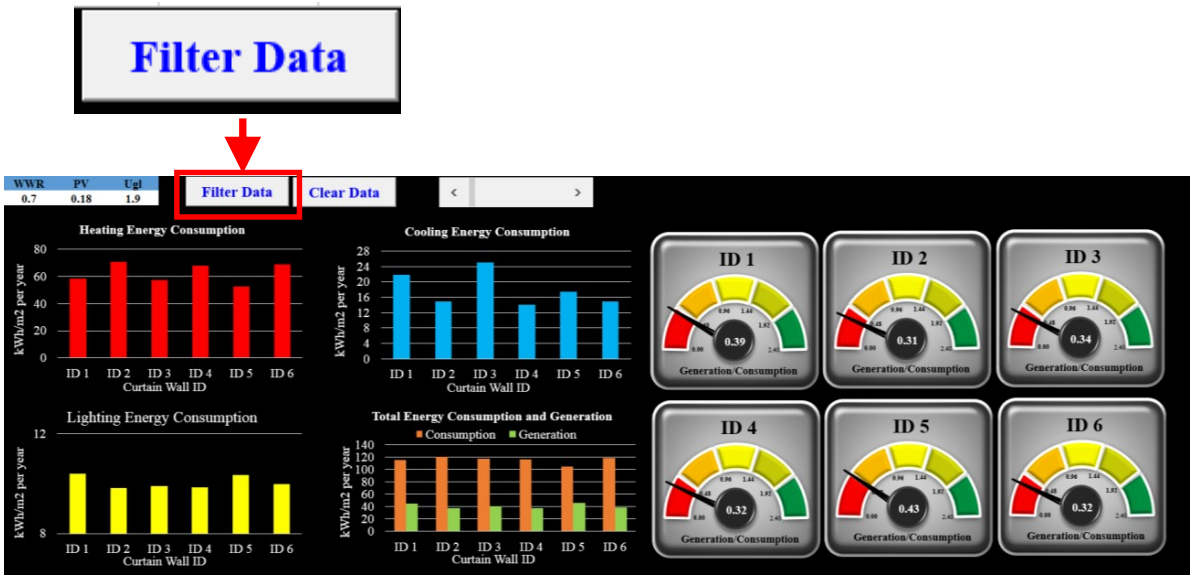

Figure 5.4. The “Filter Data” button.

Figure 5.5 highlights the “Clear Data” button. To investigate the impact with another set of input values, the users only need to “Clear Data” and extract configurations again with “Filter Data”.

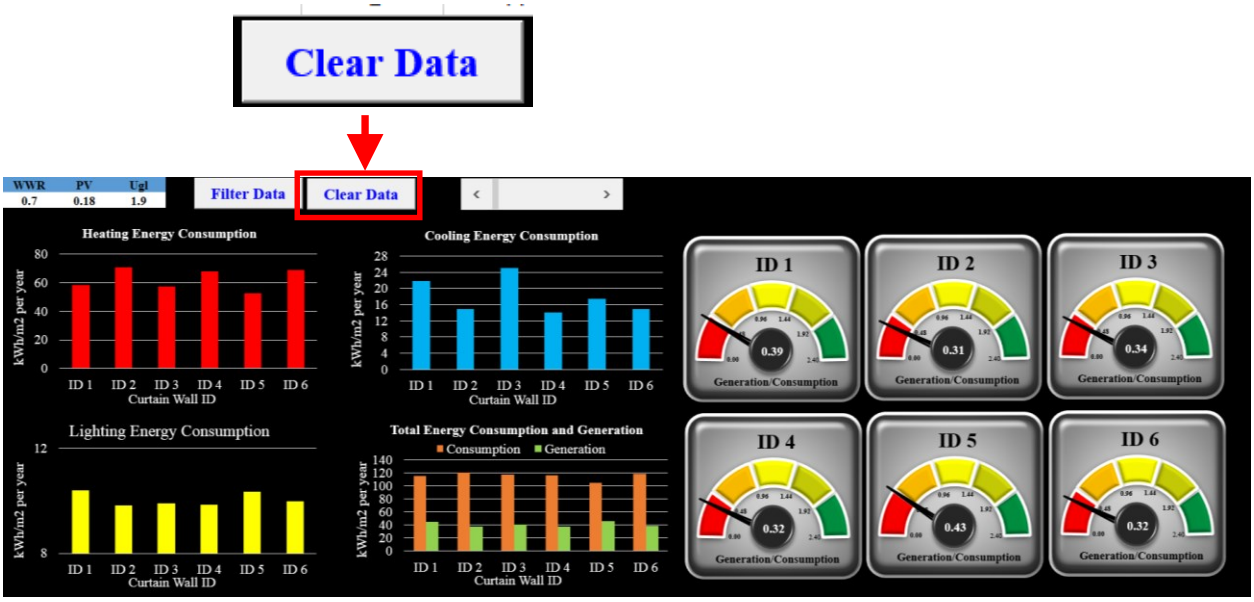

Figure 5.5. The “Clear Data” button.

The configurations will be displayed six at a time in the result display area. To help users to navigate through all possible configurations, Figure 5.6 highlights the slide bar that allows users to switch from one screen to another, in which each contains six configurations at a time.

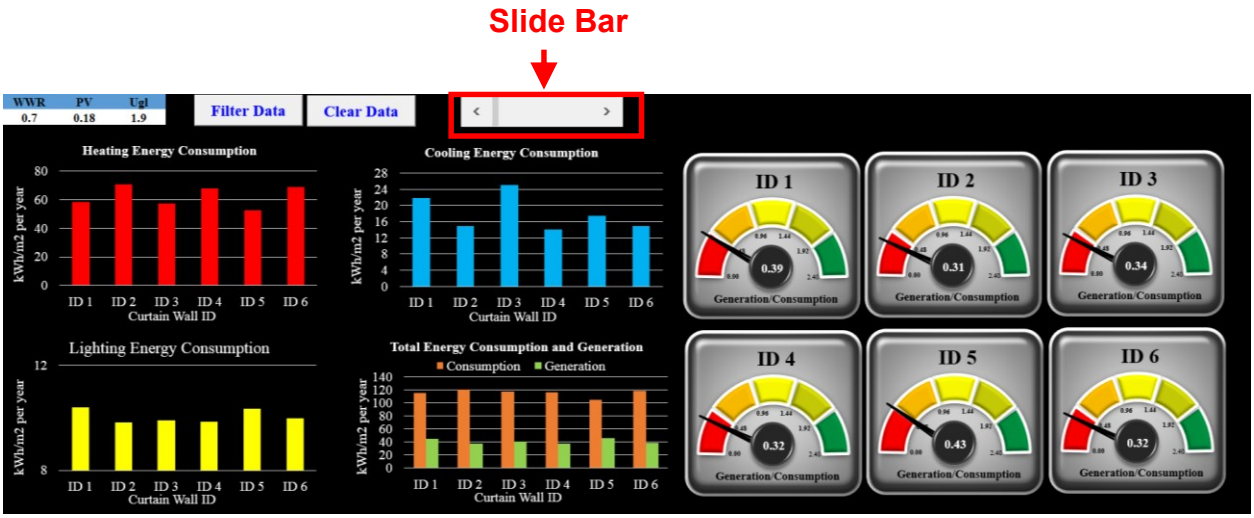

Figure 5.6. The Slide Bar to navigate through configurations.

Figure 5.7 highlights the result display area. The result includes the performance details of each configuration.

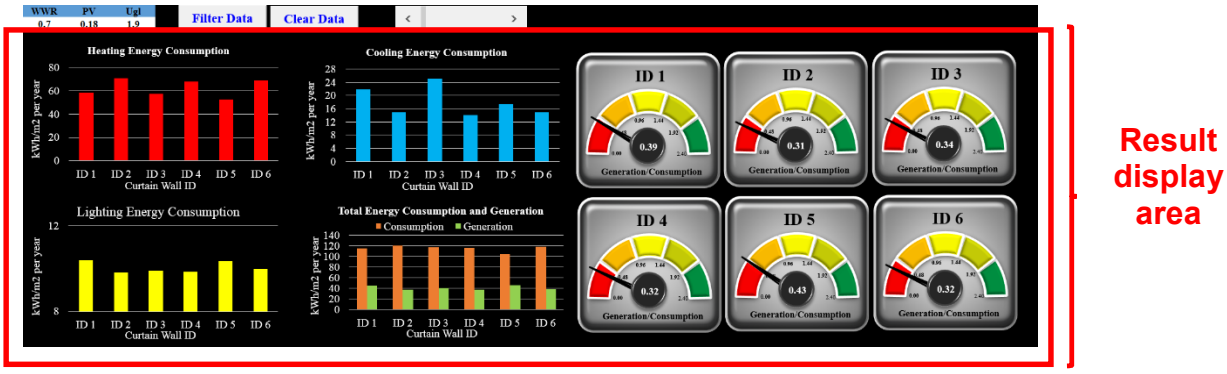

Figure 5.7. The result display area.

In the result display area, five different pieces of information are presented, namely:

1. Bar chart that displays the heating energy consumption
2. Bar chart that displays the cooling energy consumption
3. Bar chart that displays the lighting energy consumption
4. Bar chart that displays the total energy consumption and generation
5. Dial that indicates the energy generation / consumption ratio. Value passes beyond 1 (yellow to green region) represents a plus-energy configuration.

On a separate spreadsheet in Figure 5.8, numerical values of performance details and specification of the configurations (values of other design parameters) of all filtered configurations are listed.

ID	Ugl	SHGC	Tv	Ufr	Usp	WWR	iltration R	Depth	Inclination	PV	Heating	Cooling	Lighting	Total	Net	Ratio	Generation
1	1.925195	0.38998	0.65834	1.471875	0.274668	0.545313	5.88E-05	0.966602	116.1914	0.182383	51.5375	9.892429	10.10626	95.20762	-32.129	0.662537	63.07858
2	1.855371	0.560166	0.498994	1.698438	0.18415	0.517969	6.52E-05	0.285449	115.9277	0.180527	38.1401	20.38625	10.05751	92.86357	-24.9485	0.731342	67.91505
3	1.851563	0.601719	0.642344	4.675	0.212969	0.4875	7.23E-05	0.957813	167.3438	0.179063	45.05321	11.71421	11.10752	91.52685	-20.0073	0.781405	71.51953
4	1.876953	0.340117	0.216602	4.64375	0.185039	0.503125	0.000145	0.504297	112.8516	0.184141	54.65373	10.50486	11.51973	100.533	-29.3386	0.708169	71.19438
5	1.874414	0.50416	0.594355	2.409375	0.223379	0.476563	7.77E-05	0.242383	111.6211	0.175742	54.29762	15.60362	9.889384	104.0401	-31.8701	0.693675	72.17008
6	1.917578	0.331445	0.443008	6.83125	0.168789	0.515625	0.00014	0.314453	127.6172	0.177891	56.86712	10.7807	10.20268	101.7348	-34.4906	0.660975	67.24416
7	1.866162	0.566851	0.25813	8.366406	0.205288	0.506641	0.000155	0.322803	174.2432	0.176768	47.9112	19.09955	10.90464	102.2127	-33.9156	0.668186	68.29709
8	1.925195	0.335059	0.65834	1.471875	0.274668	0.545313	5.88E-05	0.966602	116.1914	0.182383	64.51935	7.927503	10.10626	106.264	-43.1854	0.593602	63.07858
9	1.855371	0.362158	0.498994	1.698438	0.18415	0.517969	6.52E-05	0.285449	115.9277	0.180527	45.20489	13.10663	10.08999	92.33022	-24.4152	0.735567	67.91505
10	1.925195	0.38998	0.247363	1.471875	0.274668	0.545313	5.88E-05	0.966602	116.1914	0.182383	61.64348	9.634103	11.73808	106.8309	-43.7524	0.590452	63.07858
11	1.855371	0.560166	0.708174	1.698438	0.18415	0.517969	6.52E-05	0.285449	115.9277	0.180527	38.66306	19.92317	9.824623	92.68584	-24.7708	0.732745	67.91505
12	1.925195	0.38998	0.65834	8.440625	0.274668	0.545313	5.88E-05	0.966602	116.1914	0.182383	65.33966	9.050388	10.10626	108.2523	-45.1738	0.582699	63.07858
13	1.855371	0.560166	0.498994	4.573438	0.18415	0.517969	6.52E-05	0.285449	115.9277	0.180527	39.58364	20.1806	10.05751	94.11385	-26.1988	0.721627	67.91505
14	1.925195	0.38998	0.65834	1.471875	0.268574	0.545313	5.88E-05	0.966602	116.1914	0.182383	62.35149	9.206804	10.10626	105.4068	-42.3282	0.59843	63.07858
15	1.855371	0.560166	0.498994	1.698438	0.2329	0.517969	6.52E-05	0.285449	115.9277	0.180527	38.95239	20.26736	10.05751	93.56483	-25.6498	0.725861	67.91505
16	1.926465	0.615088	0.228291	1.385938	0.211572	0.525781	3.07E-05	0.151855	127.8809	0.181309	33.95547	25.22156	10.79217	94.43674	-27.2659	0.711279	67.17083
17	1.855371	0.560166	0.498994	1.698438	0.18415	0.494531	6.52E-05	0.285449	115.9277	0.180527	36.87925	19.51207	10.08369	90.66815	-19.2698	0.787469	71.39838
18	1.858545	0.367397	0.371333	7.678906	0.177866	0.501172	1.87E-05	0.681396	173.54	0.183799	45.43398	10.10875	10.42369	89.59882	-17.86	0.800667	71.73879
19	1.853467	0.548062	0.693716	4.272656	0.169233	0.485547	1.3E-05	0.347412	146.4697	0.175596	34.92714	17.53142	9.862822	86.32571	-15.5615	0.819735	70.76422
20	1.925195	0.38998	0.65834	1.471875	0.274668	0.545313	0.000216	0.966602	116.1914	0.182383	76.14544	8.651818	10.10626	118.7311	-55.6525	0.531273	63.07858
21	1.855371	0.560166	0.498994	1.698438	0.18415	0.517969	0.000195	0.285449	115.9277	0.180527	49.00671	19.29708	10.05751	102.7468	-34.8318	0.660994	67.91505
22	1.925195	0.38998	0.65834	1.471875	0.274668	0.545313	5.88E-05	0.491992	116.1914	0.182383	60.11385	11.95525	9.878948	105.9907	-41.7516	0.606082	64.23903
23	1.855371	0.560166	0.498994	1.698438	0.18415	0.517969	6.52E-05	0.601855	115.9277	0.180527	40.4078	16.94991	10.08805	91.5059	-24.0793	0.736856	67.42664
24	1.925195	0.38998	0.65834	1.471875	0.274668	0.545313	5.88E-05	0.966602	123.9258	0.182383	63.06092	8.732753	10.13115	105.6677	-42.5971	0.596877	63.0706
25	1.855371	0.560166	0.498994	1.698438	0.18415	0.517969	6.52E-05	0.285449	153.1934	0.180527	38.64572	19.80235	10.05635	92.73611	-24.7417	0.733203	67.99442
26	1.879492	0.677598	0.399941	8.690625	0.162441	0.510938	0.000165	0.337305	132.7148	0.177305	44.93142	22.80849	10.27556	102.4843	-34.7929	0.660505	67.69144
27	1.894727	0.346621	0.55498	3.409375	0.235059	0.526563	0.000188	0.22832	118.3008	0.177695	59.9504	11.79221	9.891885	105.6822	-40.0241	0.621278	65.65805

Figure 5.8. The spreadsheet lists specification of the configurations (values of other design parameters) of all filtered configurations.

This user interface promotes users to explore the impact of their design action (selecting different design options, in this case, the three most sensitive design parameters).

5.5 Design tool demonstration

Step 1: Defining the values of Window Wall Ratio (WWR), Effective efficiency of Photovoltaic Panels (PV), and Glazing U-values (Ugl). For example, WWR=0.3, PV=0.15, U_{gl}=1.8

Step 2: Filtering the configurations.

Figure 5.9 shows all the configurations which fulfill the specified values of three parameters in step 1.

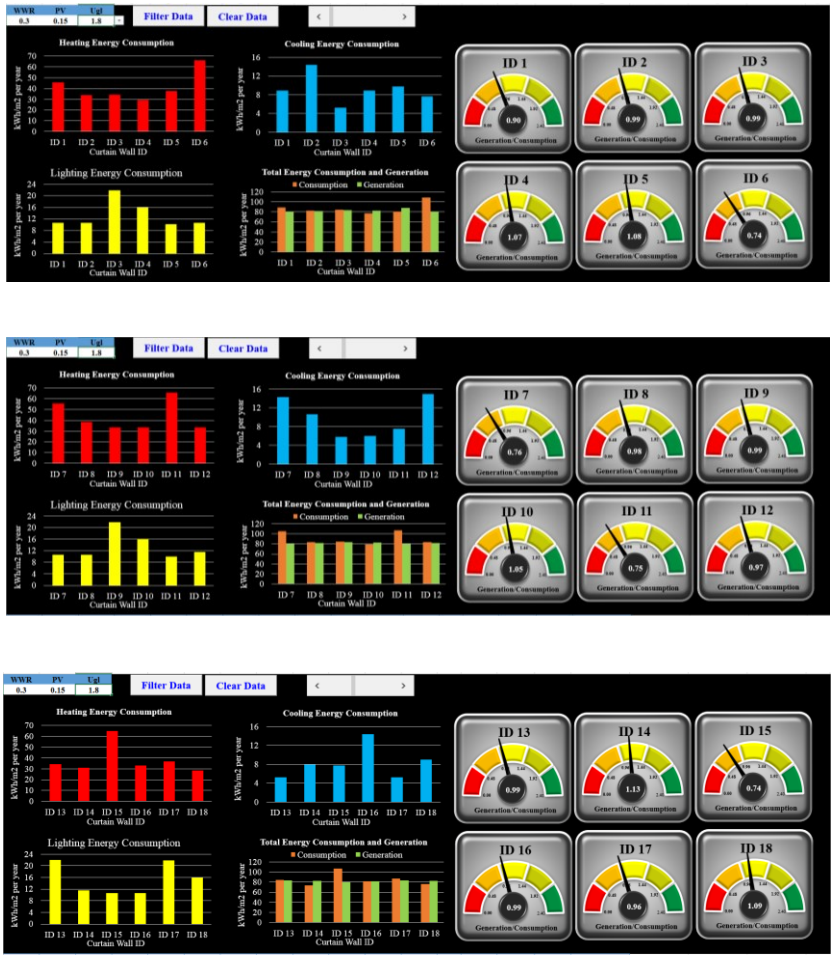

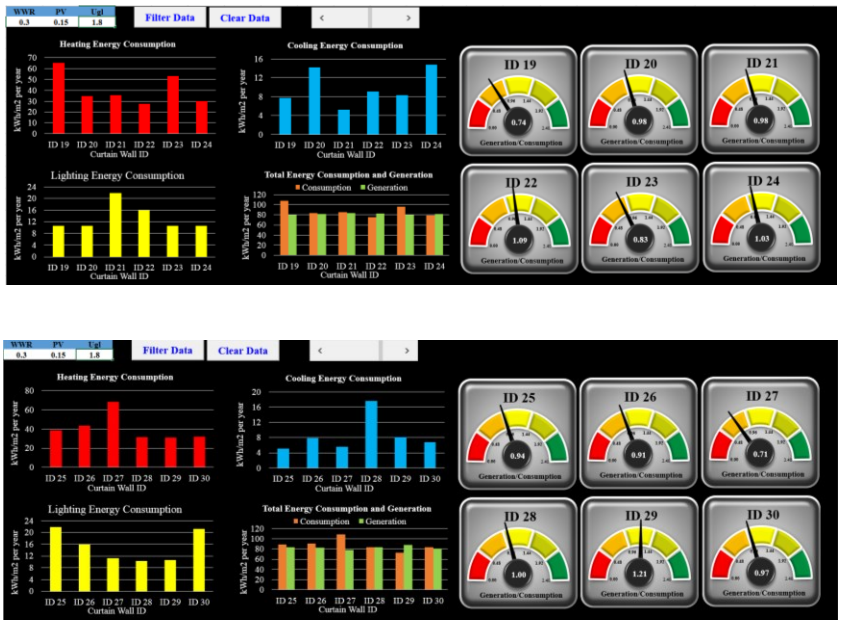

Figure 5.9. Thirty configurations which fulfill the specified values of three parameters (WWR=0.3, PV=0.15, U_{gl}=1.8).

5.6 Conclusion

As suggested, the design tool should offer a user-friendly interface to facilitate the design process. The objective in providing such interface is to allow the designers to explore the design options freely without being constrained by the tool.

The proposed design tool presented here illustrates that the design process can indeed be an interactive one. Exploration through different sets of inputs promotes the designers to have a holistic understanding of the different design options.

The tool at its present state returns all configurations correspond to the set of inputs. This design setup serves an educational purpose to the designers as it returns all filtered configurations, including both plus-energy and negative-energy one. By skimming through different sets of inputs, the designers could grasp a sense of how well a certain sets of inputs are doing (e.g. resulting in more plus-energy configurations). An improvement to the interface shall make it able to inform the users the energy performance of different set of inputs, which can be represented by a percentage that shows the proportion of plus-energy configurations over all filtered configurations.

Configurations can also be sorted in descending order from the most positive energy one to the most negative energy one.

Another enhancement to the design tool is to include an optional button to filter out only the plus-energy curtain wall configurations. In such case, some sets of inputs might return only a few potential design configurations (that achieve plus-energy curtain wall status) while some sets might return many possible configurations. The descriptive statistic of the energy performance can also be displayed. The designers will then be empowered with full knowledge of the energy performance potential of any set of inputs. In fact, it is not just about more or fewer configurations, but also the net energy generation potential. Certain sets of inputs might return fewer number of configurations with high net energy generation. This potentially higher energy generation capability introduces higher uncertainty, since fewer configurations can achieve this high energy generation potential. For example, a change in glazing U-value (one of the inputs) might readily turn a plus-energy configuration into a negative energy one. More about performance uncertainty was discussed in Chapter 4.

An extra feature to the design tool is to allow the inputs to be set over a range (rather than a single value). The resulting filtered configurations will then represent the aggregated effect of changing the input parameters collectively. This feature is particularly useful to facilitate designers to take on an integrated design approach. In this chapter, the potential application of this design tool has been demonstrated. The exact setup and the set of features of the tool shall be determined under consultation with the end users.

Chapter 6 Conclusion

With the advancement of technologies and the desire to improve building energy efficiency, there is a need to investigate the potential and opportunities to improve curtain walls from "energy sinks" to "plus-energy" façade. Given the typical large glazing area in curtain walls and the relatively low thermal performance of metal and glass, the energy performance of buildings with curtain walls, especially the perimeter zone, is more sensitive to the climatic conditions and the variation of façade design compared to buildings with opaque insulated façade. To account for the complex interacting effect of façade design parameters on the energy performance, the Analysis of Variance (ANOVA) approach is adopted for the global sensitivity analysis to identify the most significant façade design parameters and identify feasible curtain wall design configurations within available products that can achieve energy balance for the perimeter zone of office buildings.

An office unit in the perimeter zone of a typical office building located in Montreal is modeled in EnergyPlus with various curtain wall configurations. Ten design parameters including glazing U-value, solar heat gain coefficient (SHGC), and visible transmittance (Tv); U-value of the spandrel panel, U-value of the mullion, window wall ratio (WWR), infiltration rate, depth and inclination of the overhang, and efficiency of the PV modules, are studied. In total, 98,304 configurations of curtain walls are simulated for the four cardinal orientations.

The uncertainty analysis shows that:

- the variation of curtain wall configurations has generally greater impact on the cooling (υ=42-65%) followed by heating (υ=34-38%), lighting(υ=28%) and total energy consumption (υ=16-20%). The variation of curtain wall configurations has much less impact on the cooling energy consumption for north façade (υ=40%) than the other three orientations with the greatest impact on the south façade (υ=65%).
- the energy generation to energy consumption ratio has the highest coefficient of variation about 61-66%, which indicates the variation of curtain wall configurations has more significant impact on the energy balance.

The global sensitivity analysis shows that:

WWR is the most significant design parameter influencing the heating, cooling, lighting and total energy consumption and the energy balance for the office unit in the perimeter zone. Typically the total sensitivity index of WWR is 1.5 to 5.0 times greater than the second significant parameter for the energy consumption.

WWR, U-value of glazing and infiltration rate are the three most significant parameters influencing the annual heating energy consumption;

WWR, SHGC, and depth of overhang are the three most significant parameters influencing the annual cooling energy consumption for the east, south and west orientation. For the North orientation, U-value of glazing is the 3rd most significant parameter;

WWR, depth of overhang and inclination of overhang are the three most significant parameters influencing the annual lighting energy consumption for east, west and south orientations. For the north orientation, the visible transmittance Tv ranks the 3rd. The influence of inclination and Tv is comparable for all orientations.

Given that Montreal is in a heating-dominated climate, similar to the heating energy consumption, WWR, U-value of glazing, and infiltration are the three most significant parameters influencing the total annual energy consumption.

Given that WWR directly affects the spandrel surface area available for mounting PV modules, the WWR is the most significant parameter influencing the energy balance in the perimeter zone with a total sensitivity index about 8 to 13 times greater than the second most significant parameter, PV efficiency. The influence of PV efficiency is about 2 to 3.5 times greater than the third most significant parameter, i.e. U-value of glazing.

Energy balance can be achieved with the proper combination of WWR, U-glazing and PV efficiency. In general, with the increase of WWR, the number of possible configurations that can achieve the energy balance decreases.

For the east and west façade, when the WWR is greater than 40%, it is very difficult to achieve the energy balance. For the south façade, the WWR can be generally increased up to 60%. For North façade, no curtain wall configurations within the ranges studied can achieve energy balance.

A greater WWR may be specified in curtain wall design for each orientation, however, to achieve the energy balance, higher efficiency PV modules and better insulated glazing units need to be applied to offset the additional energy consumption due to the larger glazing area.

5.1 Contribution of research

- The methodology presented in this study helps facilitate the design process to resolve the issues with conflicting effects of design parameters.
- The configuration of energy generating curtain walls which perform resiliently under a certain range of building operations are proposed in this study.
- The energy impact of individual design parameters of curtain walls are investigated with considerations of all the interdependent relationship between the parameters.
- A design tool is proposed to facilitate designers to explore impact on energy performance due to different design alternatives.

5.2 Recommendation of future work

The current study assumes PV modules integrated into spandrel area and only the electricity generated by the PV modules are considered as energy generation. The contribution of thermal energy that can be collected from the PV modules will contribute to further energy generation, which will have an influence on the façade design. The current study presents the development of the methodology and its application to a cold-climate with low internal gain (i.e. assumed highly energy efficient equipment). Future studies will investigate the influence of climatic conditions, internal gains, the integration of BIPV/T, building control strategies, daylight utilization and other advanced technologies such as automated shading control, etc.

5.3 Related publication

1. Lam, T. C., Hua Ge, and Paul Fazio, 2014, "Study of different glazing modelling approaches in assessing energy performance of curtain wall systems using EnergyPlus.“,eSIM 2014 Conference Proceedings
2. Lam, T. C., Hua Ge, and Paul Fazio, 2015, Identifying plus-energy curtain wall configurations using the Analysis of Variance (ANOVA) approach, Energy and Buildings. (under revision)
3. Lam, T. C., Hua Ge, and Paul Fazio, 2015, Impact of curtain wall configurations on the building energy performance in the perimeter zone, 6th International Building Physics Conference, IBPC 2015

References

Alam, M., Singh, H., & Limbachiya, M. C. (2011). Vacuum Insulation Panels (VIPs) for building construction industry – A review of the contemporary developments and future directions. *Applied Energy*, *88*(11), 3592–3602.

Apostolakis, G. (1990). The concept of probability in safety assessments of technological systems. *Science*, *250*(4986), 1359–1364.

Archer, G. E. B., Saltelli, A., & Sobol, I. M. (1997). Sensitivity measures,anova-like Techniques and the use of bootstrap. *Journal of Statistical Computation and Simulation*, *58*(2), 99–120.

ASHRAE. (2002). ASHRAE Guideline 14-2002 Measurement of Energy and Demand Savings. American Society of Heating, Refrigerating, and Air-Conditioning Engineers.

ASHRAE. (2010). ANSI/ASHRAE Standard 55:2010 Thermal Environmental Conditions for Human Occupancy. American Society of Heating, Refrigerating, and Air-Conditioning Engineers.

ASHRAE. (2011a). Advanced Energy Design Guide for Small to Medium Office Buildings. American Society of Heating, Refrigerating and Air-Conditioning Engineers.

ASHRAE. (2011b). ANSI/ASHRAE/IES Standard 90.1-2011 -- Energy Standard for Buildings Except Low-Rise Residential Buildings. American Society of Heating, Refrigerating, and Air-Conditioning Engineers.

Attia, S., Gratia, E., De Herde, A., & Hensen, J. L. M. (2012). Simulation-based decision support tool for early stages of zero-energy building design. *Energy and Buildings*, *49*, 2–15.

Attia, S., Hamdy, M., O'Brien, W., & Carlucci, S. (2013). Assessing gaps and needs for integrating building performance optimization tools in net zero energy buildings design. *Energy and Buildings*, *60*, 110–124.

Barnett, A. M., Rand, J. A., Hall, R. B., Bisaillon, J. C., Delledonne, E. J., Feyock, B. W., … Sims, P. E. (2001). High current, thin silicon-on-ceramic solar cell. *Solar Energy Materials & Solar Cells*, *66*, 45–50.

Bieda, B. (2010). Decision support systems based on the economic feasibility assessment for Municipal Solid Waste (MSW) Management under Uncertainty using SimLab® toolpack. In *Procedia - Social and Behavioral Sciences 2* (Vol. 2, pp. 7609–7610). Sixth International Conference on Sensitivity Analysis of Model Output.

Bratley, P., & Fox, B. L. (1988). ALGORITHM 659: implementing Sobol's quasirandom sequence generator. *ACM Transactions on Mathematical Software*, *14*(1), 88–100.

Carmody, J., Selkowitz, S., Lee, E. S., & Arasteh, D. (2004). *Window Systems for High-Performance Buildings*. W. W. Norton & Company.

Chaiyapinunt, S., Phueakphongsuriya, B., Mongkornsaksit, K., & Khomporn, N. (2005). Performance rating of glass windows and glass windows with films in aspect of thermal comfort and heat transmission. *Energy and Buildings*, *37*(7), 725–738.

Chan, K., Saltelli, A., & Tarantola, S. (1997). Sensitivity Analysis of Model Output: Variance-Based Methods Make the Difference. In *Proceedings of the 29th conference on Winter simulation Conference* (pp. 261–268).

Chow, T. T., Li, C., & Lin, Z. (2010). Innovative solar windows for cooling-demand climate. *Solar Energy Materials and Solar Cells*, *94*(2), 212–220.

CIBSE. (2004). *CIBSE TM35 Environmental Performance Toolkit for Glazed Façades*. The Chartered Institution of Building Services Engineers.

Climate. (2015). climate.weather.gc.ca. Retrieved from http://climate.weather.gc.ca/climateData/almanac_e.html?timeframe=4&Prov=QC&StationID=30165&Year=2001&Month=6&Day=2

Crawley, D. B., Hand, J. W., Kummert, M., & Griffith, B. T. (2008). Contrasting the capabilities of building energy performance simulation programs. *Building and Environment*, *43*(4), 661–673.

Didonato, A. R., & Morris, A. H. (1992). Significant digit computation of the incomplete beta function ratios. *ACM Transactions on Mathematical Software*, *18*(3), 360–373.

DOE. (2013a). *EnergyPlus engineering reference: the reference to EnergyPlus calculations*.

DOE. (2013b). *EnergyPlus Input Output Reference: The Encyclopedic Reference to EnergyPlus Input and Output*.

Duffie, J. a., & Beckman, W. a. (1994). *Solar Engineering of Thermal Processes* (4th ed.). Wiley.

Dussault, J.-M., Gosselin, L., & Galstian, T. (2012). Integration of smart windows into building design for reduction of yearly overall energy consumption and peak loads. *Solar Energy*, *86*(11), 3405–3416.

Frey, H. C., & Patil, S. R. (2002). Identification and review of sensitivity analysis methods. *Risk Analysis*, *22*(3), 553–578.

Ge, H. (2002). Study on overall thermal performance of metal curtain walls. *PhD Thesis, Concordia University*.

Geoffrey, V. M., Bruyère, I., & De Herde, A. (2007). Impact of control rules on the efficiency of shading devices and free cooling for office buildings. *Building and Environment*, *42*(2), 784–793.

Gilijamse, W. (1995). Zero-energy houses in the Netherlands. In *Building Simulation '95* (pp. 276–283). Madison, Wisconsin, USA.

Gopinathan, K. K. (1991). Solar radiation on variously oriented sloping surfaces. *Solar Energy*, *47*(3), 173–179.

Gunerhan, H., & Hepbasli, A. (2007). Determination of the optimum tilt angle of solar collectors for building applications. *Building and Environment*, *42*(2), 779–783.

Gutherz, J. M., & Schiler, M. E. (1991). A Passive Solar Heating System for the Perimeter Zone of Office Buildings. *Energy Sources*, *13*(1), 39–54.

Hamby, D. M. (1994). A review of techniques for parameter sensitivity analysis of environmental models. *Environmental Monitoring and Assessment*, *32*(2), 135–54.

Hanna, S. R. (1993). Uncertainties in Air Quality Model Predictions. *Transport and Diffusion in Turbulent Fields*, *Springer N*, 3–20.

Hausladen, G. (2008). *ClimateSkin: Concepts for Building Skins That Can Do More with Less Energy*. Birkhäuser GmbH.

Helton, J. C., & Burmaster, D. E. (1996). Guest editorial: treatment of aleatory and epistemic uncertainty in performance assessments for complex systems. *Reliability Engineering & System Safety*, *54*(2), 91–94.

Hochberg, Y., & Tamhane, A. C. (2009). *Multiple Comparison Procedures* (1st ed.). Wiley.

Hoes, P., Hensen, J. L. M., Loomans, M. G. L. C., de Vries, B., & Bourgeois, D. (2009). User behavior in whole building simulation. *Energy and Buildings*, *41*(3), 295–302.

Hopfe, C. J., & Hensen, J. L. M. (2011). Uncertainty analysis in building performance simulation for design support. *Energy and Buildings*, *43*(10), 2798–2805.

Iman, Ronald L., and W. J. C. (1982). A distribution-free approach to inducing rank correlation among input variables. *Communications in Statistics-Simulation and Computation 11*, *3*, 311–334.

Jelle, B. P., Hynd, A., Gustavsen, A., Arasteh, D., Goudey, H., & Hart, R. (2012). Fenestration of today and tomorrow: A state-of-the-art review and future research opportunities. *Solar Energy Materials and Solar Cells*, *96*(7465), 1–28.

Kasinalis, C., Loonen, R. C. G. M., Cóstola, D., & Hensen, J. L. M. (2014). Framework for assessing the performance potential of seasonally adaptable façades using multi-objective optimization. *Energy and Buildings*, *79*, 106–113.

Kim, J. T., & Kim, G. (2010). Advanced External Shading Device to Maximize Visual and View Performance. *Indoor and Built Environment*, *19*(1), 65–72.

Kiureghian, A. Der, & Ditlevsen, O. (2009). Aleatory or epistemic? Does it matter? *Structural Safety*, *31*(2), 105–112.

Lam, T. C., Ge, H., & Fazio, P. (2014). Study of different glazing modelling approaches in assessing energy performance of curtain wall systems using EnergyPlus. In *eSIM 2014 Conference Proceedings*. International Building Performance Simulation Association.

Lee, E. S., & Tavil, A. (2007). Energy and visual comfort performance of electrochromic windows with overhangs. *Building and Environment*, *42*(6), 2439–2449.

Lee, I. Y. T. (2010). High Performance Window Systems and their Effect on Perimeter Space Commercial Building Energy Performance. *Master Thesis, University of Waterloo*.

Lewis, G. (1987). Optimal tilt of solar collectors. *Solar & Wind Technology*, *4*(3), 407–410.

Lorenzo, E. (2011). *Energy Collected and Delivered by PV Modules*. *Handbook of Photovoltaic Science and Engineering* (Forth). Wiley.

Macdonald, I. A. (2002). Quantifying the Effects of Uncertainty in Building Simulation. *PhD Thesis, University of Strathclyde*.

Machairas, V., Tsangrassoulis, A., & Axarli, K. (2014). Algorithms for optimization of building design: A review. *Renewable and Sustainable Energy Reviews*, *31*, 101–112.

Manz, H., & Menti, U. P. (2012). Energy performance of glazings in European climates. *Renewable Energy*, *37*(1), 226–232.

Marszal, A. J., Heiselberg, P., Bourrelle, J. S., Musall, E., Voss, K., Sartori, I., & Napolitano, A. (2011). Zero Energy Building - A review of definitions and calculation methodologies. *Energy and Buildings*, *43*(4), 971–979.

Meewissen, A. M. H., & Cooke, R. M. (1994). *Report 94-28 Tree dependent random variables*. Delft University of Technology.

Montgomery, D. C. (2012). *Design and Analysis of Experiments* (8th ed.). Wiley.

Morris, M. D. (1987). Two-stage factor screening procedures using multiple grouping assignments. *Communications in Statistics - Theory and Methods*, *16*(10), 3051–3067.

Nasrollahi, F. (2013). *Architectural Energy Efficiency* (7th ed.). Universitätsverlag der TU Berlin.

Nielsen, M. V., Svendsen, S., & Jensen, L. B. (2011). Quantifying the potential of automated dynamic solar shading in office buildings through integrated simulations of energy and daylight. *Solar Energy*, *85*(5), 757–768.

Nielsen, T. R., Duer, K., & Svendsen, S. (2000). Energy performance of glazings and windows. *Solar Energy*, *69*(SUPPLEMENT 6), 137–143.

Noguchi, M., Athienitis, A., Delisle, V., Ayoub, J., & Berneche, B. (2008). Net Zero Energy Homes of the Future : A Case Study of the ÉcoTerra House in Canada. In *Renewable Energy Congress* (pp. 2008–2112). Glasgow,Scotland.

Ott, R. L. (2008). *An Introduction to Statistical Methods and Data Analysis* (6th ed.). Duxbury Press.

Pace, L. A. (2012). *Beginning R: An introduction to statistical programming*. Apress.

Parida, B., Iniyan, S., & Goic, R. (2011). A review of solar photovoltaic technologies. *Renewable and Sustainable Energy Reviews*, *15*(3), 1625–1636.

Peter, L., Justin, W., & Mahabir, B. (2010). A comparison of window modeling methods in EnergyPlus 4.0. In *Fourth National Conference of IBPSA-USA New* (pp. 177–184). New York City, New York: SimBuild 2010.

Poirazis, H., Blomsterberg, Å., & Wall, M. (2008). Energy simulations for glazed office buildings in Sweden. *Energy and Buildings*, *40*(7), 1161–1170.

Prasad, D., & Snow, M. (2014). *Designing with solar power: a source book for building integrated photovoltaics (BiPV)*.

Roberts, S., & Guariento, N. (2009). *Building Integrated Photovoltaics: A Handbook* (First). Birkhäuser Basel.

Rosta, S., Hurt, R., Boehm, R., & Hale, M. J. (2008). Performance of a Zero-Energy House. *Journal of Solar Energy Engineering*, *130*(2), 021006.

Roy, R., Hinduja, S., & Teti, R. (2008). Recent advances in engineering design optimisation: Challenges and future trends. *CIRP Annals - Manufacturing Technology*, *57*(2), 697–715.

Saltelli, A., Chan, K., & Scot, E. M. (2000). *Sensitivity Analysis*. Wiley.

Saltelli, A., Ratto, M., Andres, T., Francesca Campolongo, J. C., Gatelli, D., Saisana, M., & Tarantola, S. (2008). *Global sensitivity analysis: the primer*. John Wiley & Sons.

Shen, H., & Tzempelikos, A. (2012). Daylighting and energy analysis of private offices with automated interior roller shades. *Solar Energy*, *86*(2), 681–704.

Silva, P. C. da, Leal, V., & Andersen, M. (2012). Influence of shading control patterns on the energy assessment of office spaces. *Energy and Buildings*, *50*, 35–48.

Singh, G. K. (2013). Solar power generation by PV (photovoltaic) technology: A review. *Energy*, *53*, 1–13.

Spitz, C., Mora, L., Wurtz, E., & Jay, A. (2012). Practical application of uncertainty analysis and sensitivity analysis on an experimental house. *Energy and Buildings*, *55*, 459–470.

Stein, M. (1987). Large sample properties of simulations using Latin hypercube sampling. *Technometrics 29*, *2*, 143–151.

Tawada, Y., & Yamagishi, H. (2001). Mass-production of large size a-Si modules and future plan. *Solar Energy Materials and Solar Cells*, *66*(1-4), 95–105.

Thalfeldt, M., Pikas, E., Kurnitski, J., & Voll, H. (2013). Façade design principles for nearly zero energy buildings in a cold climate. *Energy and Buildings*, *67*, 309–321.

Tian, W. (2013). A review of sensitivity analysis methods in building energy analysis. *Renewable and Sustainable Energy Reviews*, *20*, 411–419.

Torcellini, P., Pless, S., & Deru, M. (2006). Zero Energy Buildings : A Critical Look at the Definition Preprint. In N. R. E. Laboratory (Ed.), *ACEEE Summer Study*. Pacific Grove, California.

Tzempelikos, A., & Athienitis, A. K. (2007). The impact of shading design and control on building cooling and lighting demand. *Solar Energy*, *81*(3), 369–382.

Van Buren, K. L., Atamturktur, S., & Hemez, F. M. (2014). Model selection through robustness and fidelity criteria: Modeling the dynamics of the CX-100 wind turbine blade. *Mechanical Systems and Signal Processing*, *43*(1-2), 246–259.

Van der Zwaan, B. (2003). Prospects for PV: A learning curve analysis. *Solar Energy*, *74*(1), 19–31.

West, S. (2001). Improving the sustainable development of building stock by the implementation of energy efficient , climate control technologies. *Building and Environment*, *36*(2001), 281–289.

Yang, J., Banerjee, A., & Guha, S. (2003). Amorphous silicon based photovoltaics - From earth to the "final frontier." *Solar Energy Materials and Solar Cells*, *78*(1-4), 597–612.